# Functional Characterization of Abiotic Stress Responsive Genes from *Jatropha curcas* L., a Potential Biofuel Plant

Thesis Submitted for the Award of the Degree of

**DOCTOR OF PHILOSOPHY**

**SHALINI MUDALKAR**

**(Registration No. 10LPPH12)**


**DEPARTMENT OF PLANT SCIENECS**
**SCHOOL OF LIFE SCIENCES**
**UNIVERSITY OF HYDERABAD**
**HYDERABAD 500046**

**MARCH 2017**

# ACKNOWLEDGEMENTS

*I express my profound gratitude and sincere thanks to my supervisor* **Prof. Attipalli Ramachandra Reddy,** *Department of Plant Sciences for introducing me to this fascinating work and allowing me to work under his valuable guidance. I thank him for his kind support. The discussions with him during the course of my Ph.D. provided a great deal of encouragement towards completion of this work. I am fortunate to have had him as my Supervisor and I consider working with him is the greatest privilege I ever had.*

*I am thankful to my Doctoral committee members* Prof. A. S. Raghavendra *and* Prof. K. P. M. S. V. Padmasree *for periodically evaluation my progress in research and also for their interest, advice and support.*

*I thank present and former Heads of Department of Plant Sciences* Prof. Ch. Venkataramana, Prof. Attipalli R. Reddy, *and* Prof. Appa Rao Podile *and also present and former Deans of School of Life Sciences for their valuable suggestions and providing research facilities.*

*My most sincere thanks go to* Sri. Ghatti Srinivas*, Tree Oils India Pvt. Ltd. (Toil) for providing seed material for my experiments and allowing me to visit their experimental farm.*

*I am extremely thankful to Faculty members, Department of Plant Sciences and School of Life Sciences for their help and valuable suggestions.*

*I thank CSIR-UGC, New Delhi for my fellowship. I also thank DST-SERB, New Delhi and UPE, University of Hyderabad for the travel support to Vienna, Austria to attend conference on Plant gene discovery and omics technologies.*

*Funding in lab from DBT, DST, DST-Nanotechnology, DST-FIST, UGC-SAP, DBT-CREEB, BASF is highly acknowledged.*

*I wish to extend my thanks to all the non-teaching staff of School of Life Sciences. I thank* Mr. Vinodh, Mr. Laxman, Mr. Sateesh Yadav *for their help in the lab and field work.*

*I express my sincere thanks to* Dr. G. Ramesh, *who laid the foundation for my career and for his invaluable patience in teaching me the molecular biology techniques. Also, I thank him for his constant support, encouragement and valuable suggestions.*

*Diction is not enough to express my gratitude and regards to* Dr. Debashree Sengupta and Mr. Rachapudi Venkata Sreeharsha *for their endless love, affection, cooperation, encouragement and patience. They were a great source of motivation and support throughout my Ph.D. tenure. I thank them from the bottom of my heart for all the help they have done which cannot be put in words that easily.*

*I wish to express my heartfelt gratitude to* Dr. Girish Kumar Rasineni, Dr. Anirban Guha, Dr. A. S. V. Chalapathi, Mr. Bharatula Srikrishna Chaitanya, Mr. Kalva Madhana Sekhar, Mr. Sumit Kumar, Mr. Konubothula Sitarami Reddy, Mr. Marriboina Suresh Babu, Ms. Tamna Singha, and Ms. Divya K. Unnikrishnan *for maintaining cheerful environment in the lab and also for their help and support during my Ph.D. tenure.*

*I express my heartfelt thanks to all my friends for their kind support, love and affection and I especially thank* Ms. Annapurna, Mr. Shyam *for cheering me up during my tough times and extending a helping hand whenever needed.*

*I owe immensely to my* Family members *especially my maternal grandparents, aunts and uncles who raised me up and whatever I achieved today is only because of their blessings, love, care and support. I thank my* Parents *and my dear most brother* (Sandeep) *for their everlasting love, affection, cooperation motivation in every walk of life and for their patience till the completion of the Ph.D. work. The acknowledgement is incomplete without a mention about my loveable cousins* (Aditya, Akshay, Vishnu, Sachin, Supriya, Lakshita and Khushal) *who would always create a cheerful environment when they were around. I express my sincere thanks to all my well wishers and who so ever, who has helped me the least way possible and finally, I thank the Almighty for his blessings.*

***Dedicated to* Ajji *and* Ajja . . .** 

## TABLE OF CONTENTS

## LIST OF FIGURES AND TABLES

### Figures

antibody. In all planes, lane 1 represents GST protein and lane 2 the corresponding GST fused targeted protein.

**Fig. 30.** Bacterial cells expressing GST and GST-JcGLYI, II and GR were grown in LB broth supplemented with ampicillin till $O.D_{600}$-0.5, the cultures were induced with 1mM IPTG (A) untreated control (B) 200mM NaCl, (C) 5% PEG or (D) 5% PEG+200mM NaCl for salt, osmotic and osmotic+salt stress, respectively and $O.D_{600}$ was measured respectively for each treatment. Data are the mean ± SD (n=3).

**Fig. 31.** Yeast growth for abiotic stress tolerance. Vector p424 and the construct p424-JcGLYI, II and GR were introduced into Yap-1 cells and the transformed cells were selected by their capacity to grow in complete synthetic medium (SC), lacking Trp (p424 selection marker). To determine the abiotic stress tolerance, yeast cells were grown in liquid SC-TRP medium supplemented independently with NaCl (200mM), PEG (5%), PEG+NaCl or MG (5mM) and the growth was observed by measuring the OD at 600nm for 36 h at 30°C for (A) JcGLYI, (B) JcGLYII and (C) JcGR. Data are the mean ± SD (n=3).

**Fig. 32.** qRT-PCR analysis of targeted genes. JcGLYI (A) leaf (B) root. JcGLYII (C) leaf (D) root and JcGR (E) leaf, (F) root at 7, 15 and 21DAS during salt, drought and drought + salt stress. Data are the mean ± SD (n=3).

**Fig. 33.** Enzyme activities of targeted genes. JcGLYI (A) leaf (B) root. JcGLYII (C) leaf (D) root and JcGR (E) leaf, (F) root at 7, 15 and 21DAS during salt, drought and drought + salt stress and untreated control, with 2mM MG as substrate. Data presented is the mean ± SD (n=3).

**Fig. 34.** Total glutathione content. Ratio of reduced (GSH) and oxidised glutathione (GSSG) in control and treated plants at 7, 15 and 21 DAS**.** Mean± SD (n=3) was taken for presentation of the data.

**Fig. 35.** Sequence alignment of MT2 from different plants which were used to design primers JcMTF and JcMTR from the conserved regions highlighted in blue using Clustal W.

or with 20 μM and 40 μM $CdCl_2$. (B) Functional complementation of yeast mutants on selective media. DTY4 (Copper sensitive) mutant was transformed with empty vector P424 or with p424-JcMT2a and DTY3 (parental cells with single CUP1 gene) were taken for the study. The cells were grown to $OD_{600}$=1.0, 10-fold dilutions were performed. 3μl of each dilution were spotted on SC-URA-TRP plates supplemented without or with 75 μM and 125 μM $CuSO_4$.

**Fig. 44.** Transcript analysis of JcMT2a gene under heavy metal stress: qRT-PCR analysis of *JcMT2a* gene under heavy metal stress from leaf tissue cadmium(A), copper (B) stress and root tissue cadmium (C), copper (D) stress at different time points (12, 24, 48 hours) and concentrations (250, 500, 1000 μM) of the metals respectively. Total RNA was isolated from control and treated plants, converted to cDNAs, subjected to qRT-PCR. The relative expression of gene *JcMT2a* was expressed by $2^{-\Delta\Delta C_T}$. The vertical bars represent the mean ± SD.

## Tables

# Abbreviations and symbols

| | |
|---|---|
| ABA | Abscisic acid |
| ADRs | Aldehyde reductases |
| AKRs | Aldo - keto reductases |
| ANOVA | Analysis of variance |
| APx | Ascorbate peroxidase |
| ASC | Ascorbate |
| CAT | Catalase |
| $CO_2$ | Carbon dioxide |
| Ct | Threshold cycle |
| DAS | Days after stress |
| DAT | Days after treatment |
| DHA | Dehydro ascorbate |
| DHAR | Dehydro ascorbate reductase |
| E | Transpiration rate |
| EDTA | Ethylene diamine tetrachloride |
| ETR | Electron transport rate |
| FAD | Flavin adenine dinucleotide |
| $F_M$ | Maximum fluorescence |
| $F_o$ | Initial fluorescence |
| $Fv/F_m$ | Maximal photochemical efficiency of PS – II |
| GLY I & II | Glyoxalase I and II |
| GPx | Glutathione peroxidase |
| GR | Glutathione reductase |
| $g_s$ | Stomatal conductance |
| GSH | Glutathione |
| GST | Glutathione S transferase |
| GSSG | Glutathione |
| $H_2O_2$ | Hydrogen peroxide |
| HNE | 4-Hydroxynonenal |
| HRP | Horse radish peroxidase |
| IPTG | Isopropyl β-D-1-thiogalactopyranoside |
| LEA | Late embryogenesis abundant proteins |
| MDA | Malondialdehyde |
| MDHA | Monodehydroascorbate reductase |
| MG | Methylglyoxalase |
| MTs | Metallothionein |
| $NAD^+$/NADH | Nicotinamide adenine dinucleotide |
| $NADP^+$/NADPH | Nicotinamide adenine dinucleotide phosphate |
| PCR | Polymerase chain reaction |
| PEG | Polyethylene glycol |
| $P_n$ | Photosynthetic rate |
| POx | Peroxidase |
| RACE | Randomly amplified cDNA ends |
| RC | Reaction centers |
| ROS | Reactive oxygen species |
| RuBp | Ribulose 1,5- bis phosphate |
| RWC | Relative water content |
| SD | Standard deviation |
| SDS-PAGE | Sodium dodecyl sulphate poly acrylamide gel electrophoresis |
| SLG | S- lactoyl glutathione |
| SOD | Superoxide dismutase |
| TF | Transcription factor |
| UTR | Untranslated region |
| $WUE_i$ | Water use efficiency |

# Chapter I

# Rationale & Objectives

# Chapter - I

Any external factor that imposes negative impact on growth and development of the plant is known as stress. Depending upon whether the factors involved are living or non-living, environmental stress can be categorized as biotic (plant pathogens) or abiotic stress (environmental conditions) respectively. The sessile nature of plants make them susceptible to various kinds of abiotic stresses including light, heat, salinity, drought, cold and heavy metals causing more than 50% yield losses in some of the major crops worldwide (Polle and Chen 2015). Further, anthropogenic contributions and climate change continue to exacerbate the detrimental effects of these stresses on crop yield, thereby threatening sustainable agriculture globally. However, plants are flexible enough to exhibit a plethora of morphological patterns depending on the growth conditions to which they are exposed. In fact, they have evolved from primal living organisms by adapting various morphological, physiological and biochemical modifications in response to abiotic and biotic environmental changes (Choudhary et al. 2003). In the current scenario, to meet future food and fuel demands, obtaining increased plant yields in environmentally challenging conditions is essential.

Water stress in its broadest sense encompasses both drought and salt stress. Moreover, stressful conditions generally do not occur as isolated events but as crosstalk of multiple stresses (Mittler and Blumwald 2010). For example, among abiotic stresses, drought and salt stress are most frequent and affects virtually every aspect of plant physiology and metabolism and the changes that occur under these stresses have been documented broadly either as adaptive or pathological consequences (Zhu 2002). Most studies on water stress signalling have focused on salt stress primarily because plant responses to

salt and drought are closely related and the mechanisms overlap (Mahajan and Tuteja 2005; Zhu 2002). Heavy metal toxicity is the next crucial abiotic stress that poses a serious problem for global agriculture. Heavy metals such as copper and zinc, are essential micronutrients for a range of plant physiological processes through the action of Cu- and Zn-dependent enzymes. However, these essential and other nonessential heavy metal ions, such as cadmium, lead, and mercury are highly reactive and consequently can be toxic to plants when present in excess (Clemens 2006). As a result, plants have evolved mechanisms which can control and respond to the uptake and accumulation of both essential and nonessential heavy metals.

The responses of plants to various abiotic stresses can broadly be classified into following three categories:

## 1. Physiological responses

Plants employ a fine metabolic coordination involving several inter-related processes, especially a close balance between photochemical activity and Calvin cycle reactions. Abiotic stresses disturb this balance and affect $CO_2$ assimilation by means of stomatal and non-stomatal limitations. Net $CO_2$ uptake is declined due to reduction in stomatal aperture which further decrease the intercellular $CO_2$ concentration and ribulose-1,5-bisphosphate carboxylase/oxygenase (Rubisco) carboxylation capacity. Non – stomatal limitations contribute by means of decreased ribulose – 1,5 – bisphosphate (RuBP) regeneration and diminished ATP synthesis and metabolism (Cornic 2000; Escalona et al. 2000). Stomatal conductance ($g_s$) limit net photosynthesis ($A_{sat}$) at low stress levels whereas RuBP and ATP supply contribute under severe stress conditions. And, it is the stomatal opening rather than stomata density that play a crucial role in water loss during drought stress. Thus, $A_{sat}$ is a function of the activity of Rubisco as well as regeneration of RuBP. Reduction in chloroplast volume and acidification of chloroplast stroma due to desiccation may also lead to conformational changes in Rubisco resulting in inhibition of its activity. Further, increased mesophyll $CO_2$ diffusion conductance, Chl a/b ratio, leaf nitrogen partitioning in Rubisco and bioenergetics have been reported as the crucial elements to mediate physiological plasticity under long-term stress conditions. In addition, there are reports that the activities of fructose 1, 6 bis-

phosphatase and sucrose phosphate synthase decline with reduced water potential, indicating that the sucrose synthesis is strongly influenced by abiotic stress, especially by drought (Reddy et al. 2004). The limitation of photosynthesis during drought could lead to a decrease in starch and sucrose metabolism which ultimately results in decrease in dry matter production (Reddy et al. 2004). Moreover there has been an enormous change in the growth and anatomy during various abiotic stresses wherein many plants showed inhibition in the growth of shoot and root, cell division and cell expansion (Zhu 2002).

The performance of the photosynthetic apparatus in terms of photosystem II (PS – II) efficiency can be measured by chlorophyll *a* fluorescence. PS – II efficiency can be explained in terms of Fv/Fm, a dependent parameter for minimum ($F_0$) and maximum fluorescence (Fm). Fv/Fm along with Fv'/Fm' ratios are the reliable diagnostic indicators of PS – II efficiency under any climatic conditions (Sreeharsha et al. 2015). Abiotic stress causes reduction in number of open PS – II reaction centers thereby impeding the light harvesting and energy transduction and eventually leads to impairment of $CO_2$ assimilation. This also creates an imbalance in the utilization of absorbed light energy in the process of photochemical quenching resulting in enhanced dissipation in the form of heat energy (non-photochemical quenching). Thus PSII efficiency is key for determining the ability of plant to survive under various abiotic stress conditions.

Water flow from the soil to the roots depends on the water potential gradient between the soil and plant, which is affected by the water needs of the plant, the hydraulic conductivity of the soil, soil type, moisture content in the soil and the atmospheric demand, which directly affects transpiration, generating considerable tension in the xylem. Water potential ($\Psi$), which is a combination of pressure potential (p) and osmotic potential (s) along with relative water content (RWC) acts as indicator of plant water status (Kiani et al. 2007). The continued inflow of water contributes to growth processes, as turgor pressure is responsible for cell elongation. Plant growth is the result of daughter-cell production by meristematic cell divisions in the shoot and root and the subsequent massive expansion of the young cells. The constant inflow of water exerts pressure within the cell, causing the cell wall to stretch and inducing the elongation or

growth of the cell in both size and volume. This physical process is repeated until the cell becomes mature, at which point cell size is no longer significantly altered. These two processes (cell division and expansion) are important to the growth and development of tissues and organs. When moisture availability in the soil decreases and there is continuity in the loss of water through transpiration, cavitation can occur, causing the interruption of water flow through the xylem due to the formation of air bubbles. Dry soil and the loss of water through high transpiration rates make the plant experience drought stress, which leads to the loss of turgor. Thus, plants are generally shorter in dry environments. During abiotic stresses, plants try to maintain pressure potential by means of increased cell solute concentration thereby mediating osmotic adjustment. The lowering water potential due to the accumulation of compatible solutes allows rapid water intake from rather dry soil, thus mitigating water stress effects.

## 2. Biochemical responses

One of the common plant responses upon stress perception is an alteration in the redox state of the cell due to enhanced production of reactive oxygen species (ROS) and decreased activities of antioxidant mechanisms. The evolution of aerobic metabolic processes such as respiratory and photosynthesis unavoidably led to the production of ROS in mitochondria, chloroplast, peroxisomes by cell wall NADPH oxidases, peroxidases (Apel and Hirt 2004; Mittler et al. 2004). Under normal conditions, ROS such as superoxide ($O_2^{\bullet -}$), hydrogen peroxide ($H_2O_2$), hydroxyl radicles ($OH^{\bullet -}$) and singlet oxygen ($O^{-}$) act as important secondary messengers at the core of signaling pathways in plants thus maintaining normal metabolic fluxes and other cellular functions. The level of ROS determines whether it will be defensive or destructive molecule and its level is maintained through coordination between ROS production and turnover (Miller et al. 2010; Mittler et al. 2004). Function of ROS is also governed by its site of production, site of action and duration of action. Increase in ROS turnover under abiotic stress leads to certain detrimental modifications to lipids, carbohydrates, proteins and also to DNA thus becoming lethal to the plant cell (Apel and Hirt 2004). In such scenario, plant activates a genetically controlled process, called programmed cell death to specifically eliminate damaged tissues. In this process, plants produce excess of ROS which help in destroying damaged tissue. The plant cell and its

organelles – peroxisomes, chloroplasts, and mitochondria contain multiple enzymes or enzyme systems to operate signal transduction pathways for removing ROS by utilizing the reducing power derived from NADPH or ferridoxin thereby protecting the plant from adverse effects of ROS (Bowler and Fluhr 2000; Mittler et al. 2004). Osmolytes such as glycine betaine, mannitol, trehalose and proline accumulate in plants during various abiotic stresses such as drought, salinity and metal stress and they help in maintaining the integrity of membrane by osmotic adjustments thus maintaining the turgor pressure of the cell (Ashraf and Foolad 2207). The other metabolites such as glutathione, polyamines and α-tocopherol are also known to accumulate during various environmental stresses (Reddy et al. 2004).

ROS generated during these stress conditions, eventually cause lipid peroxidation, protein and nucleic acid oxidation leading to the formation of toxic reactive carbonyls including acrolein, malondialdehyde (MDA), 4-hydroxy-2-nonenal (HNE) and MG (Mano, 2012; Martins et al., 2001; Mittler et al., 2004; Oberschall et al., 2000; Saito et al., 2013; Simpson et al., 2009; Yamauchi et al., 2011). Among reactive carbonyls, methylglyoxal (MG) is highly cytotoxic and usually escalates during various stress conditions. MG is produced endogenously in plant cell as a result of both enzymatic and non-enzymatic reactions (Kaur et al. 2014). The key enzymes that catalyze the formation of MG include methylglyoxal synthase that participates in glycolytic bypass, cytochrome P450 of acetone metabolism and amine oxidase which involved in amino acid breakdown. MG is also formed spontaneously under physiological conditions, by non-enzymatic mechanisms from glycolysis and photosynthetic intermediates, glyceraldehyde-3-phosphate (GAP) and dihydroxyacetone phosphates (DHAP) (Mano 2012; Rabbani and Thornalley 2012; Sato-Masumoto and Ito 2014; Sengupta et al. 2015). The cellular turnover of MG depends on two metabolic systems which include glutathione dependent glyoxalase pathway and glutathione independent pathways involving enzymes such as oxido-reductases and dehydrogenases (Mudalkar et al. 2016).

## 3. Molecular responses

At molecular level, plants respond to abiotic stresses by differentially regulating the expression of various genes belonging to different metabolic pathways including late

embryogenesis protein (LEA), dehydrins, heat shock proteins, proteins involved in ion homeostasis and various transcription factors (TF's). Further, plant adaptive signaling mechanisms under abiotic stress conditions can be categorized conceptually into three groups:

a) Signaling related to ion or osmotic homeostasis
b) Detoxification signaling to control and repair stress damages
c) Signaling related to coordination of cell division and expansion which regulate growth.

The three signalling events are interdependent and coordinate with each other. For instance, homeostasis signalling negatively regulates components of detoxification signalling and the effective functioning of the former two, leads to relieving of growth inhibition. Plants show large variations in their response to unfavourable environmental conditions that include the activation of specific transcription factors (TFs). Many TFs which are part of various signalling pathways have been reported to regulate the response of the plant to abiotic stresses (Kim et al. 2008; Sokol et al. 2007; Stockinger et al. 2001; Sunkar et al. 2007). The key signalling pathways that operate during drought, salt and metal stresses include, (i) SOS regulatory pathway for ion homeostasis where a calcium – responsive SOS3-SOS2 protein kinase complex controls the expression and activity of ion transporters such as SOS1. (ii) Protein kinase pathways including mitogen-activated kinases, which may mediate osmotic homeostasis and/or detoxification responses. (iii) Phospholipid signalling activated by osmotic stress which function upstream of the osmotic stress – activated protein kinases. (iv) ABA mediated osmotic stress signalling which modify expression of transcription factors thereby activating the downstream stress tolerance effector genes (Agrawal et al. 2015; Choudhary et al. 2003; Cushman and Bohnert 2000; Mahajan and Tuteja 2005).

Among the tolerance mechanisms mediated by osmotic stress signalling, protein kinase (MAP kinases) and phospholipids ($IP_3$, DAG, PA etc.) are also playing a significant role in various plant species. Abscicic acid (ABA) which has a broad functions in plant growth and development, also participate in plant water balance and osmotic stress tolerance. Recent reports had evidenced the increased accumulation and decreased degradation of ABA in *Arabidopsis*, tobacco, tomato and maize during osmotic stress. The role of ABA in drought and salt stress is at least two fold: water

balance by guard cell regulation and cellular dehydration tolerance by inducing genes that encode dehydration tolerance proteins. In addition, ABA is required for freezing tolerance, which also involves in the induction of dehydration tolerance genes.

As for metal stress is concerned, plants have evolved certain mechanisms that respond to the uptake and accumulation of heavy metals. These mechanisms include the chelation and sequestration of heavy metals by particular ligands like phytochelatins (PCs) and metallothioneins (MTs) (Freisinger 2008; 2009). Till now, many tree and crop species have been identified as potential heavy metal sequesters thereby attributing phytoremediation properties (Chang et al. 2004; Cozza et al. 2013; Du et al. 2012; Gong et al. 2003; Liu et al. 2014). An outline of physiological, biochemical and molecular responses of plants in response to abiotic stresses are represented in Fig. 1.

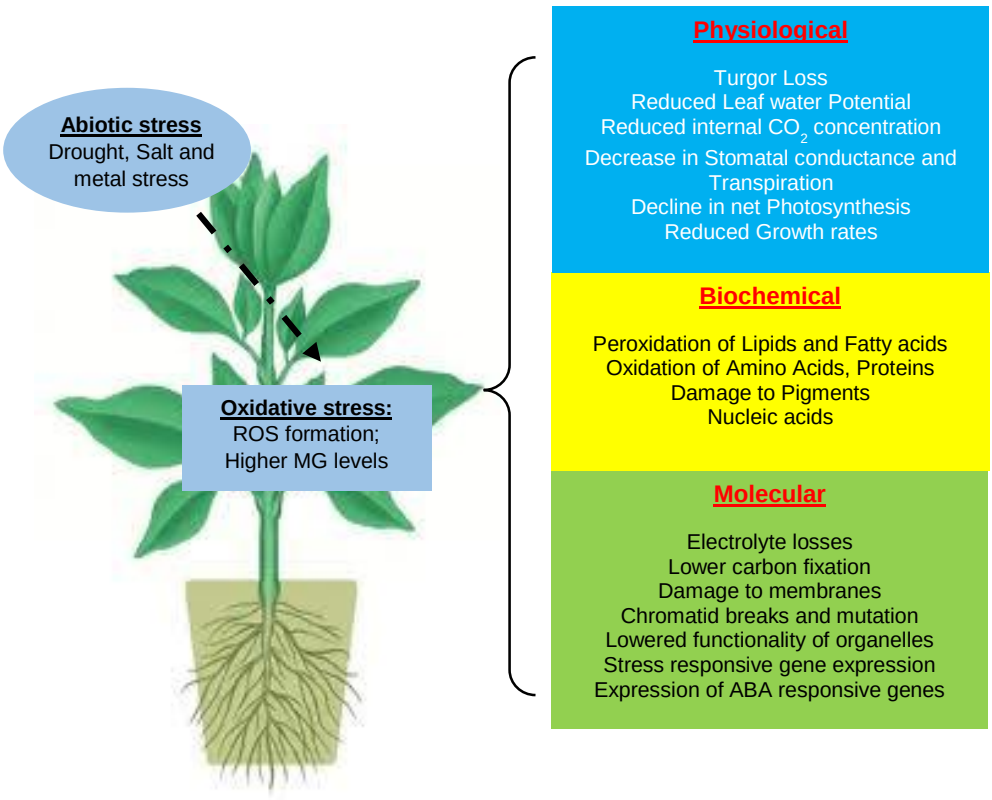


**Fig. 1.** Schematic representation of abiotic stress responses in plants. Severe abiotic stress leads to oxidative damage which eventually effects cellular, molecular and physiological components plant metabolism.

## Stress combating strategies in plants

Plants have evolved complex mechanisms to survive under challenging conditions. Tolerance, avoidance, and resistance are three major strategies followed by plants to counter the recurring biotic and abiotic stresses. These mechanisms involve genes associated with several interconnected pathways which lead them towards better stress tolerance (Mahajan and Tuteja 2005). Also, severe and prolonged stress can lead to genome alterations which may sometimes contribute towards better adaptation. The basic information guiding the behaviour of plant lies in the DNA sequence and alterations in DNA sequence by mutation or genetic recombination leading to new alleles which may confer enhanced stress tolerance to the plant. However, the rate of formation of new gene combinations is too slow in comparison to the occurrence of different stresses in the environment. Therefore, the survival of plant in these conditions depends largely on the regulation of various stress responsive genes through epigenetic mechanisms (Chen et al. 2010; Chinnusamy and Zhu 2009; Peng and Zhang 2009; Tariq and Paszkowski 2004). In plants, a complex signalling network operates to transduce any external stimuli to inside of the cell for an appropriate cellular arrangement giving rise to a particular response. The response is such that it helps the plant to cope up with environmental stresses that it experiences throughout its life. To exhibit a particular response, it is important for the plant to perceive the stimulus and transmit it into the nucleus of the plant cell. The perception is specifically done by cell wall receptors which then by several mechanisms activate internal signalling components. Further, long distance signalling within a plant is important for plant adaptation, wherein, guard cell signalling is a critical component because it is a key determinant of plant water budget.

Depending on the type and intensity of stress, plants adopt a wide range of strategies to cope up with adverse conditions. The plant defence system employs different strategies to detoxify cytotoxic ROS, reactive carbonyls and to maintain ion homeostasis. The major stress combating mechanisms briefly are of the following types.

## 1. Antioxidant systems

To mitigate oxidative damage from ROS, plants possess a complex antioxidative system that involves both non-enzymatic and enzymatic antioxidant defences. Non-enzymatic defences include hydrophilic compounds, such as ascorbate and reduced glutathione, which are capable of quenching ROS. Enzymatic defences including an array of superoxide dismutase, peroxidases and catalases are needed for the regeneration of the active forms of antioxidants. Peroxidases constitute a class of enzymes that catalyse the oxidoreduction between hydrogen peroxide and various reductants. There are three classes of plant peroxidases, ascorbate peroxidase (APX), guaiacol-type peroxidase (POX) and glutathione peroxidase (GPX) which are considered to be the most important related to the antioxidative defence system.

Ascorbate peroxidase (EC 1.11.1.11) catalyses the reduction of $H_2O_2$ to $H_2O$ in the presence of two ascorbate (ASC) molecules and produce two monodehydroascorbate (MDHA) molecules. MDHA is a short-lived radical that can either spontaneously dismutase to ascorbate and dehydroascorbate (DHA) or be reduced to ascorbate by NAD(P)H via monodehydroascorbate reductase (MDHAR; EC 1.6.5.4), which is found in different cell compartments (Jaleel et al. 2009). DHA is reduced to ascorbate by the action of dehydroascorbate reductase (DHAR; EC 1.8.5.1), using reduced glutathione (GSH) as the reducing substrate. This reaction generates oxidised glutathione (GSSG), which in turn, re-reduced to GSH by glutathione reductase (GR; EC 1.6.4.2) using NADPH. The removal of $H_2O_2$ through this series of reactions is known as the ascorbate-glutathione cycle or the Halliwell-Asada pathway (Macháčková 1995). Ascorbate and glutathione are not consumed in this pathway, but participate in the cyclic transfer of reducing equivalents, which allows the reduction of $H_2O_2$ to $H_2O$, with NADPH as the reducing equivalent donor.

The different types of GPX (EC 1.11.1.9) form a large family of diverse isozymes that reduce $H_2O_2$ and organic and lipid hydroperoxides using GSH as a reducing agent. In plants, however, it has been suggested that GPX preferably uses thioredoxin as a reductant (Herbette et al. 2002; Jung et al. 2002). Selenocysteine

participates directly in electron donation to the peroxide substrate and becomes oxidised in the process. The enzyme then uses reduced glutathione as a hydrogen donor to regenerate selenocysteine. GPX uses two GSH molecules to reduce $H_2O_2$ to water and produce a GSSG molecule. Taken together, the major ROS-scavenging pathways in plants include SOD, found in almost all cell compartments, CAT in peroxisomes, POX in the cytosol, vacuole and cell wall and the ascorbate-glutathione cycle in the chloroplasts, cytosol, mitochondria, apoplast and peroxisomes. As mentioned above, CAT has extremely high maximal catalytic rates, but low substrate affinities, while APX has a much higher affinity for $H_2O_2$ than CAT. The high affinity of APX for $H_2O_2$, in conjunction with the finding of the ascorbate-glutathione cycle in nearly all cell compartments, suggests that this cycle plays a crucial role in controlling the level of ROS in these compartments. Moreover, APX might also be responsible for the fine modulation of $H_2O_2$ for signalling. In contrast, CAT, which is only present in peroxisomes, is indispensable to $H_2O_2$ detoxification during stress, when high levels of ROS are produced.

## 2. Salt Overly Sensitive (SOS) pathway

One of the well-established and possible pathways for salt signalling is $Ca^{2+}$ dependent salt overly sensitive (SOS) pathway that emerged recently as a result of genetic, molecular, and biochemical analysis. Salt stress induces a cytosolic calcium signal that is different from the calcium signal that triggered by drought, cold, or other stimuli. A myristoylated calcium- binding protein encoded by SOS3 presumably senses the salt-elicited calcium signal and translates it to downstream responses (Angelopoulos et al. 1996; Tsimilli-Michael and Strasser 2008). SOS3 together with SOS2, a serine/threonine protein kinase regulate the expression and activity of SOS1, a $Na^+/H^+$ antiporter (Boo and Jung 1999). A yeast mutant strain lacking all endogenous Na+-ATPases and $Na^+/H^+$ antiporters showed slightly increased salt tolerance upon expression of SOS1, while, co-expression of SOS3 and SOS2, together with SOS1, dramatically enhanced the salt tolerance.

## 3. Glyoxalases and aldehyde reductases

The glyoxalases which have been reported in various plant species are believed to be key players in the plant stress response, and their overexpression confers significant tolerance to multiple stresses such as salinity and heavy metal stress. The glyoxalase pathway in plants operates in both cytosol and mitochondria. There are two important classes of glyoxalases Gly I and Gly II where the former operates in cytosol since their substrate MG is produced majorly as a by-product of the cytosol-based glycolytic pathway, while the latter are present in both cytosol and mitochondria. In addition to MG detoxification, glyoxalases also play a crucial role in cell division and microtubule assembly and act as mainstream players in glycolysis.

The aldo-keto reductases (AKRs) encompass a large superfamily of NAD(P)(H)-dependent oxido-reductases which are found across the biological kingdoms including prokaryotes as well as yeast, plants, amphibian and mammals. They are characterized by the presence of $(\alpha/\beta)_8$ – barrel motif and contain approximately 320 amino acids per monomer. They catalyze the oxidation of hydroxysteroids and trans-dihydrodiols of polycyclic aromatic hydrocarbons. The AKR superfamily contain nearly 14 families (AKR1 – AKR14) where aldehyde reductases, hydroxysteroid dehyderogenases and steroid 5β-reductases represent majorly. They were reported to play a crucial role in abiotic stress tolerance mechanisms by detoxifying MG which is a potent electrophile.

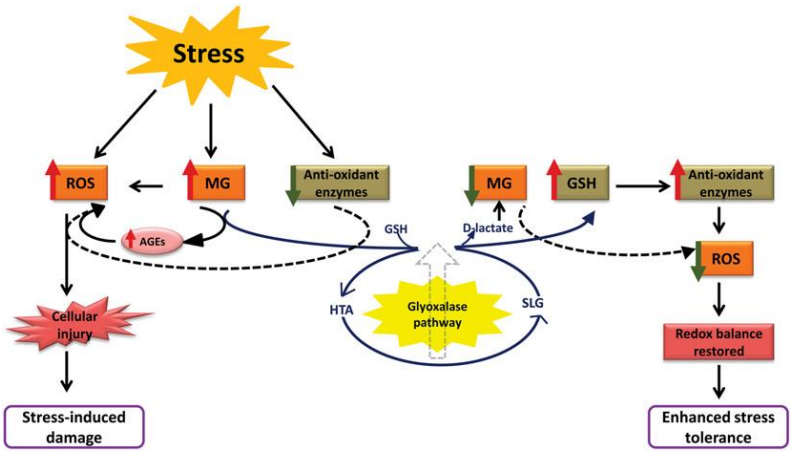


**Fig. 2.** Overview of ROS and MG generation and Glyoxalases pathway in plants.

## Experimental model - *Jatropha curcas* L.

*Jatropha curcas* (L.), commonly known as physic nut is a shrub belonging to Euphorbiaceae family and produce non-edible oil with minimum agricultural inputs. It is known for its high seed oil content, easy propagation, rapid growth and adaptation to a wide range of agro-climatic conditions. The phytoremediation capacity of J. curcas makes it suitable to grow in non-arable and metal contaminated soils. The oil quantity of Jatropha seeds ranged from 35 – 50% and can be used as a potential feedstock for biofuel production and also in making of soaps and bio pesticides. The fatty acid composition of Jatropha is predominately composed of oleic acid (56%) followed by linoleic acid and linolenic acid. Trans-esterification of Jatropha seed oil containing majority of unsaturated fatty acids produce ideal biodiesel. The seed cake is used as organic fertilizer, combustible fuel and for the production of biogas. *Jatropha* is also known for its tolerance to different abiotic stresses (Eswaran et al. 2010; Gao et al. 2008; Yadav et al. 2009). Of late *Jatropha* has been proposed as a potential crop for phytoremediation of heavy metals such as nickel, copper, arsenic, chromium, zinc, lead, cadmium and coal fly ash (Mangkoedihardjo 2008; Yan et al. 2008) and also for the soils contaminated with lubricating oils (Agamuthu et al. 2010). The current status of scientific research done on Jatropha was summarised in Table 1.

Picture has taken from public source for fair use

**Fig. 3.** Experimental model plant Jatropha grown in the field of Tree oils India limited. Representation of Jatropha flower, inflorescence and seeds.

**Table 1.** Brief review of literature on characterization of Jatropha genes under different environmental conditions.

| S.No | Protein | Type of study | Observation | References |
|---|---|---|---|---|
| **1.** | Cu/Zn superoxide dismutase | Overexpression of JcCu/ Zn-SOD in *Arabidopsis* | Salt tolerance | Liu Z.B. et al., 2015 |
| **2.** | AP2/ ERF - type transcription factor | Overexpression of *JcERF2* in Tobacco and *Arabidopsis* | Drought and salt; salt and freezing tolerance | Wang X.et al., 2015; Tang M. et al., 2007 and 2011 |
| **3.** | Betaine aldehyde dehydrogenase | Overexpression of *JcBD1* in *E.coli* | Salt tolerance | Zhang F. et al., 2008 |
| **4.** | Ascorbate peroxidase | Overexpression in Tobacco; Overexpression of *JctAPX* in *Arabidopsis* | Salt tolerance | Liu Z. et.al., 2014; Chen Y. et al., 2015 |
| **5.** | NAC transcription factor | Overexpression of *JcNAC1* in *J. curcas*, Differential gene expression | Abiotic stress (Salinity) and pathogen infection | Qin X. et al., 2014; Wu Z.et al., 2015; |
| **6.** | D-myo-inositol-3-phosphate synthase (MIPS) | Differential Display technology (DDRT) targeted gene is *JcMIPS* | ABA, drought, and NaCl | Wang Y. et al., 2011 |
| **7.** | Plant dehydrin proteins | EST of developing seed emphasis on *JcDHN1 and JcDHN2* | Natural dehydration process during seed development | Omar S. A. et al., 2013 |
| **8.** | Plant small heat shock proteins | Jatropha embryo cDNA libraries emphasis on *JcHSP-1 and JcHSP-2* | Natural dehydration process during seed development | Omar S. A. et al., 2011 |

| S.No | Protein | Type of study | Observation | References |
|---|---|---|---|---|
| **9.** | ADP-ribosylation factors (ARF) | Overexpression of *Jcarf1* in *E. coli* | Environmental stresses | Qin X. et al et al., 2011 |
| **10.** | Allene oxide cyclase | Overexpression of *JcAOC* in *E.coli* | Salt and low temperature | Liu B. et al., 2010 |
| **11.** | Dehydrationresponsive element-binding protein | Overexpression of *JcDREB* in *Arabidopsis* | Salt and freezing tolerance | Tang M. et al., 2011 |
| **12.** | Cation/proton antiporter | Overexpression of *SbNHX1* in *Jatropha* | Salt tolerance | Jha B. et al., 2013 |
| **13.** | Aquaporins | Overexpression of *JcPIP2.7; JcTIP1,3* in *Arabidopsis* | Drought and salt tolerance | Khan K. et al., 2015 |
| **14.** | Aldo-Keto Reductase | Overexpression of *JcAKR* in *E.coli* and yeast | Drought and salt tolerance | Mudalkar S. et al., 2016 |
| **15.** | Metallothionein | Overexpression of *JcMT2a* in *E.coli* and yeast | Metal stress | Mudalkar S. et al., 2014 |
| **16.** | H+ -pyrophosphatase | *JcVP1 Escherichia coli* and *Saccharomyces cerevisiae* | salt tolerance | Yang Y. et al., 2016 |
| **17.** | MYB proteins | Overexpression of *JcMYB2* in *Arabidopsis* | salt and cold stres | Peng X. et al., 2016 |
| **18.** | Glycine sarcosine methyltransferase and sarcosine dimethylglycine methyltransferase | Overexpression of Synechococcus GSMT and DMT in *Jatropha* | Drought tolerance | Tsuchimoto S et al., 2012 |

Due to the commercial importance of Jatropha in biofuel industry and its innate tolerant property to abiotic stresses, it is of prime significance to study the mechanisms involved in stress tolerance and to characterize the genes involved in those mechanisms. Though, substantial research has been done in the areas of abiotic and metal stresses in Jatropha, the key molecular mechanisms and genes related to drought, salt and metal stress especially the glyoxalases and reductases are far from being characterized.

## OBJECTIVES

Based on the above background on abiotic stress responses in higher plants and importance of Jatropha as biofuel feedstock, following four objective were framed for the present work:

1. **Growth and photosynthetic responses of *Jatropha curcas* L. during drought and salinity stress conditions.**
2. **Detoxification potential and expression analysis of aldo-keto reductase (*JcAKR*) from *J. curcas.***
3. **Characterization of glyoxalase genes (*JcGly1* and *JcGly2*) from *J. curcas* and elucidation of their role in glyoxalase - glutathione cycle.**
4. **Molecular cloning and characterization of type 2 metallothionein gene (*JcMT2*) from *J. curcas* to understand its role in metal stress tolerance**

## Experimental layout

The seeds of *J. curcas* were obtained from Directorate of Oilseed Research (DOR, Rajendranagar, Hyderabad, India). They were surface sterilized with 0.4% sodium hypochlorite for 5 minutes and were washed thoroughly with sterile water. Sterilized seeds were germinated in petri plates containing sterile wet blotting paper. After germination, the seedlings were transferred to pots containing red soil and sand (1:1). Plants were grown in a glasshouse under controlled conditions at 28±2ºC and ~70% humidity for one month. For the experiments on stress treatment, one month old plants were divided into four groups, group 1-control, group 2 - NaCl treated (200mM), group 3- drought stress (complete water withdrawal), group 4 - drought salt (200mM salt water treatment followed by complete water withdrawal) for 21 days (Fig. 5 ). Following the treatment, roots and leaves of the treated as well as the control plants were collected at 7, 15 and 21 days after stress and were frozen in liquid nitrogen and stored at -80$^0$C. All physiological and biochemical measurements were recorded at regular intervals throughout the experimental period. For heterologous expression studies, the key genes involved in MG detoxification including aldo-keto reductase (JcAKR), Glyoxalase I, II (JcGly I, II) and glutathione reductase (JcGR) as well as genes involved in metal detoxification were cloned and characterized in bacterial and yeast system. Detailed methodology for individual experiments was given at respective chapters.

**Fig. 4.** Growth of Jatropha plants in 20 L pots in green house conditions

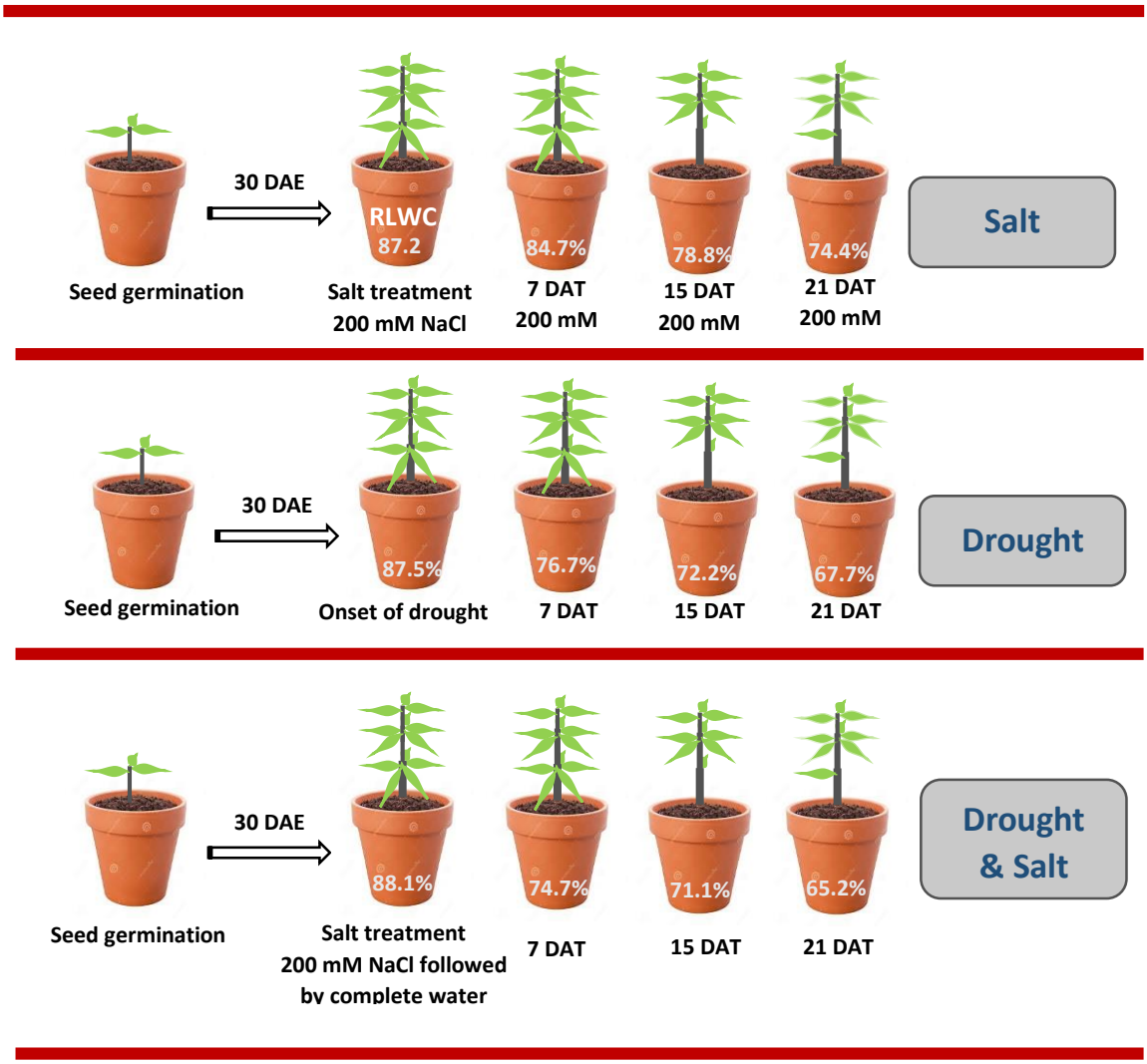


**Fig. 5.** Representation of experimental layout of Jatropha plants for drought, salt as well as combined drought and salt experiments. Pots were grown in glass house conditions throughout the experimental period. The relative leaf water content (RLWC) was mentioned on top of each pot.

# Chapter II

# Photosynthetic, growth and biochemical responses of Jatropha to salt and drought stress

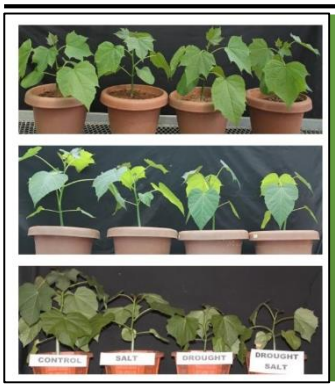


# Chapter - II

Dwindling fossil fuel resources intensified the pressure to replace traditional fuels with alternative sources based on bio-feedstock. But there is a competing interest over whether land is to be used for feed and food production or for biomass as a raw material for industrial purposes and energy. This unlikely situation arises due to the unavailability of major portion of world's land area for intense cropping systems because of unfavourable climatic and soil conditions. If the biofuel feedstock trees can be grown on soils unsuitable for arable crop production, most of the challenges related to feedstock production and environmental issues can be answered. Bringing the marshy or saline soils under cultivation would also enhance the agronomical productivity and accomplish demands of growing population. Further, characterizing the physiological and morphological responses of plant to various adverse conditions serves as a preliminary marker for identifying tolerant and susceptible species or varieties. Hence, it is necessary to identify potential tree species which can grow well under unfavourable soil and climatic conditions using photosynthetic physiology.

Abiotic stresses including salinity, drought are major factors responsible for loss of arable land and agriculture productivity worldwide. Primary and/or secondary salinization leads to the ionic toxicity of the soil with $Na^+$, $Cl^-$ and $Ca^+$ which results in low osmotic potential and eventually disrupts the nutrient uptake of the plant. Whereas, drought stress lowers the water potential of the plant thereby generating oxidative free radicals and reactive oxygen species. In most cases, they primarily effect the photosynthesis which is essential for growth and development of plants, by a series of

preceding events including loss of chlorophyll, inactivation of photochemical reaction centers and reducing PS II efficiency. Also, excess salt in the soil prevent plants from taking up water, exposing them to drought stress and resulting in stomata closure to conserve water. Closure of stomata eventually reduces the $CO_2$ availability at carboxylation site of Rubisco and reduces the photosynthetic rate which ultimately halt the growth of the plant. To cope up with salt and drought stresses plants have evolved through certain developmental, physiological and biochemical adaptations which nevertheless varies among the species and within the accessions of the same species.

*Jatropha curcas* belonging to the family Euphorbiaceae, produce non-edible oil with minimum agricultural inputs. The phytoremediation capacity of *J. curcas* makes it suitable to grow in non-arable and metal contaminated soils. The molecular responses of Jatropha to various abiotic stresses including drought, salt and metal stresses have been well characterized. However, the physiological and morphological responses of this potential biofuel plant to drought and salt stresses have not yet been reported. The objective of the present study is to elucidate the physiological, morphological and biochemical responses of Jatropha to interactive treatments of salt and drought stress. Our results on progressive stress treatments provide a comprehensive evidence for the stress tolerance levels as well as biochemical markers for stress intensity in Jatropha.

## Materials and methods

### *Photosynthesis and Chlorophyll a fluorescence measurements*

Leaf gas exchange parameters were measured on fully expanded upper canopy leaves, between 0900 h – 1000 h using a portable infrared $CO_2/H_2O$ gas analyzer (IRGA) (LC Pro+, ADC Bioscientific Ltd., U.K.). A saturating photosynthetically active radiation (PAR) of 1600 µmol $m^{-2}$ $s^{-1}$ was supplied by a LED light source (LC pro Lamp 32070 – Broad, ADC Bioscientific Ltd. UK) attached to leaf chamber. Relative humidity was set to 55-60%. Net photosynthetic rate (*A*), stomatal conductance ($g_s$), transpiration rate (E) and intercellular $CO_2$ concentration ($C_i$) were measured in control and stressed plants. Leaf level water use efficiency ($WUE_i$) was calculated from gas exchange data by dividing photosynthetic rate (*A*) with transpiration rate (E). Response of *A* to

photosynthetic photon flux density (PPFD) was measured by using light response curves (*A*/Q curves), measured at increasing PPFD from 0 to 1600 µmol $m^{-2}$ $s^{-1}$. The apparent quantum efficiency of $CO_2$ fixation (AQE) was calculated as the slope of the linear portion of the response curves. Light - saturated photosynthetic rate ($A_{Sat}$) was calculated from the asymptote of fitted response function. Chlorophyll *a* (Chl *a*) fluorescence parameters were determined on the same leaves used for the gas exchange measurements using MINI-PAM (Heinz Walz GmbH, Effeltrich, Germany) on the adaxial side of the leaves. From these measurements we calculated maximal photochemical efficiency of photosystem-II [$(F_m-F_o)/F_m = F_v/F_m$] on leaves which were pre dark adapted for 30 minutes, effective quantum yield of the Photosystem-II [$(F_m'-F_o')/F_m' = F_v'/F_m'$] under natural light conditions and non-photochemical quenching [$NPQ = (F_m–F_m')/ F_m'$] according to Rascher *et al.* (2000). The high light flash used to measure saturated fluorescence had a PPFD of 4000 µmol $m^{-2}s^{-1}$ and duration of 0.8s.

### *Growth and destructive biomass measurements*

Leaf area was measured using a portable laser leaf area meter (CI-202) (CID Biosciences, Inc.) equipped with a laser scanner with built - in control unit. Growth parameters like plant height, stem girth, number of branches, number of nodes and internodes were calculated periodically in control and treated plants. Total aboveground and belowground fresh biomass of Jatropha plants grown under drought and salinity were recorded for three experimental seasons. Samplings were dried at 70$^oC$ for four days and dry biomass was calculated.

### *Quantification of ROS*

ROS were determined spectrofluorometrically using the specific reaction of ROS with the dye 2, 4 - dichlorofluorescein diacetate (DCF-DA) to give fluorescing DCF. Two grams of fresh leaves were incubated in 100 ml of 5 µM of DCF-DA. The tissues were rinsed once in 50 mM potassium phosphate buffer (pH 7.0) and once in DDW and were blotted dry. They were then homogenized in liquid nitrogen. 1 ml of 40 mM Tris - HCl buffer (pH 7.0) was added and the sample was mixed and centrifuged at 10000 rpm for 10 min. Fluorescence was determined using an LS-5 spectrofluorometer at an excitation

wavelength of 488 nm and an emission wavelength of 522 nm. A standard graph with concentrations of DCF ranging from 10 to 1000 nmol was used for determining concentration of unknowns.

### *Lipid peroxidation*

Lipid peroxidation in leaves was measured using the thiobarbituricacid (TBA) test, which determines MDA as an end product of lipid peroxidation (Hodges et al., 1999). Briefly, leaf material (500 mg) was homogenized in 5ml 0.1% (w/v) TCA solution and centrifuged at 10000 g for 20 min. 0.5 ml of supernatant was added to 1 ml of reaction mixture containing 0.5% (w/v) TBA in 20% TCA. The mixture was incubated in boiling water for 30 min, and the reaction was stopped by placing the reaction tubes on ice bath. Then the samples were centrifuged at 10,000 g for 5 min, and the absorbance of supernatant was read at 532 nm. The amount of MDA-TBA complex (red pigment) was calculated from extinction coefficient of MDA (155 $mM^{-1}$ $cm^{-1}$.)

### *Quantification of ascorbate and glutathione*

Leaf tissue (500 mg) was ground in liquid nitrogen and homogenized with 5ml of 2.5M of perchloric acid and centrifuged at 7400g for 15 min. 100µl of clear homogenate was added with 1ml of reaction mixture containing 2 % (w/v) TCA, 8.8% ortho-phosphoric acid, 0.01% α-dipyridyl, 10mM ferric chloride and incubated for 1 hour at 40ºC. The colour developed was estimated spectro-photometrically at 525 nm for ASC. 100µl of clear homogenate previously incubated with 5µl of 100mM DTT for 1 hour at room temperature. DTT was subsequently inactivated by addition of 5µl of 5% (w/v) N-ethylmalamide and calibrated by 10 to 300 nmol of ASC in reaction mix.

GSSG and GSH levels were determined by Contreras et al (2005). 0.5g leaf tissue was extracted with 5% w/v sulfosalicylic acid and total glutathione (GSH+GSSG) was detected by incubating with reaction mixture containing 60µM 5,5-dithio-bis-(2-nitrobenzoic acid),and 0.66U of GR and NADPH. The colour developed was estimated at 412 nm by using spectrophotometer.100µl of neutralized homogenate was incubated with 20µl of 1M 2-Vynil pyridine for 1hour at room temperature. Then reaction mixture

was added and calibration curve was prepared using 2 to 40 nmol of GSH in the same reaction mixture.

### *Methylglyoxal content*

The assay was performed according to (Mustafiz et al. 2010). 250 mg of plant tissue was ground in liquid nitrogen and 2.5 mL 0.5 M perchloric acid was added and homogenised. It was incubated on ice for 15 min. The extract was centrifuged for 10 min at 11000×*g* at 4°C. The supernatant was transferred to a fresh tube and charcoal (10 mg/mL) was added. This mixture was kept at room temperature for 15 min and was centrifuged at 11,000×*g* for 10 min. The clear supernatant was taken in fresh micro centrifuge tube and the solution was neutralized with saturated potassium carbonate and the pH of the supernatant was checked using a pH paper. The extract was kept at room temperature for 15 min and centrifuge at 11000×*g* for 10 min. The supernatant was taken for MG estimation. The amount of MG in the sample was measured by taking standard curve of MG at different concentrations (10-100µM), using 7.2 mM 1,2-diaminobenzene and 5M perchloric acid. The absorbance was taken at 336 nm using spectrophotometer (Eppendorf, Germany).

### *Statistical analysis*

Samples from three biological replicates were collected at regular intervals and mean values were represented together with standard deviation (SD), for *in vitro* experiments. Analysis of variance (ANOVA) was used for further data analysis and the comparisons were tested with Holm-Sidak method, the level of significance was set to 0.05. Statistical significance of the differences within a treatment at different time periods was indicated with capital letters and between the treatments was represented with small letters. Microsoft excel 2010 was used for data processing. Statistical analysis was performed using software, Sigma plot 11.0.

## Results and Discussion

The present study has been primarily focussed on the photosynthetic and growth responses of a potential biofuel tree Jatropha to adverse climatic conditions including drought, salt stresses. The stress tolerance capacity of Jatropha was assessed by subjecting it to progressive stress conditions using some key biochemical parameters. Our results provide a comprehensive understanding of Jatropha stress tolerance ability in terms of physiology and biochemistry.

### *Photosynthetic gas exchange measurements*

The leaf gas exchange measurements were recorded at regular intervals during 7 DAS, 15 DAS and 21 DAS and found that the results varied with type and intensity of stress treatment. The photosynthetic rates ($P_n$) in control plants were maintained constantly at 11±1 throughout the experimental period. Salt stress reduced the $P_n$ rates significantly where there was a reduction of 85% at 21 DAS (Fig. 6). Whereas, drought stress showed much significant impact on Pn rates wherein, there was a significant decrease of 83% by the end of 15 DAS and by 92% at the end of 21 DAS (Fig. 6). Our results also showed that the combined treatment of drought and salt stress imply much significant impact on Pn rates of Jatropha. Further, we measured Pn rates at increasing light intensities (A/Q curves) to deduce photorespiration rates (Fig. 7). The A/Q curve analysis showed that the apparent quantum efficiency (AQE) was reduced significantly after 7 DAS though the decrease was less in salt treated plants when compared to drought and combined stress treatments. Photosynthesis is the prime factor influenced by any form of abiotic stress to conserve reducing equivalents and energy. However, the decrease in $P_n$ rates depends on the level of tolerance of a plant to particular abiotic stress. Osmotic or ionic stress affect the $P_n$ in a complex manner where either it lowers the carboxylation capacity of Rubisco or decrease the regeneration capacity of RuBP by lowering the metabolism of ATP under the conditions of mild and severe stresses respectively. Jatropha plants responded differently to drought and salt stresses during progressive stress treatments, where drought stress caused significant decline in gas exchange physiology by the end of 15 days. Stomatal conductance ($g_s$) and transpiration rates (E) were also decreased significantly as the stress progressed and drought stress

had higher impact when compared to alone salt stress. Also, the combined stress treatments caused much higher damage to photosynthetic physiology of Jatropha than the individual stress treatments. Leaf level water use efficiency which is a function of Pn and E, showed little variation among the stress treatments. During 7 DAS there was a slight increase in the $WUE_i$ in all the three treatments while at 21 DAS there was a significant decrease of $WUE_i$ from 2.51 to 1.25 mmol $CO_2$/mol $H_2O$ (drought + salt stress) which indicated that the prolonged stress periods are lethal to Jatropha (Fig. 6).

### *Chlorophyll a fluorescence kinetics*

Chlorophyll *a* fluorescence measurements including photochemical yield ($\Delta F/F_m$), $F_V/F_m$ and non-photochemical quenching (NPQ) were measured on upper canopy leaves using MINI-PAM to understand PSII efficiency. Photochemical yield ($\Delta F/F_m$) was not altered at 7 DAS, while it was reduced from 0.78 to 0.71, 0.67 at 15 DAS and to 0.62, 0.58 at 21 DAS in salt and drought treated plants respectively (Fig. 8). $F_V/F_m$ values showed no significant differences during moderate stress but showed slight decrease during severe stress. Further, we measured dynamic changes of fluorescence parameters to increasing light intensities (PPFD) using MINI-PAM to understand the photosynthetic efficiency of Jatropha under different stress treatments. The electron transport rates (ETRs) showed an exponential increase against light intensities and reached a maximum ($ETR_{max}$) of 113.29 in control plants which decreased by 36%, 30% and 40% during 7 DAS and by 69%, 68% and 79% during 21 DAS in salt, drought and salt + drought treated plants (Fig. 9). The other parameters like yield and photochemical quenching showed a downtrend towards the increasing levels of PPFD which is more significant in stress treated plants (Fig. 10). Non photochemical quenching (NPQ) which is positively correlated with PPFD showed no significant difference between control and stress treated plants at 7 DAS but significantly increased during 15 and 21 DAS particularly in combined stress conditions (Fig. 10).

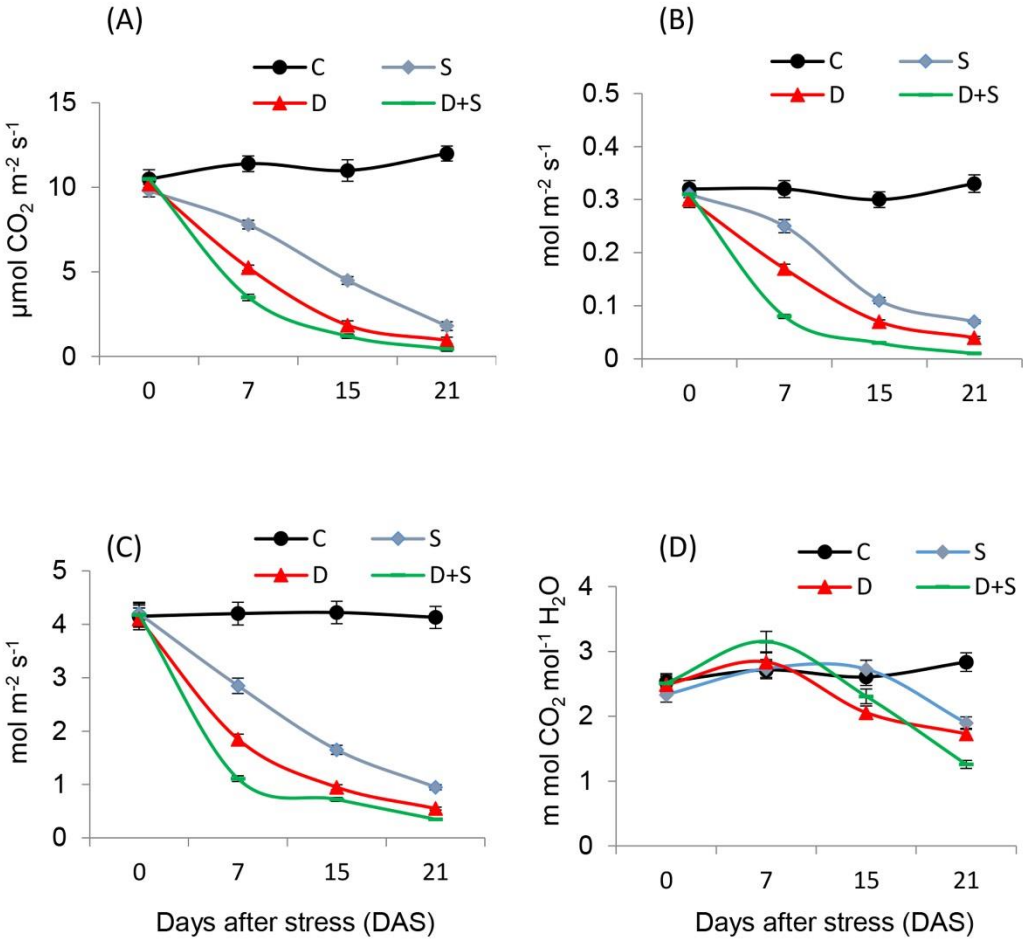


**Fig. 6.** Photosynthetic gas exchange parameters of Jatropha plants grown under drought, salt and combined stress treatments. (A) photosynthetic rate (B) stomatal conductance (C) transpiration rate (D) instant water use efficiency at 0, 7, 15 and 21 days after stress

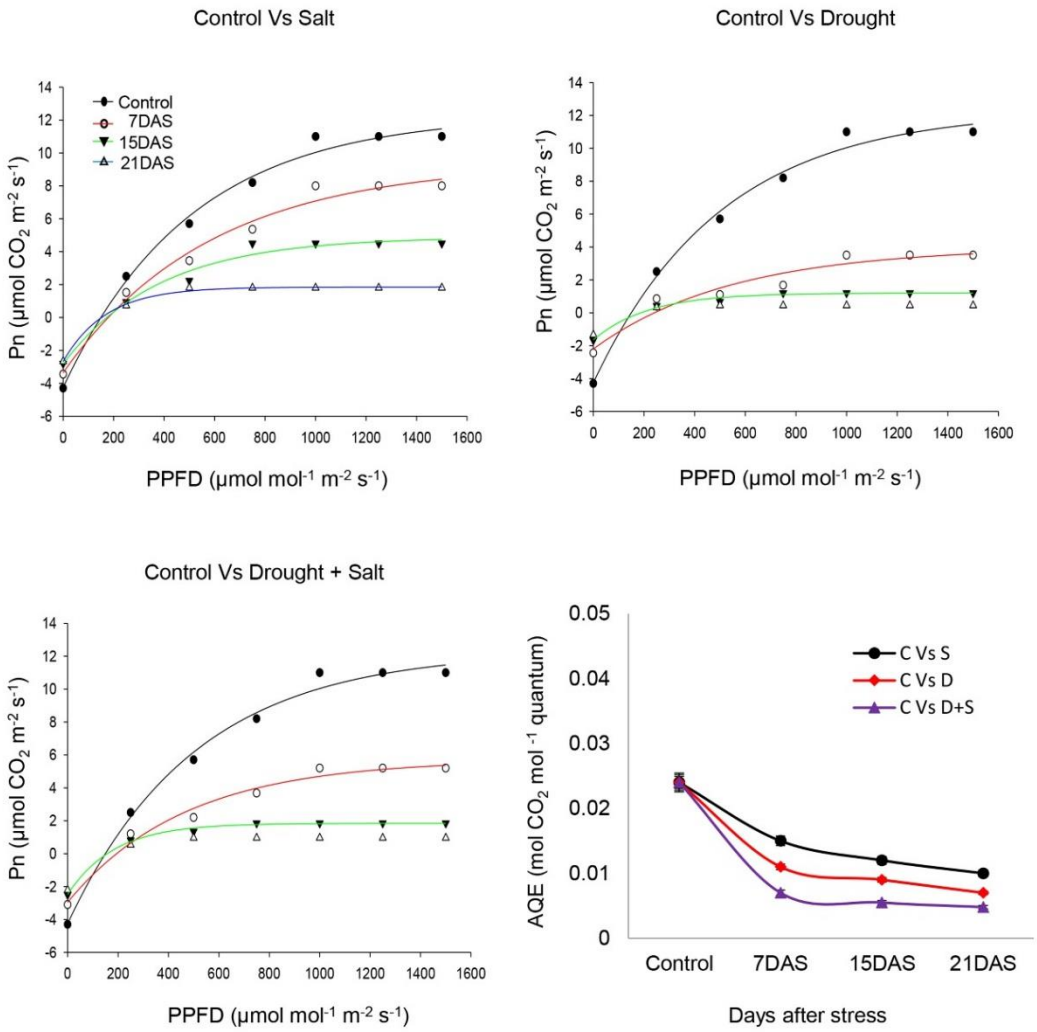


**Fig. 7.** Response of photosynthesis to photosynthetic photon flux density (PPFD) (A/Q curves) in Jatropha plants grown under drought, salt and combined stress conditions. Also shown the apparent quantum use efficiency (AQE) under different stress treatments.

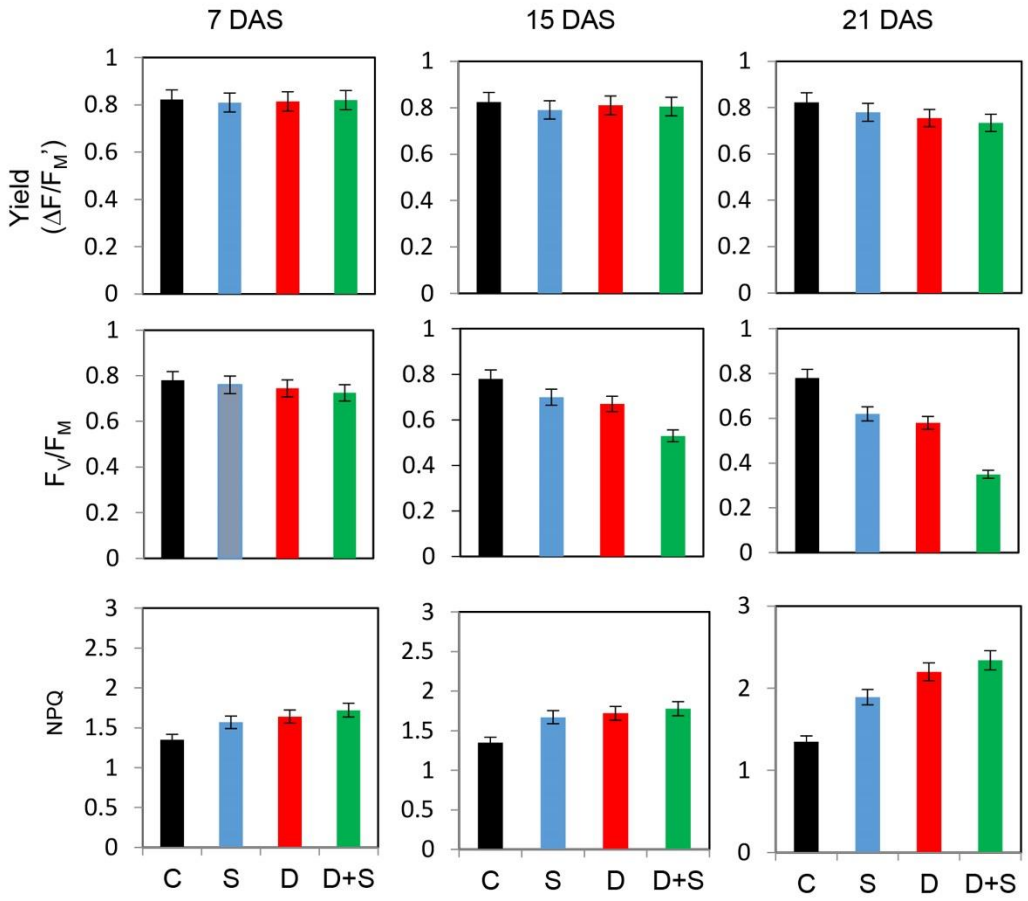


**Fig. 8.** Chlorophyll *a* fluorescence parameters deduced from MINI-PAM in Jatropha plants grown under drought, salt and combined stress conditions at 7, 15 and 21 DAS.

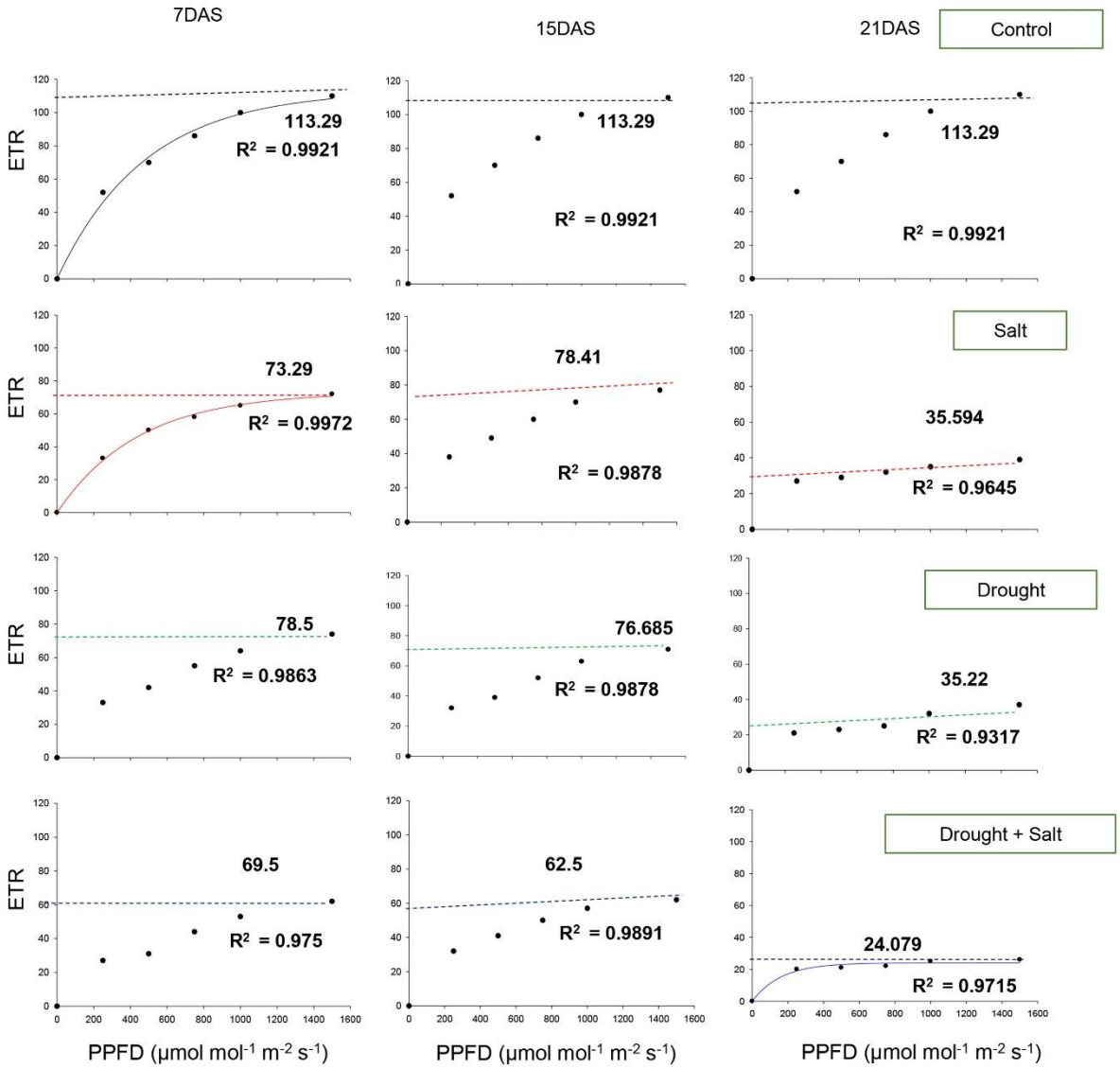


**Fig. 9.** Response of electron transport rate (ETR) to photosynthetic photon flux density (PPFD) in Jatropha plants grown under drought, salt and combined stress conditions at 7, 15 and 21 DAS. The analysis was performed using mini – PAM.

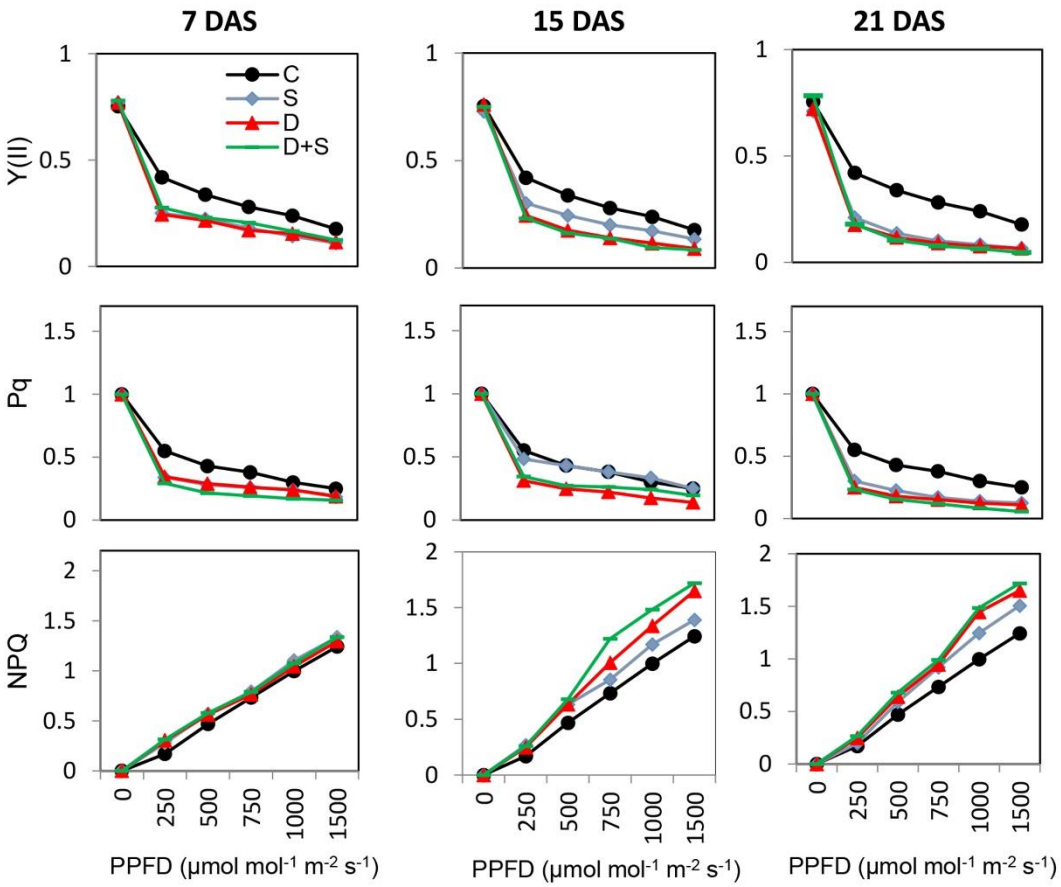


**Fig. 10.** Response of chlorophyll a fluorescence parameters to photosynthetic photon flux density (PPFD) in Jatropha plants grown under drought, salt and combined stress conditions at 7, 15 and 21 DAS. The analysis was performed using MINI – PAM.

### *Growth, morphology and biomass*

We assessed growth of Jatropha under drought and slat stress in terms of plant height, number of nodes, specific leaf area (SLA), and number of branches (Fig. 11). Growth was significantly inhibited under drought stress, wherein control plants reached a height of 40 cm by the end of 21 DAS which was more by 38.5% and 42% in salt and drought treated plants respectively. Significant difference was also observed in case of number of nodes and branches where, the control plants showed 46 and 53% increase over salt and drought treated plants respectively. The effect was more pronounced in combined stress treatment wherein the treated plants only reached a height of 22.6 cm and showed only 6 nodes per plant (Fig. 11). Interestingly, the growth rate was higher in later phases of stress treatments (14-21 DAS) compared to initial phases (0-15 DAS) indicating that Jatropha plants were slowly adjusted the internal metabolism and accustomed the growth to the environmental changes.

### *Quantification of ROS, lipid peroxidation and methylglyoxal*

Reactive oxygen species produced due to various abiotic stress conditions were measured in Jatropha at regular intervals of time. As the stress intensity progressed, the ROS levels also shoot up particularly in combined stress treatments. Salt and drought treated plants showed similar pattern of increase in ROS contents upon progression of stress intensity but combined stress treated plants showed ROS levels of 215 and 423 nmol/gFW at 7 DAS and 21 DAS which is more than 90% and 94% respectively than their respective control plants (Fig. 12).

Further, we quantified malanaldehyde (MDA), which is produced as a result of lipid peroxidation and an indicative of oxidative damage at regular intervals of stress treatments. Our results showed that at 7 DAS there was no significant lipid peroxidation but as the stress progressed, the MDA content increased to a maximum of 32 µmol/gFW indicating considerable lipid peroxidation. It was evident from our results that the salt stress caused more damage to the lipids by the end of 21 DAS (Fig. 12).

Methylglyoxal (MG) is produced form sugar and amino acid metabolism in bacteria, yeast, animals and plants. In our study, the levels of MG increased in *J. curcas* with increasing drought and salinity stress showing an increase of up to 80% in stressed plants compared to control plants (5 – 6 µM of MG), which gradually increased to a maximum of 35 µM at 21 DAS in all three stress conditions (drought, salt, drought + slat) (Fig. 12). Thus, MG can act as a signalling molecule and could be considered as a marker for determining the stress as well as the tolerance levels of Jatropha.

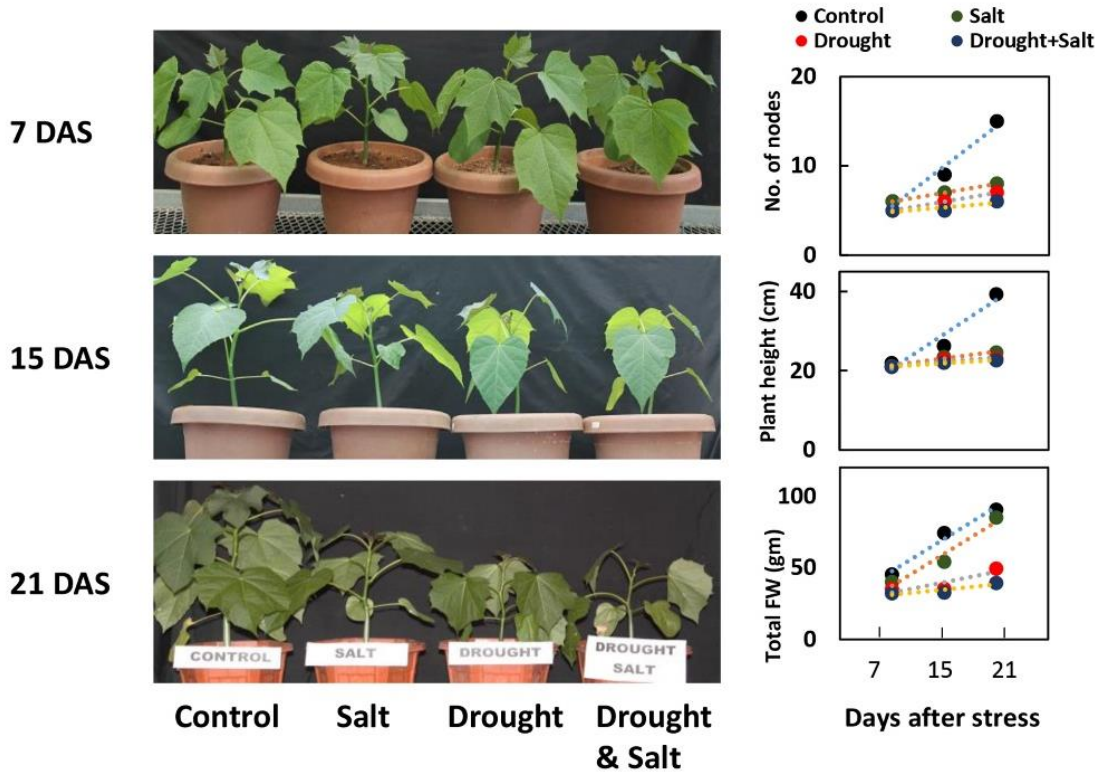


**Fig. 11.** Growth and morphology of Jatropha plants grown under drought, salt and combined stress treatments at 7, 15 and 21 DAS. Also represented the morphological parameters like number of nodes, plant height and total fresh weight of Jatropha during 7, 15 and 21 DAS under different stress conditions.

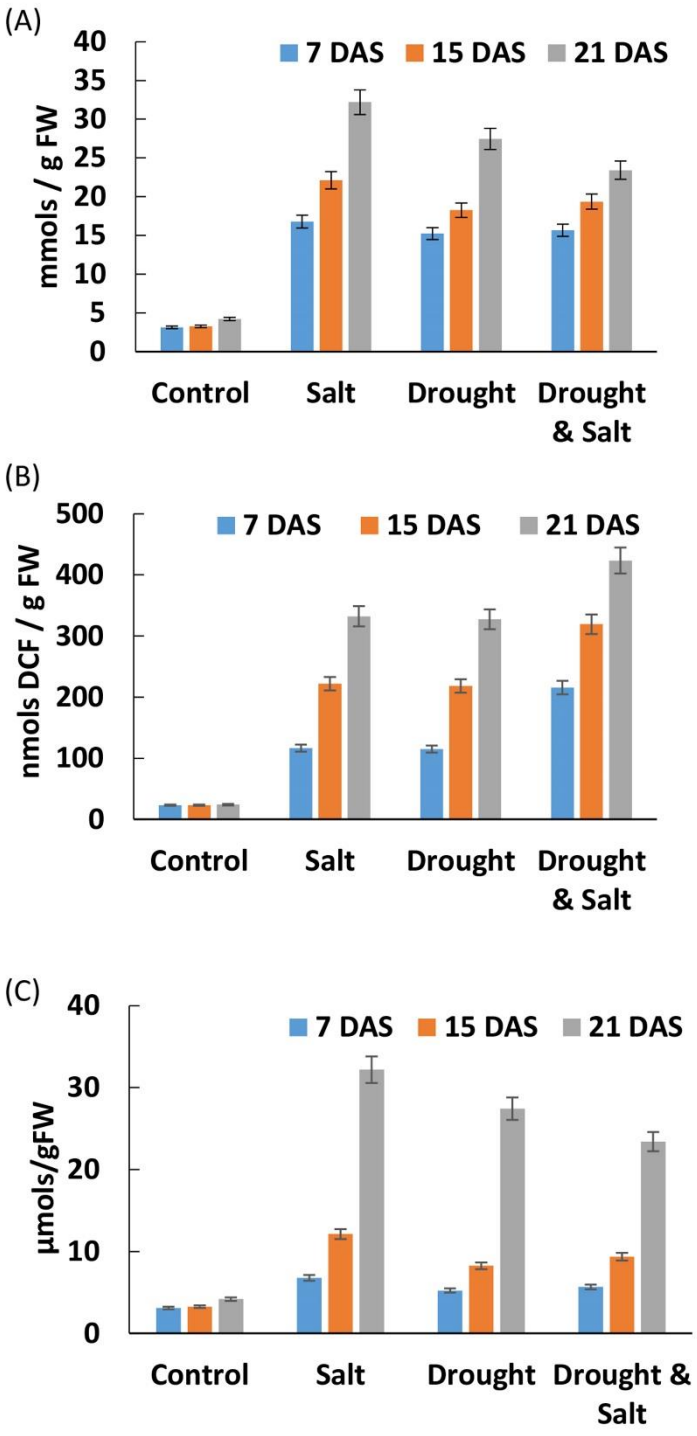


**Fig. 12.** Biochemical parameters including (A) lipid peroxidation (B) reactive oxygen species (C) methylglyoxal content in Jatropha grown under drought, salt and combine stress treatments at 7, 15 and 21 DAS.

## Conclusion

The current study on *J. curcas* under interactive drought and salt stress provide insights into physiological, morphological and biochemical responses that serves as basis for understanding the regulation of photosynthetic machinery. Under progressive stress conditions, there was an increase in lipid peroxidation and ROS generation along with synthesis of stress signalling molecule, MG. Also, there was a decrease in photosynthetic rates and stomatal conductance as the stress progressed to conserve water by preventing transpirational loss. As a result there was growth and biomass inhibition. Severe stress hampered the photochemical quenching and the captured light was dissipated in the form of heat which was corroborated by MINI-PAM data. Further, there was an increase in ascorbate and reduced glutathione levels which could play a protective role against excess energy generated through antioxidant system. The enhanced MG levels under drought and salt stress could be of potential interest to investigate for the relevant metabolic pathways involved in its detoxification which are discussed in the next chapters.

# Chapter III

## Functional characterisation of aldo-keto reductase (JcAKR) to understand its role in methylglyoxal detoxification

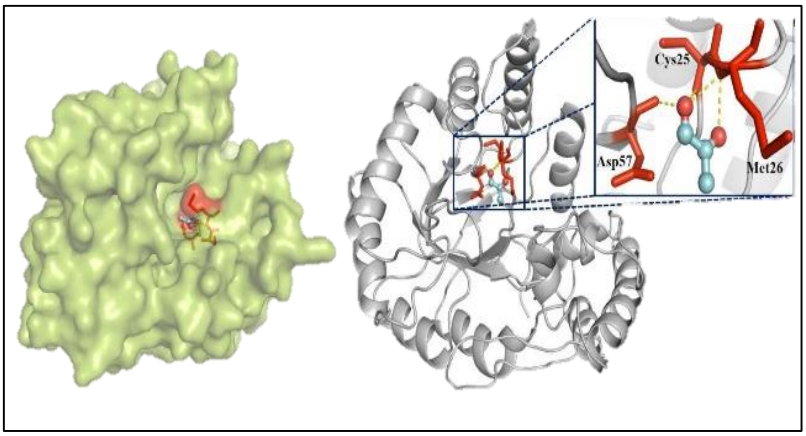

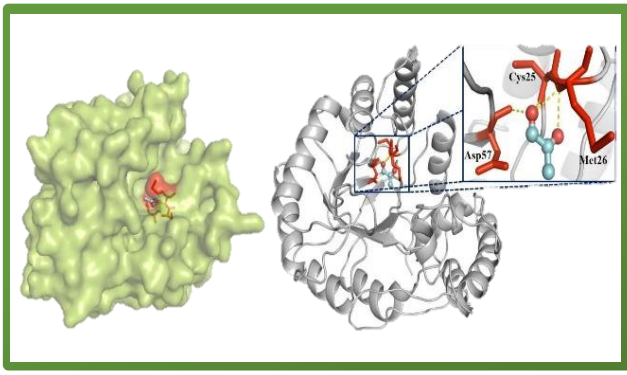


# Chapter - III

Plants are subjected to various abiotic stresses including drought, salinity, cold, high temperatures and flooding which leads to dehydration, cell injury and cell death, ultimately resulting in functional impairment. However, in the course of evolution, plants have developed various complex mechanisms including strategies such as avoidance, tolerance and adaptive changes that vary with genotype (Petrov et al. 2015). Primarily, abiotic stress leads to the generation of ROS which cause lipid peroxidation, protein and nucleic acid oxidation leading to the formation of toxic reactive carbonyls including acrolein, MDA, HNE and MG (Mano 2012; Martins et al. 2001; Mittler et al. 2004; Oberschall et al. 2000; Saito et al. 2011; Simpson et al. 2009; Yamauchi et al. 2011). Among these, MG, a cytotoxic α,β-dicarbonyl aldehyde, that is formed due to amino acid metabolism as well as impairment in glycolysis, acts as a signalling molecule during various abiotic and biotic stresses (Kalapos 1999; Kaur et al. 2014b). MG can be oxidized or reduced and hence serves as a substrate for various enzymes involved in oxidation and/or reduction including glyoxalases, aldehyde dehydrogenases (SDRs), aldehyde reductases (ADRs), aldose reductases (ALRs) and AKRs, resulting in its detoxification into non-toxic alcohol or carboxylic acid (Fehér-Juhász et al. 2014; Kalapos 1999; Saito et al. 2013; Sengupta et al. 2015; Yamauchi et al. 2011). Among these enzyme families, AKRs are a family of NADPH dependent oxido-reductases known to play a key role in carbonyl metabolism with diverse metabolic roles in plants, although the functional importance of most of these remain unknown. AKRs participate in four different metabolic events in plants including (i) detoxification of reactive aldehyde, (ii) osmolyte production, (iii) secondary

metabolism and (iv) membrane transport (Sengupta et al. 2015). AKR superfamilies' comprise of members from bacteria, archaebacteria, yeast, plants and animals with broad physiological activity and substrate specificity (Hyndman et al. 2003; Jez et al. 1997; Vander Jagt et al. 1992). The mechanism behind AKR-mediated stress tolerance appears to be the detoxification of cell damaging reactive carbonyls which are produced during abiotic stress conditions. Most AKRs reduce aldehydes and ketones to their respective alcohols and are NADPH-dependent, although there is evidence that AKRs can use NADH as a cofactor and reduce other substrates, such as monosaccharides, steroids, prostaglandins and polycyclic hydrocarbons (Mano 2012).

*J. curcas* L. is a multipurpose, abiotic stress tolerant as well as a perennial biofuel plant belonging to the family Euphorbiaceae. It is a tropical commercial crop plant that can be grown in low to high rainfall areas either in the farms or in non-arable wasteland. The seeds of *Jatropha* yield non-edible oil (30-40%) which is economically important for biodiesel production, making soaps and biopesticides. In the present study, we have identified an AKR from *Jatropha curcas* (JcAKR) which was cloned and heterologously expressed in bacteria and yeast to show its role in abiotic stress tolerance and MG detoxification. Further, the transcript levels and enzyme activity of JcAKR were investigated during drought and salinity stress in leaves and roots of *J. curcas*.

## Materials and methods

### *Plant material and experimental layout*

The seeds of *J. curcas* were obtained from Directorate of Oilseed Research (DOR, Rajendranagar, Hyderabad, India). They were surface sterilized with 0.4% sodium hypochlorite for 5 minutes and were washed thoroughly with sterile water. Sterilized seeds were germinated in petri plates containing sterile wet blotting paper. After germination, the seedlings were transferred to pots containing red soil and sand (1:1). Plants were grown in a greenhouse under controlled conditions at 28±2ºC and ~70% humidity for one month. For the experiments on stress treatment, one month old plants were divided into four groups, group 1-control, group 2 - NaCl treated (200mM), group 3- drought stress (complete water withdrawal), group 4 -drought+salt (200mM salt

water treatment followed by complete water withdrawal) for 21 days. Following the treatment, roots and leaves of the treated as well as the control plants were collected at 7, 15 and 21 days after stress and were frozen in liquid nitrogen and stored at -80$^0$C.

Transcriptome analysis was done according to (Mudalkar et al. 2014a). Briefly, Total RNA, isolated from control sample, was subjected to cDNA library construction following Illumina TruSeq RNA library protocol outlined in ‘‘TruSeq RNA Sample Preparation Guide’’. The library was quantified using Nanodrop and validated for quality by Bioanalyzer Chip (Agilent Technologies, USA) and was sequenced on the Illumina HiSeq 2000 sequencer platform as paired end 100 bp reads following the manufacturer’s recommendations (Genotypic technology, Bangalore, India). The sequences were assembled with velvet (1.2.10) and oases (0.2.08). 52771 transcripts were generated after sequence assembly and these were annotated with TrEMBL, Swiss-prot, KEGG and KOG databases against Euphorbiaceae members. The transcriptome data generated was submitted to NCBI biosample database with biosample accession number SAMNO3145040 and bioproject ID-PRJNA265009.

### *RNA isolation and first strand cDNA synthesis*

Total RNA was isolated from 100 mg of frozen leaves and roots of 7, 15, 21 days after stress samples along with control using Plant Spectrum RNA isolation kit (Sigma-Aldrich, USA). RNA purity was checked by means of spectrophotometer (Nano drop 2000 spectrophotometer, Thermo Fisher Scientific, Germany) and its integrity was checked by agarose gel electrophoresis. Following isolation, cDNA synthesis was performed by using RevertAid$^{TM}$ first strand synthesis kit (Fermentas Life Sciences, Germany) according to the manufacturer's protocol. The cDNA was stored at −20 °C until use.

### *Primer synthesis, cDNA amplification and phylogenetic analysis*

Transcriptome analysis of *J. curcas* generated 52771 transcripts, of which 35 transcripts represented putative AKRs and one had highest homology with AKRs of *Manihot esculenta* and *Populus trichocarpa*. 50 ng of cDNA prepared from *Jatropha* leaf was

used to amplify JcAKR using emerald PCR master mix (Takara, Tokyo, Japan), JcAKR Fwd: ATGGCAGGAGCAACAGTGAAG; JcAKR Rev: TTATGCTGCTTTCCATGA and a PCR program: cycle of 5 min at 95 $^0$C, followed by 45 cycles of 30s at 95$^0$C, 30s at 55$^0$C annealing temperature and 30 s at 72$^0$C to obtain JcAKR sequence. The PCR product was cloned in pTZ57RT vector (Fermentas Life Sciences, Germany) and later sequenced.

MEGA6 was used for the construction of phylogenetic tree using Clustal W and neighbour-joining analysis by taking the amino acid sequences of known AKRs from upenn.edu/akr/members and deduced amino acid of JcAKR (Tamura et al. 2013). Evolutionary analyses with MEGA6 software showed differences in base composition bias per site (Kumar et al., 2016). The analysis involved 34 amino acid sequences and all positions containing gaps and missing data were eliminated. There were a total of 110 positions in the final dataset.

### *Cloning, heterologous expression, protein purification and confirmation*

The coding region of *JcAKR* was obtained by PCR amplification with the following primers: JcAKRBF: gtaggatccATGGCAGGAGCAACAGTGAAG and
JcAKRER: ccggaattccggTTATGCTGCTTTCCATGA
The amplified product encompassed the BamH I and EcoR I sites, respectively, *Pfu* DNA Polymerase and a PCR program: cycle of 5 min at 95$^0$C, followed by 45 cycles of 30 s at 95$^0$C, 1 min 30 s at 60$^0$C annealing temperature and 30 s at 72$^0$C to obtain JcAKR sequence. The amplified fragment was digested with the restriction endonucleases, and ligated into a pGEX-4T-1 (Amersham Pharmacia Biotech) expression vector digested with the same enzymes. The recombinant plasmid, pGEX-4T1-JcAKR, was transformed in *E.coli* TOP10F' cells, positive clones were identified by colony PCR, plasmid was isolated from these positive clones and the presence of insert was further confirmed by sequencing. pGEX-4T1-JcAKR construct was then transformed into competent cells of *E. coli* BL21 (DE3) for protein expression. A parent vector without inserts was used as a negative control. Expression of GST-AKR protein was carried out according to (Mudalkar et al. 2014b). JcAKR fusion protein was expressed in *E. coli* and induced with 1 mM isopropyl β-D-thiogalactoside (IPTG) for

6 h at 30 °C. Cells were harvested by centrifugation for 15 min at 8000g and resuspended in 1xPBS containing 0.5% β-mercaptoethanol to prevent protein oxidation and later the cells were lysed by sonication. After sonication, cellular debris was pelleted by centrifugation for 20 min at 10000g and the fusion protein (GST-JcAKR) was isolated from the supernatant by affinity chromatography using CL-Agarose column from Genei™ GST-fusion protein purification kit (Bangalore Genei, Bangalore, India). Selected fractions were confirmed by 12% SDS-PAGE stained with coomassie brilliant blue R 250. 10µg of purified GST and GST-AKR proteins were loaded on 15% SDS-PAGE. The separated proteins were transferred on polyvinylidene fluoride (PVDF) membrane (Immobilon-P, Millipore, MA, USA) using biorad apparatus (Bio-Rad laboratories ltd., USA). Anti-GST antibody was used as a primary antibody (1:10000) and HRP-conjugated goat anti-mice IgG (1:20000) was used as secondary antibody and the blot was developed using *supersignal west pico chemiluminescent substrate* (Thermoscientific, USA) following manufacturer's instruction. The image was developed by Kodak image station 4000 (USA).

### *Modelling and molecular docking studies*

*JcAKR* sequence was taken from transcriptome analysis and BLAST search of the deduced amino acid sequence was done against Protein Data Bank (PDB) to identify the three-dimensional structures that could share high sequence homology. The model of JcAKR was generated with Modeler9v12 (Sali and Blundell 1994) by multi template modelling using four crystal structures with PDB Ids: 1PYF, 1YNP, 3N2T, 3V0T as templates. The structural validation and stereochemical quality examination of the generated three-dimensional models was performed using Verify_3D. Secondary structure of JcAKR and Ramachandran plot were generated by PROCHECK analysis (Liithy et al. 1992; Ramachandran et al. 1963).

Molecular docking study for JcAKR with MG was performed by Autodock 4.2 (Morris et al., 2009). Polar hydrogens and atomic charges were added to receptor molecule by Auto Dock Tools (ADT) graphical user interface according to default parameters (Morris et al., 2009). Torsion and rotatable bonds were defined and gasteiger charges were added to ligand molecule using ADT graphical user interface. Ligand was allowed

to dock to receptor within a grid box space of 40 × 40 × 40 grid points along X, Y and Z axes with 0.26 Å grid spacing. The centre of the grid was set to 6.673, 32.415 and 19.746 on XYZ coordinates. Docking was employed by using Lamarckian Genetic Algorithm (LGA) available in Autodock 4.2 with parameters set to GA population size: 150; GA runs: 10 and maximum number of energy evolutions: 25,000,000. During docking, a maximum numbers of top 10 conformers were considered, and the root-mean-square (RMS) cluster tolerance was set to 0.2 nm. Among ten ligand confirmations which were docked to protein, the conformation which scored well was visualized for detailed interactions in PyMol Molecular Graphics System.

### *Abiotic stress tolerance of recombinant JcAKR in Escherichia coli*

To investigate the stress tolerance of transformed *E.coli*, the cells harbouring GST and GST-JcAKR protein were induced in presence of 1mM IPTG and 200mM NaCl (Salt), 5%PEG (Drought) and 5%PEG+200mM NaCl (Drought+Salt). Bacterial growth was monitored at 1 h. intervals at $OD_{600}$.

### *Growth analysis of yeast under abiotic stress*

The yeast vector p424-JcAKR was constructed as follows: the JcAKR coding region was excised from pGEX-4T-1-JcAKR by digestion with BamHI/EcoRI and ligated into the yeast expression vector p424 under the transcriptional control of the yeast glyceraldehyde-3-phosphate dehydrogenase (GPD) promoter. The p424 vector also contains the CYC1 (cytochrome c oxidase) terminator, the 2 µ replication origin and the TRP1 tryptophan marker. Oxidative stress sensitive *Saccharomyces cerevisiae* strain $W_3O_31A$ was used for the study. Vector p424 and the construct p424-JcAKR were introduced into $W_3O_31A$ cells using Frozen EZ-yeast transformation II$^{TM}$ kit (Zymo Research, USA). The transformed cells were selected by their capacity to grow in complete synthetic medium (SC), lacking Trp (p424 selection marker). To determine the abiotic stress tolerance, yeast cells were transformed with p424 and p424-JcAKR, the transformed cells were grown on SC-TRP medium supplemented independently with NaCl (200mM), PEG (5%), PEG+NaCl or MG (5mM) and the growth was observed by measuring the OD at 600nm for 36 h at 30$^{o}$C.

### *Quantification of foliar MG levels under abiotic stress*

The assay was performed according to (Mustafiz et al. 2010). 250 mg of plant tissue was ground in liquid nitrogen and 2.5 mL 0.5 M perchloric acid was added and homogenised. It was incubated on ice for 15 min. The extract was centrifuged for 10 min at 11000×*g* at 4°C. The supernatant was transferred to a fresh tube and charcoal (10 mg/mL) was added. This mixture was kept at room temperature for 15 min and was centrifuged at 11000×*g* for 10 min. The clear supernatant was taken in fresh micro centrifuge tube and the solution was neutralized with saturated potassium carbonate and the pH of the supernatant was checked using a pH paper. The extract was kept at room temperature for 15 min and centrifuge at 11000×*g* for 10 min. The supernatant was taken for MG estimation. The amount of MG in the sample was measured by taking standard curve of MG at different concentrations (10-100µM), using 7.2mM 1,2-diaminobenzene and 5M perchloric acid. The absorbance was taken at 336nm using spectrophotometer (Eppendorf, Germany).

### *Real-time PCR (qRT-PCR) of JcAKR gene*

Expression levels of mRNA for *JcAKR* was measured by qPCR using Eppendorf Realplex MasterCycler (Eppendorf, Germany), KAPA SYBR FAST (Mastermix (2X) Universal) (KAPA Bio systems, USA) and the following primer pair AKRqRTF: TATCGTCGCATACAGTCCCC and AKRqRTR: GTGCATTGTTTCCTTGCTGC. To establish reference points for AKR-expression, primers were designed for *J. curcas* 18SrRNA mRNA partial sequence (genbank accession number- AB233567.1): Jc18F-CCTGCGGCTTAATTTGACT and Jc18R- TTAGCAGGCTGAGGTCTC. Expression levels of the target gene was calculated by comparing the cycle threshold value (Ct) to the reference gene. The relative quantification (comparative method) was calculated using the $2^{-\Delta\Delta Ct}$ method (Livak and Schmittgen 2001). All samples were normalized to the ΔCt value of a reference gene sample to obtain a ΔΔCt value = (ΔCt treated−ΔCt control). The final relative expression was calculated using the following formula:

$$F = 2^{-(\Delta Ct\ treated - \Delta Ct\ control)}$$

The experiment was performed twice in triplicates for each sample.

### *Enzyme activity and enzyme kinetics*

Enzyme activity of JcAKR was done according to Turóczy et al., 2011. The reaction mixture contained 0.1 M sodium phosphate buffer (pH 7), 0.1mM of NADPH/NADH and 1mM MG as substrate and 25µg of extracted leaf, root and purified protein. The decrease in absorbance was measured for 1 min for purified protein and 3 min for leaf and root samples at 340nm using a spectrophotometer (Eppendorf, Germany) at 25$^{o}$C. Specific activity was measured by taking ε of 6.2 $mM^{-1}$ $cm^{-1}$. $K_m$, $K_{cat}$ and catalytic efficiency ($K_{cat}/K_m$) were calculated from the non-linear regression of Michaelis-Menten data. GraphPad PRISM version 5.04 program was used for the enzyme kinetics of purified JcAKR protein.

### *Statistical analysis*

Samples from three biological replicates were collected at regular intervals and mean values were represented together with standard deviation (SD), for *in vitro* experiments. Analysis of variance (ANOVA) was used for further data analysis and the comparisons were tested with Holm-Sidak method, the level of significance was set to 0.05. Statistical significance of the differences within a treatment at different time periods was indicated with capital letters and between the treatments was represented with small letters. Microsoft excel 2010 was used for data processing. Statistical analysis was performed using software, Sigma plot 11.0.

## Results and Discussion

*Jatropha* is known for its tolerance to various abiotic stresses such as drought and salinity. Abiotic stress tolerance characteristics which include enhanced heat shock protein levels, LEA proteins, proline and betaine aldehyde have been reported in *Jatropha* (Liang et al. 2013; Omar et al. 2011; Yang et al.). MG is a highly reactive dicarbonyl compound that accumulates in plants with stress; however, the biochemical mechanisms driving its production and detoxification are not well understood although, stress-induced MG production and its detoxification mechanisms in plants have not

been well understood. Synthesis and accumulation of MG is known to occur mainly due to the impairment in glycolysis in plants, and its detoxification has been linked to glyoxalases and AKRs, which differ mechanistically. In a glutathione independent pathway, AKR converts MG into hydroxyacetone (acetol) in presence of NADPH whereas the glyoxalases use reduced glutathione (GSH) to metabolise MG into lactate (Kaur et al., 2014; Yadav et al., 2005). The alternate MG detoxification routes depend on the availability of either GSH or NADPH which in turn depends on external environment and plant species. With respect to industrial applications, AKRs are more suitable than glyoxalases for the generation of renewable bioenergy in prokaryotic systems, since they convert toxic aldehydes into non-toxic alcohols. To date, biochemically characterized plant AKRs show a large variation with respect to homology and substrate specificity. Several plant AKRs, characterised till date, show a large variation with respect to homology and substrate specificity (Narawongsanont et al., 2012; Oberschall et al., 2000; Saito et al., 2013; Sengupta et al., 2012; Turóczy et al., 2011; Yamauchi et al., 2011). Thus, it is of great relevance to identify and characterise potent AKRs in plants with high substrate specificity. In the present study, we identified a putative AKR from *J. curcas* and demonstrated the recombinant protein, expressed in heterologous systems, utilizes MG as a substrate. The mechanism of action was confirmed with molecular docking studies.

### *Cloning, sequencing and analysis*

The analysis of transcriptome data revealed the presence of 35 putative AKRs of which, one had highest similarity with other plant AKRs and this putative gene sequence was selected for further experiments. The PCR amplification of cDNA prepared from leaf yielded a 1035 bp product (Genbank accession number KU513391). *In silico* translation of the nucleotide sequence yielded a polypeptide sequence of 344 amino acids with a molecular weight of 37.7 kDa and a theoretical pI of 6.11. The conserved domain analysis through NCBI-BLAST revealed JcAKR to be a member of soluble NADP(H) oxidoreductase superfamily, which catalyses reduction of aldehydes and ketones to primary and secondary alcohols. Furthermore, JcAKR had homology with the beta subunit of voltage-gated potassium channels of plants and animals that are known to be

involved in ion transport across membranes (Table 2). JcAKR was 77-87% similar at the amino acid to AKRs from *Manihot esculenta*, *Populus trichocarpa*, *Theobroma cacao*, *Arabidopsis lyrata subsp.lyrata* and *Medicago trunculata*; the protein shared 81% similarity with an NAD(P)-linked oxido reductase superfamily protein from *Theobroma cacao* (Fig. 14). Multiple sequence alignment of JcAKR with other AKRs showed the conservation of amino acids at N and C terminal region where, at N-terminal region amino acids such as G(33), G(52), D(57), Y(62), E(68), G(72), V(109), L(117), L(120), D(123), **DLY**(126-128), **H**(131) and those at C-terminal region such as A(258), Q(267), QN(294-295), E(306) were conserved in *J. curcas* and were correlated with AKR4/A9-like proteins of other Euphorbiaceae members that are involved in abiotic stress tolerance (Sengupta et al., 2015). A phylogenetic analysis demonstrated JcAKR is part of a small clade consisting of an AKR from *Glycine max* and perakine reductase (AKR13D) from *Rauvolfia serpentina*; this implies that JcAKR might be active against other endogenous aldehydes (Fig. 15) (Rosenthal et al., 2006).

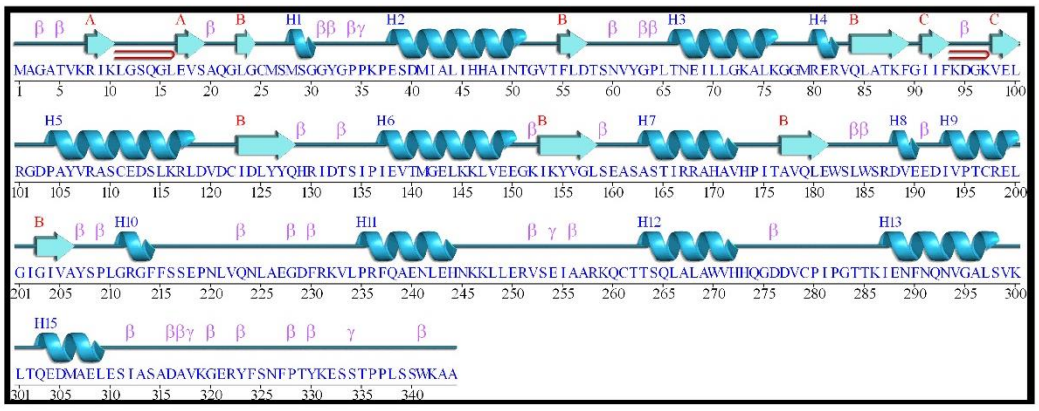


**Fig. 13.** Secondary structure of JcAKR protein obtained from deduced amino acid sequences.

**Table 2:** Conserved regions of JcAKR

| Protein identified | Specific hit | Non-specific hits | Superfamily | Multi domains |
|---|---|---|---|---|
| JcAKR (*Jatropha curcas* Aldo-keto reductase) | Cd0660<br><br>Aldo-keto reductases (AKRs) | 1. Pfam00248-Ald_ket_red<br><br>2. ARA1-COG0656-Ald_ket_red<br><br>3. PRK10376- Aldo/keto reductase, related to diketogulonate reductase<br><br>4. PLN02587- L-galactose dehydrogenase | 1. cl00470- Aldo-keto reductases (AKRs), a superfamily of soluble NAD(P)(H) oxidoreductases | 1. Tas-COG0067- Predicted oxidoreductase (related to aryl-alcohol dehydrogenase)<br><br>2. kv-beta TIGR01293- voltage-dependent potassium channel beta subunit |

**Table 3:** Enzyme kinetics of GST-JcAKR with different substrates

| Substrate | Substrate concentration (mM) | Specific activity (µmol $min^{-1}$ $mg^{-1}$) | $K_m$ (µM) | $K_{cat}$($min^{-1}$) | $K_{cat}/K_m$( $min^{-1}/M^{-1}$) |
|---|---|---|---|---|---|
| Methylglyoxal | 1 | 5.9±0.02 | 4.9±0.01 | 18.5±0.01 | $3.77x10^6$ |
| p-Dimethyl amino benzaldehyde | 1 | 1.2±0.15 | 56.5±1.4 | 10.9±0.02 | $1.92\ x10^5$ |
| Glutaraldehyde | 1 | 0.3±0.09 | 366±0.3 | 4.1±0.05 | $1.12\ x10^4$ |

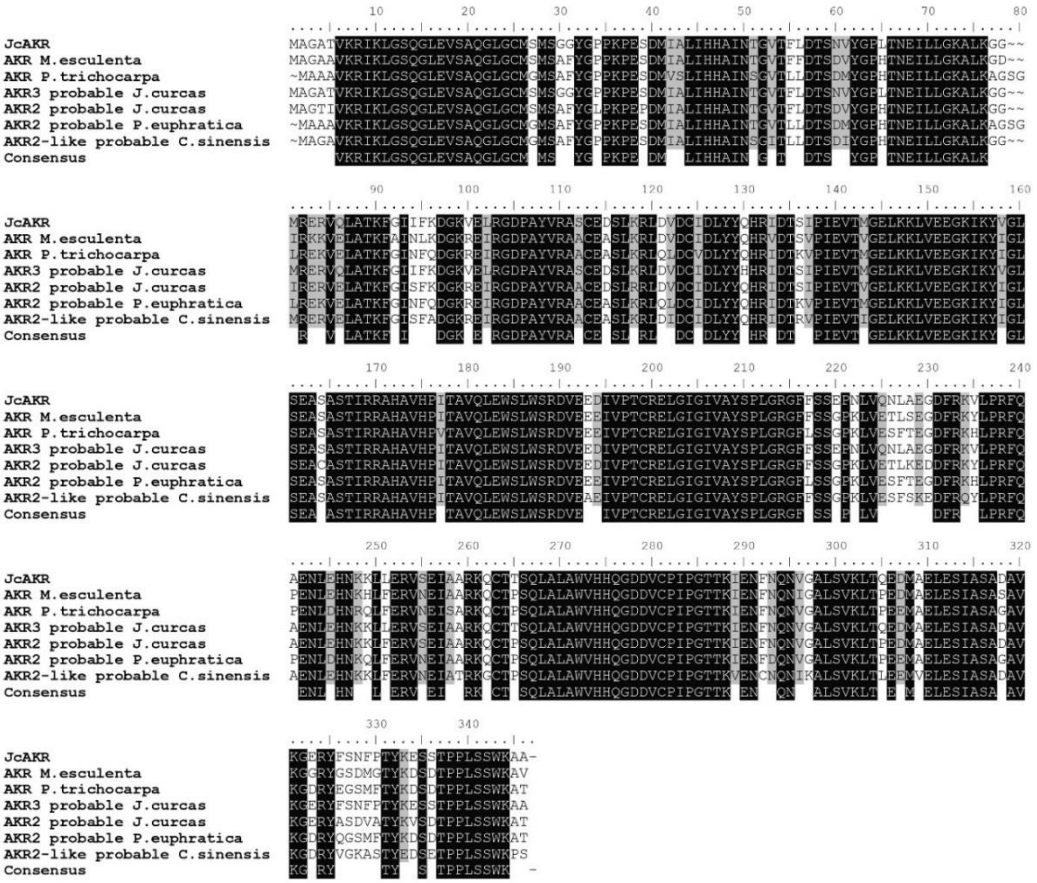


**Fig. 14.** Multiple sequence alignment of JcAKR with deduced amino acid sequence of other plant AKRs obtained after BLAST analysis.

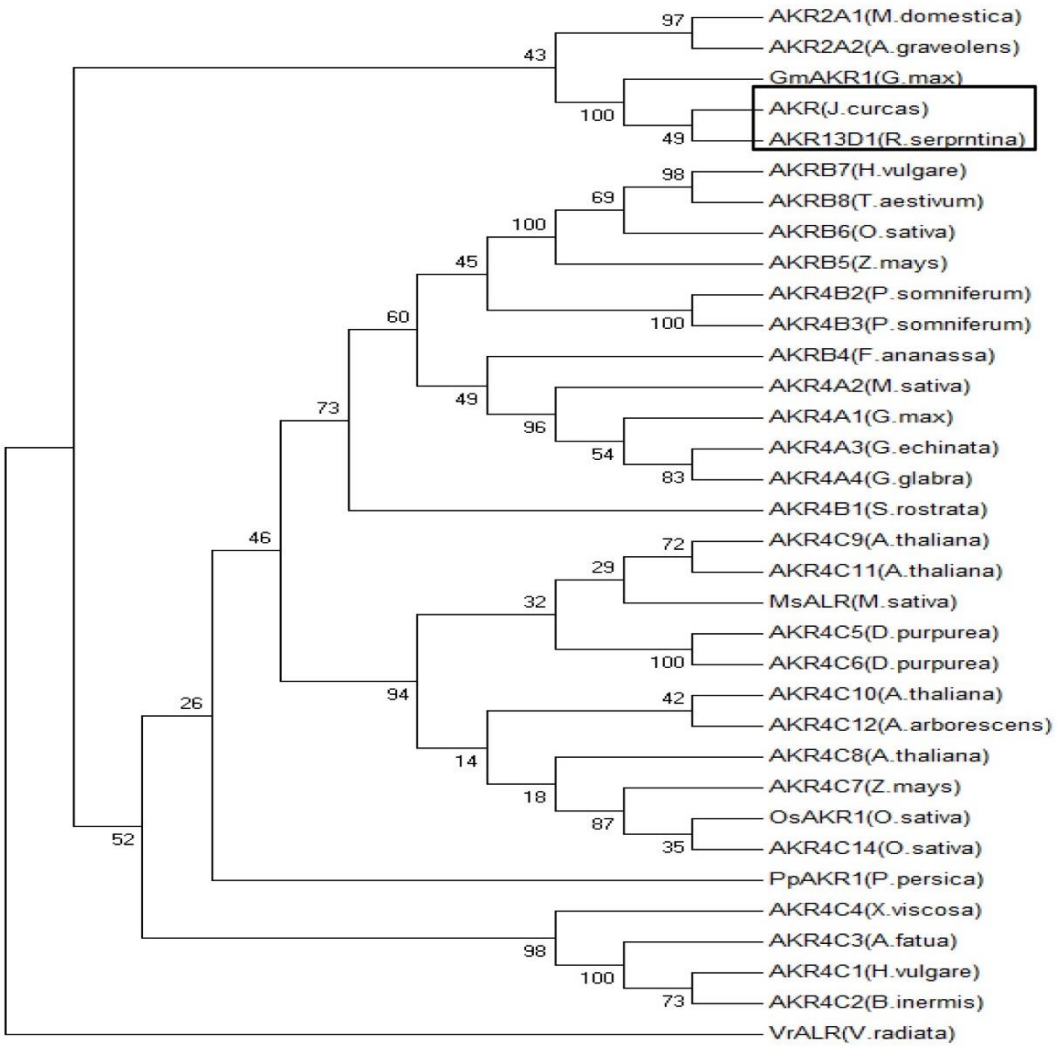


**Fig. 15. Phylogenetic analysis:** JcAKR and its relationship with other published plant AKRs. MEGA6 was used for the construction of the tree using neighbour joining method and clustal W program, with boot strap method taking 500 replicates. The branch numbers refer to the bootstrap confidence. The accession numbers of JcAKR, PpAKR1 and VrALR are KU513391, AB183148 and AAD53967.1 respectively, whereas the accession codes for the other AKRs used in the construction of phylogenetic tree are available at www.med.upenn.edu/akr.

### *Protein expression, purification, enzyme assay and kinetics*

To determine the ability of JcAKR to detoxify MG, JcAKR was expressed along with GST, as a fusion protein. In SDS-PAGE analysis, a protein corresponding to GST (26.5 kDa) was detected in crude lysate of induced *E. coli* BL21 (DE3) cells containing the vector pGEX4T-1 (GST without insert) and a unique protein, corresponding to the predicted size of the GST-JcAKR (64 kDa) was observed in crude lysates of cells transformed with plasmid pGEX4T-1+JcAKR (Fig.16A). Also, column purified GST-AKR gave a clear band of 64kDa (Fig. 16B). Purified GST and GST-JcAKR proteins were subjected to western blot analysis with anti-GST antibody. 26 and 64kDa proteins corresponding to GST and GST-fused AKR were seen on the membrane (Fig. 16C). Further, GST-AKR was confirmed by MALDI-TOF analysis, wherein three peptide fragments were generated (Table. 4). These peptide fragments were subjected to MASCOT search which gave hit to AKRs of other Euphorbiaceae members including *Manihot esculenta*, *Ricinus communis* and probable AKR3 of *J. curcas.*

AKRs have wide range of substrate specificity ranging from steroids to reactive aldehydes and ketones. AKR4C8 and 9 of *Arabidopsis* showed the ability to reduce a group of aliphatic aldehydes including MG with a catalytic efficiency of 0.96 and 32.7 $s^{-1}$ $mM^{-1}$, respectively (Simpson et al. 2009). AKR4C14 from rice was capable of metabolizing sugars and reactive aldehydes such as MG, trans-hexenal and glutaraldehyde (Narawongsanont et al. 2012). At1g4870, At3g04000 and At2g37770 from *Arabidopsis thaliana* exhibited a catalytic efficiency of 0.51, 5.76 and 48 $s^{-1}$ $mM^{-1}$ respectively (Yamauchi et al. 2011). Also, the overexpression of OsAKR1 from rice was able to detoxify MG both in bacteria and transgenic plants with a catalytic efficiency of 18 $s^{-1}$ $mM^{-1}$ (Turóczy et al. 2011). Similarly, JcAKR showed a higher specific activity of 5.9 µmol $mg^{-1}$ $min^{-1}$ with MG when compared to other substrates which had specific activities of 1.2 and 0.3 µmol $mg^{-1}$ $min^{-1}$ for 2, 4-dimethyl amino benzaldehyde and glutaraldehyde respectively.

Also, JcAKR exhibited a high catalytic efficiency ($K_{cat}/K_m$) of 62.83 $s^{-1}$ $mM^{-1}$ with MG as substrate and NADPH as co factor (Table 3). The catalytic efficiency of JcAKR with MG was higher when compared to that in rice and *Arabidopsis* by 60% and 22%

respectively. Therefore, MG was taken as substrate for all further studies. NADP(H) is the preferred cofactor for carbonyl reduction and NADH is used to convert aromatic aldehydes to corresponding alcohols whereas $NAD^+$ promotes oxidation of hydroxyl groups (Yamauchi et al. 2011). JcAKR did not show any activity with NADH but had highest activity with NADP(H) as cofactor and hence it could be inferred that it is actively participating in the reduction of reactive carbonyls. *Jatropha* being a biofuel crop, the ability of *JcAKR* to reduce harmful reactive carbonyls to alcohols could be used for the production of renewable biofuels as reported in the case of YqhD of *E.coli* (Jarboe 2011).

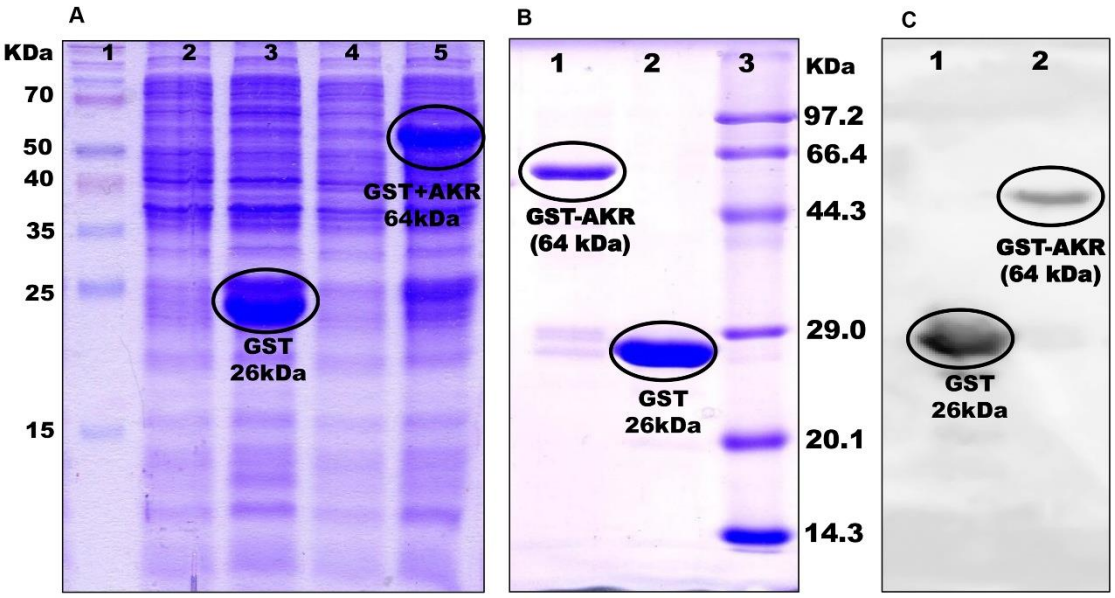


**Fig. 16. Overexpression, purification of JcAKR & western blot analysis**: 12% SDS-PAGE of GST and GST fused AKR and stained with coomassie brilliant blue R 250. (A) Lane 1 medium range molecular weight marker; Lane 2 *E. coli* BL21 with GST, uninduced cell lysate; Lane 3 *E. coli* BL21 with GST cell lysate induced with IPTG; Lane 4 Uninduced GST-JcAKR; Lane 5 GST-JcAKR cell lysate induced with IPTG; (B) Lane 1 GST-JcAKR affinity purified by GST chelating column; Lane 2 Affinity purified GST; Lane 3 medium range molecular weight marker; (C) Lane 1 Western blot for GST using anti-GST antibody; Lane 2 Western blot for GST-AKR using anti-GST antibody.

### *Modelling and molecular docking studies*

The NCBI-BLAST search of the JcAKR against PDB database showed 58, 31, 30 and 29% sequence identity with **3V0T (**Crystal structure of perakine reductase from *Rauvolfia serpentina*), **3N2T (**Structure of the glycerol dehydrogenase AKR11B4 from *Gluconobacter),* **1YNP (**Aldo-keto reductase AKR11C1 from *Bacillus halodurans),* **1PYF** (Structure of NADPH-dependent family 11 aldo-keto reductase from *Bacillus subtilis*) structures respectively. The modelled structure of the JcAKR was validated using PROCHECK and Verify_3D wherein 90.6% of the residues were in the most favored region and 91.57% of the residues had an averaged 3D-1D score >= 0.2 (Fig. 17).

Docking studies on MG with JcAKR protein revealed that all the ligand confirmations were found to be restricted to catalytic site of the protein. Out of ten ligand confirmations, 9 confirmers of MG were almost with same binding free energies at one binding site confirming the binding of ligands at that site. Among these, top ranked confirmations, MG had a binding free energy ($\Delta G$ in kcal/mol) of −3.13 and this confirmation was viewed and analysed for interactions in PyMol (Fig.18A). The residues of protein forming interactions with MG were Cys25, Met26 and Asp57 (Fig. 18B).

## ***Bacterial and yeast growth curve analysis***

### *Bacterial growth curve*

AKRs from bacteria such as YqhD of *E.coli* are known to covert MG and other aldehydes to their non-toxic derivative acetol (Grant et al. 2003; Jarboe 2011; Ko et al. 2005; Pérez et al. 2008). Similarly, many AKRs from other organisms were overexpressed in bacteria to show protection or tolerance against various stress-inducing factors. For example, VrALR from *Vigna radiata* could protect the bacteria from external $H_2O_2$; when OsAKR1 from rice was overexpressed in bacteria in presence of MG, it could detoxify and accept MG as substrate; also the cells expressing OsAKR1 were more resistant to MG compared to control. AKR4C14 from rice reduces MG to corresponding alcohol (Narawongsanont et al. 2012; Sengupta et al. 2012; Turóczy et

al. 2011). Here, we report that bacteria, containing a GST-AKR fusion protein, tolerated multiple abiotic stresses when LB broth was supplemented with either NaCl (200mM), PEG (5%) or both and MG (5mM) relative to cells expressing GST alone (Fig. 19), thus

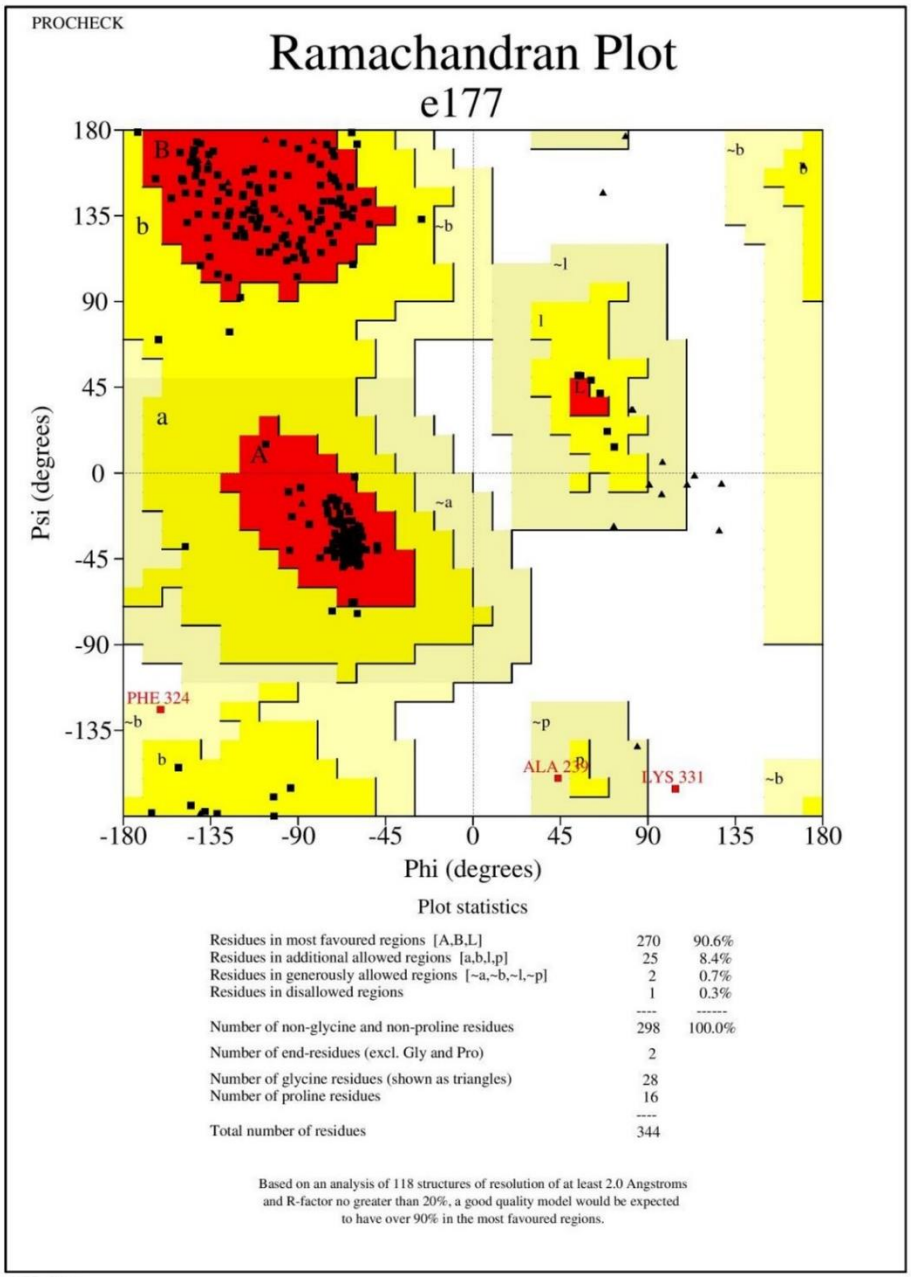


**Fig. 17.** Validation of JcAKR Protein model through Ramachandran plot.

protecting the bacteria from a wide range of stresses including oxidative stress, caused by NaCl and/or PEG and by detoxification of a reactive aldehyde, MG.

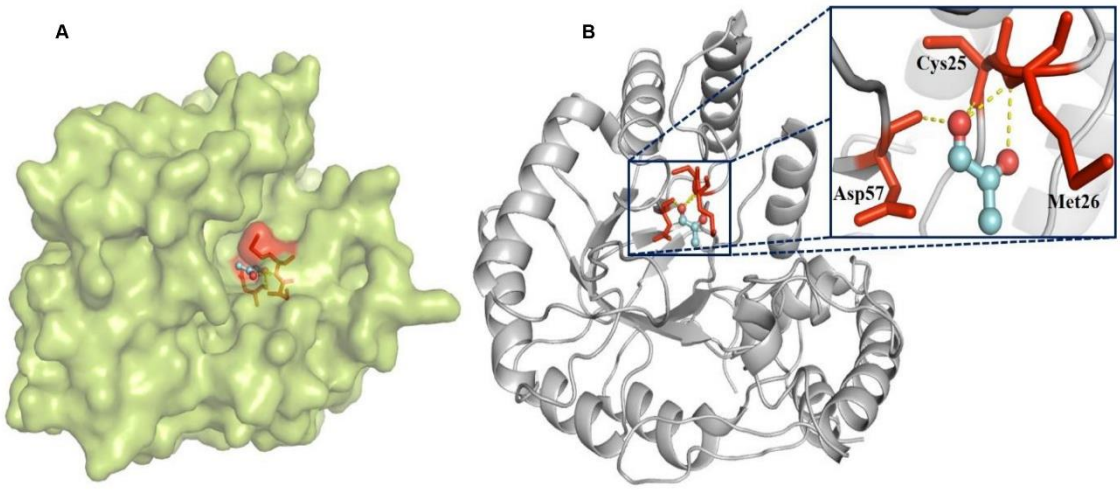


**Fig. 18. Three-dimensional model of JcAKR with MG:** (A) Surface representation of JcAKR modelled protein with docked MG structure (B) Cartoon representation of AKR and docked MG with enlarged view. The structure of MG is shown in sky blue ball and sticks representation and residues interacting with ligand are shown in red color in sticks representation.

**Table 4:** Identification of JcAKR with MALDI and MASCOT search analysis

| **Protein identified** | **Peptide sequences matched** | **Theoretical Mr/pI** | **Accession no./ Coverage** | **Reference organism** | **MS/MS score** |
|---|---|---|---|---|---|
| Aldo-keto reductase | 1. R.ELGIGIVAYSPLGR.G<br>2. R.GFFSSEPNLVQNLAEGDFR.K<br>3. R.GFFSSEPNLVQNLAEGDFRK.V | 38kDa/6.11 | gi\|802599781/<br>9% | *M. esculenta*<br>*J. curcas*<br>*R. communis* | 247 |

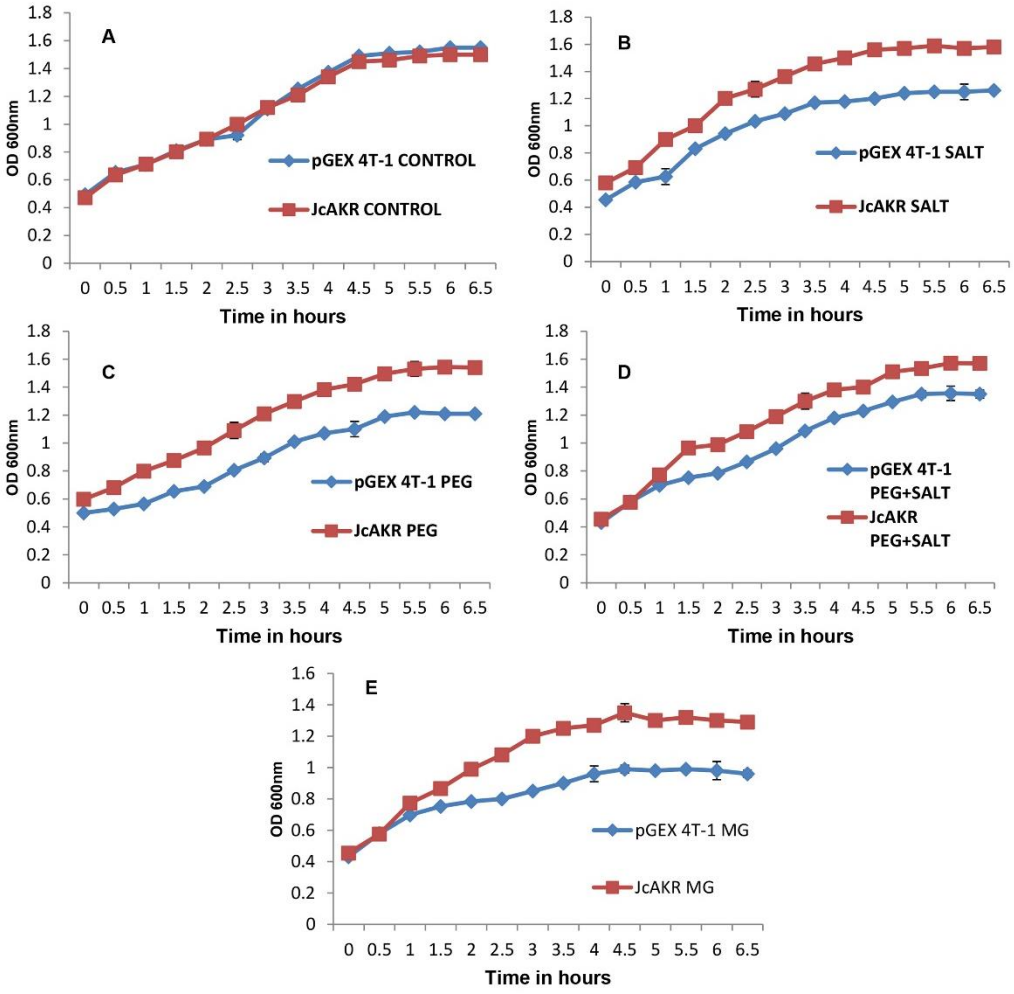


**Fig. 19. Bacterial growth curve**: Bacterial cells expressing GST and GST-JcAKR were grown in LB broth supplemented with ampicillin till $O.D_{600}$-0.5, the cultures were induced with 1mM IPTG along with 200mM NaCl, 5% PEG or 5% PEG+200mM NaCl for salt, osmotic and osmotic+salt stress and $O.D_{600}$ was measured respectively for each treatment along with untreated controls.

### *JcAKR expressing yeast and abiotic stress tolerance*

Yeast serves as a eukaryotic model to study the functional characterization of genes from higher organisms (plants and animals). To check if AKRs have a potential role against MG and abiotic stress, growth analysis was done in yeast cultures. Aldehyde reductases and aldose reductases from *Saccharomyces cerevisiae* are known to play important roles in oxidative stress as well as in regulation of transcription, associated with MG metabolism (Aguilera and Prieto 2001; Chang and Petrash 2008). In this study, an oxidative stress-sensitive *Saccharomyces cerevisiae* mutant strain, $W_3O_3$-1-A was used. It has a mutation in ybp1-1. Ybp1-p (Yap1p-binding protein) is responsible for oxidative stress tolerance in yeast and strains with mutated Ybp1-p were sensitive to $H_2O_2$ oxidative stress (Gulshan et al. 2004). The yeast cells, harbouring p424-JcAKR, showed more tolerance to abiotic stress compared to the cells expressing p424 alone. Further, $W_3O_3$-1-A could show higher tolerance for MG in cells expressing JcAKR (Fig. 20). Similarly, AKRs from *Arabidopsis* such as AKR4C10 and AKR4C11 and *sakR1* from *Synechococcus* were reported to be involved in MG reduction (Saito et al. 2011; Xu et al. 2006). Our study showed the ability of JcAKR to protect bacteria and yeast from oxidative stress resulting from NaCl and/or PEG and MG. Thus, JcAKR could act as a stress protective enzyme in plants by shielding the harmful effects of abiotic stress. Also, it could be exploited for its dual function of detoxification of harmful reactive carbonyls as well as for the generation of renewable bioenergy from the detoxified product in the form of biofuel.

### *Quantification of foliar MG levels under abiotic stress*

MG is produced from sugar and amino acid metabolism in bacteria, yeast, animals and plants (Aguilera and Prieto 2001; Hossain and Fujita 2009; Jarboe 2011; Vander Jagt et al. 1992; Yamauchi et al. 2011). In our study, the levels of MG increased in *J. curcas* with increasing drought and salinity stress showing an increase of upto 80% in stressed plants compared to control plants (5-6 µM of MG), which gradually increased to a maximum of 35 µM at 21DAS (days after stress) in all the three stress conditions (drought, salt, drought+salt) (Fig. 21). Thus, MG can act as a signalling molecule and could be considered as a marker for determining the stress as well as the tolerance levels of *Jatropha*.

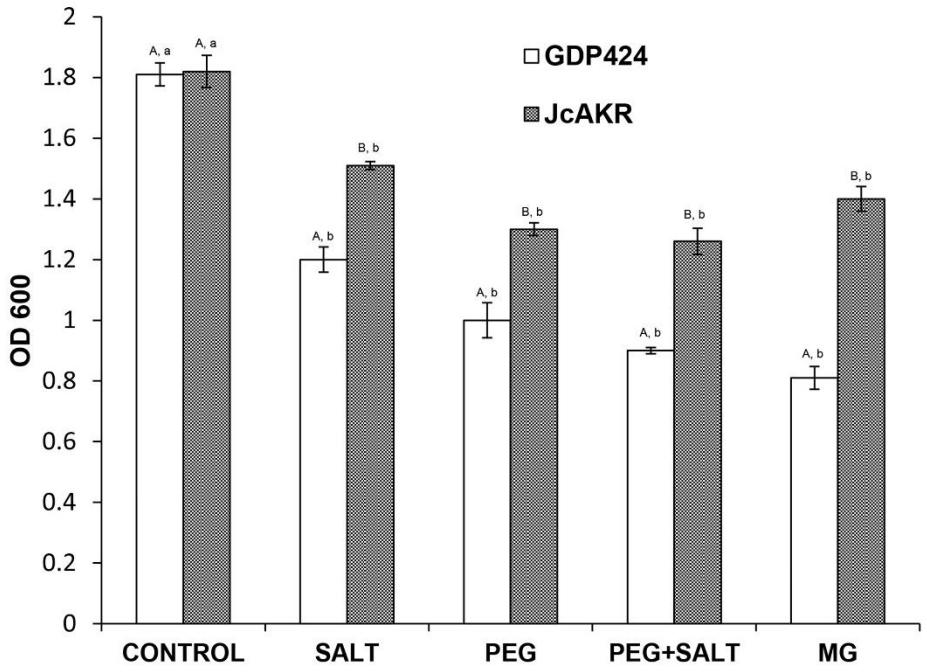


**Fig. 20. Yeast growth for abiotic stress tolerance**: Vector p424 and the construct p424-JcAKR were introduced into $W_3O_31A$ cells and the transformed cells were selected by their capacity to grow in complete synthetic medium (SC), lacking Trp (p424 selection marker). To determine the abiotic stress tolerance, yeast cells were grown in liquid SC-TRP medium supplemented independently with NaCl (200mM), PEG (5%), PEG+NaCl or MG (5mM) and the growth was observed by measuring the OD at 600nm for 36 h at 30°C. Data are the mean ± SD (n=3).

### *qRT- PCR analysis and JcAKR activity*

To understand the role of JcAKR under drought and salinity stress, transcript abundance was analysed by qRT-PCR. JcAKR transcripts were increased in leaves in response to increased drought and salinity stress; a 12-fold enhancement was apparent 7 days after exposure to drought and salt stress (Fig. 22A, B). Though there was an increased expression at 15DAS and 21DAS, the fold change decreased when compared to 7DAS. Also, there was an upregulation of *JcAKR* in the root tissue in all the treatments at 7DAS with a fold change of 4, 2, and 2 for salt, drought and drought+salt respectively, but with the progression of the stress the levels of JcAKR transcripts decreased. Comparatively, the mRNA levels of *JcAKR* were more in leaf tissue when compared to root tissue, which was also reported in rice AKR4C14 (Narawongsanont et al. 2012). From our data on qRT-PCR analysis, it could be inferred that the expression of *JcAKR* was triggered by drought and salinity in leaves and roots, thus protecting the plant from abiotic stress. JcAKR enzyme activity in leaf followed the same trend as that of JcAKR mRNA expression wherein, the activity was more at 7DAS which decreased gradually as the stress progressed. Although the levels of mRNA expression decreased at 15DAS in roots, the enzyme activity was several times higher compared to controls. Aldehyde reductases (At2g37770) and aldo-keto reductases (At1g54870 and At3g04000) of *Arabidopsis thaliana* which are a class of NADPH-dependent reductases are known to be contributing together for the detoxification of reactive carbonyls (Yamauchi et al. 2011). Similarly, the activity of JcAKR which was higher in the roots could be due to the fact that the enzyme activity was the sum of the activities of all the AKRs present in *Jatropha* (Fig. 22 C, D). Usually, drought and salinity stress reduce photosynthetic rates resulting in impairment of energy metabolism and electron transport (Reddy et al. 2004). This leads to decrease in reducing equivalents and ATP which were otherwise involved in various metabolic pathways. Under severe stress (21DAS), the decrease in AKR expression and activity could be attributed to the lower photosynthetic rates. Our results on *JcAKR* in this study correlated with other plant AKRs including, *PpAKR1* from peach, *OsAKR1* from rice, AKR4C8 and AKR4C9 from *Arabidopsis*, DpAR from *Digitalis purpurea and MsALR* from alfalfa (Gavidia et al. 2002; Kanayama et al. 2014;

Oberschall et al. 2000; Simpson et al. 2009; Turóczy et al. 2011). Also, increased *JcAKR* expression in salinity stress could be correlated with the presence of multidomains in the conserved core region of the beta subunit of voltage-gated potassium channels of plants and animals.

MG is also known to be involved in stomatal opening and closure during abiotic stresses by inhibiting the $K^+$ influx in the guard cells, thus acting as a signalling molecule in plant stress responses (Hoque et al. 2012). Although other enzymes including alkenal reductases, aldehyde dehydrogenases are known to be involved in detoxification of reactive carbonyls, the present study demonstrates that AKRs could potentially play a crucial role in the detoxification of MG. Thus, a co-ordinated regulation between AKRs and other stress protective enzymes could be an important strategy for MG detoxification in plants subjected to unfavourable environmental growth conditions.

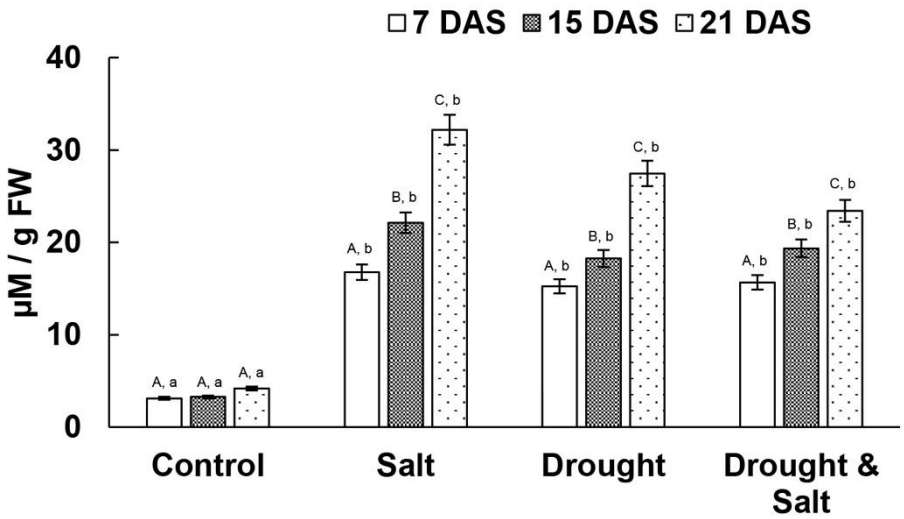


**Fig. 21. Quantitative changes in methylglyoxal under abiotic stress**: MG content of salt, drought and drought+salt treated plants. Data are the mean ± SD (n=3).

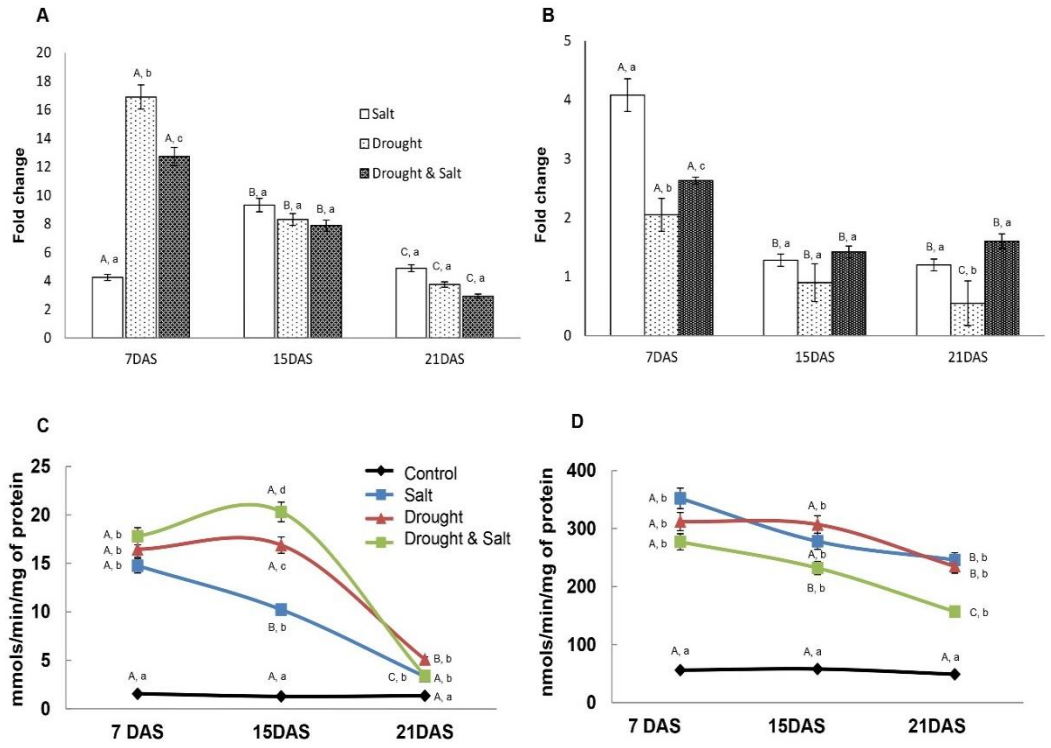


**Fig. 22. qRT-PCR analysis and JcAKR enzyme activity**: qRT-PCR analysis of *JcAKR* gene in leaf (A) and root tissue (B) at 7, 15 and 21DAS during salt, drought and drought +salt stress. JcAKR activity in leaf (C) and root tissue (D) at 7, 15 and 21DAS during salt, drought and drought +salt stress and untreated control, with 2mM MG as substrate. Data presented is the mean ± SD (n=3).

## Conclusion

Our experiments on salinity and drought stress on *Jatropha* clearly implied a role for *JcAKR* in protecting the plant from abiotic stress as well as conferring resistance in transformed bacterial and yeast cells. JcAKR protein sequence was confirmed by MALDI-TOF analysis. The transcript levels and enzyme activity of AKR increased in response to drought and salt stress. Our data demonstrate that, *JcAKR* from *J. curcas* is involved in MG detoxification and could be a possible candidate for use in genetic engineering approaches to confer abiotic stress tolerance in crop plants.

# Chapter IV

## To study the involvement of glyoxalases and glutathione reductase in conferring abiotic stress to *Jatropha curcas* L.

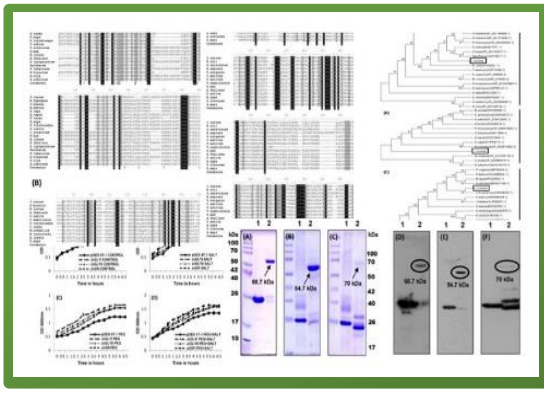

# Chapter - IV

The sessile nature of plants make them susceptible to various abiotic stresses which cause more than 50% of the crop losses and the situation has been further aggravating by fast changing global climate. The major abiotic stresses that affect growth, development and yield of the plants include drought and salinity which have environmental, social and economic impact on developing world. Salinity causes osmotic shock, ionic imbalance and toxicity to the plants due to excessive salt concentration whereas drought leads to photosynthetic inhibition, stomatal closure, dehydration and disturbances in ion transport. Moreover, plants are subjected to a combination of these stresses thus imposing additive effects and causing physiological, molecular and biochemical changes in the plants (Mittler and Blumwald 2010). The major outcome of any stress in plants is the change in redox state and generation of reactive oxygen species (ROS) such as superoxide, hydrogen peroxide and hydroxyl radicals. These molecules cause DNA nicking, oxidation of amino acids, proteins, photosynthetic pigments and lipids eventually leading to their degradation which further generates various reactive carbonyls including MG that cause cellular damage (Apel and Hirt 2004; Asada 1999; Kaur et al. 2014; Suzuki et al. 2012).

MG, a 2-oxo propanal or pyruvaldehyde is a by-product of lipid, amino acid metabolism and glycolytic pathway. It shows significant accumulation during abiotic stresses such

as drought and salinity, thus acting as a signalling molecule in plants (Mustafiz et al. 2014; Phillips and Thornalley 1993). Increased MG levels are toxic to cell and hence it is imperative to identify and characterize key genes regulating its detoxification and entail tolerance. MG is believed to be detoxified through expression of certain genes such as aldo-keto reductases and glyoxalases (Sengupta et al. 2015; Turóczy et al. 2011; Yamauchi et al. 2011). Glyoxalases are superfamily of proteins which include glyoxalse I, II and are identified from bacteria, yeast, animals and plants (Kaur et al. 2014a). Glyoxalase I (GLYI) contains a glyoxalase domain functioning as lactoyl glutathione lyase whereas glyoxalase II (GLYII) has beta-lactamase domain which functions as hydroxyacyl glutathione hydrolase and together they detoxify the harmful MG using reduced glutathione (GSH). MG reacts with GSH to form hemithioacetal which is later converted to SLG through GLYI resulting rapid increase in SLG. If the amount of SLG exceeds to its normal, it tends to be toxic to the plants since it exhausts the GSH which is important for other enzymatic and non-enzymatic anti-oxidants and hence SLG needs to be detoxified which is taken care by GLYII, resulting the release of trapped GSH (Kalapos 1999). Glutathione reductase (GR) is a member of NADPH – dependent oxidoreductase family and is known to act as an important antioxidant enzyme in ASA – GSH pathway which is crucial for ROS detoxification (Couto et al. 2016). It is present in both prokaryotes and eukaryotes either as homodimer, heterodimer or tetramer. The higher ratio of GSH/GSSG is important for salt and drought tolerance which requires an efficient GR that aids in the conversion of GSSG to GSH (Yadav et al. 2005a; Yadav et al. 2005b). Moreover, GSH acts as a metabolic hub between MG and ROS detoxification where it coordinates with glyoxalases and peroxidases respectively as a reductant. Hence the stoichiometry of glutathione and methylglyoxal is achieved by interplay between glutathione reductase and glyoxalase cycles which are two independent complex mechanisms connected to other metabolic events. Thus, it is very crucial to understand the role of these enzymes under different abiotic stress conditions including drought and salt stress.

With increasing population and depleting fossil fuel reserves there is a huge demand for renewable bioenergy resources including biofuels which can be derived from non-edible plants such as *Jatropha*, *Pongamia* and *Camelina*. *J. curcas* is known for its high seed oil content, easy propagation, rapid growth and adaptation to a wide range of agro climatic conditions. Till date, very little is known on the adaptive strategies of this biofuel tree species to grow even under semi-arid tropics. In the previous study we characterised JcAKR which was proved to be a potential candidate gene in stress tolerance. Now, in the present study, glyoxalase I, II and GR were identified, isolated, cloned and characterized from *J. curcas*. This study aid in understanding the glutathione dependent MG detoxification potential during interactive progressive drought and salinity stress.

## Materials and methods

### *Plant material and stress treatment*

*Jatropha curcas* seeds were surface sterilized with 0.4% sodium hypochlorite and were kept for germination in dark for 7 days. The germinated seeds were transferred to pots containing a mixture of sand, red soil and manure (2:2:1). One month old plants were subjected to either salinity (200mM), drought (complete water withholding) or a combination of drought +salt (200mM+ complete water withholding) stresses in a progressive manner wherein, the measurements were taken at 7, 15 and 21 days and a set of plants which served as controls were not subjected to any stress. Leaves and roots were collected and frozen in liquid nitrogen from all the stressed and control samples and stored at -80$^{o}$C until use.

### *cDNA synthesis and gene amplification*

100mg of total RNA isolated using Plant Spectrum RNA isolation kit (Sigma-Aldrich, USA) was used for cDNA synthesis (RevertAid$^{TM}$ first strand synthesis kit, Fermentas Life Sciences, Germany). Transcripts showing highest homology with the glyoxalases and GR were obtained from transcriptome data of *J. curcas* (biosample accession number SAMNO3145040 and bioproject ID-PRJNA265009) and primers were

designed based on these sequences (Table 5). cDNA was amplified and PCR product was cloned in pTZ57RT vector (Fermentas Life Sciences, Germany) and later sequenced.

### *Multiple sequence alignment and phylogenetic analysis*

All the known amino acid sequences showing homology with glyoxalases and GR were collected from NCBI database. Bioedit was used for multiple sequence alignment whereas MEGA7 software was used for evolutionary analysis (Tamura et al. 2013). The Phylogenetic tree was constructed based on Neighbour-joining method and bootstrap method was used for test of phylogeny. The number of replications was 500. The model used was Poisson model. All positions containing gaps and missing data were eliminated.

### *Heterologous protein expression and MALDI analysis*

ORF region of JcGLYI, II and GR were considered for designing primers containing restriction enzyme sites based on multiple cloning sites of pGEX4T$^{-1}$ vector (Table 5). PCR amplification of genes was carried out using cDNA, *Pfu* DNA polymerase and Eppendorf PCR. The amplified products were gel eluted and restriction enzyme digestion was performed to these gel eluted products and the vector which were then ligated and transformed in *E. coli* BL-21 DE3 cells. Plasmid was isolated using GenElute™ HP Plasmid Miniprep Kit (Sigma-Aldrich, USA) from transformed colonies and the presence of insert was further confirmed by sequencing. JcGLYI, II and JcGR proteins were expressed by induction with 1mM isopropyl β-D-thiogalactoside (IPTG) for 6 h at 30 °C and centrifuged at 8000g for 10 min. The pellets were dissolved and sonicated in 1xPBS containing 0.5% β-mercaptoethanol and centrifuged again for 20 min at 10000g to pellet the debris. The supernatant was subjected to affinity chromatography by using CL-Agarose column from Genei™ GST-fusion protein purification kit (Bangalore Genei, Bangalore, India). 10µg of purified GST and GST-GLYI/II/GR proteins were loaded on 15% SDS-PAGE. The separated proteins were transferred on polyvinylidene fluoride (PVDF) membrane (Immobilon-

P, Millipore, MA, USA) using biorad apparatus (Bio-Rad laboratories ltd., USA). 1:10000 dilutions of primary anti-GST antibody, was used and 1:20000 of HRP-conjugated goat anti-mice IgG was used as secondary antibody. S*upersignal west pico chemiluminescent substrate* (Thermoscientific, USA) was used for developing blot and the image was developed by Kodak image station 4000 (USA).

### *Bacterial growth analysis under abiotic stress*

Stress tolerance of *E.coli* cells transformed with GST and GST-JcGLYI/II/GR were assessed by growing the bacteria in LB broth until $OD_{600nm}$ reached to 0.5 and then supplementing with either 200mM NaCl (Salt), 5% PEG (Drought) and 5% PEG+200mM NaCl (Drought+Salt) or in the absence of salt/PEG that served as control. Further, the growth was monitored for every one hour at $OD_{600nm}$.

### *Yeast growth analysis under abiotic stress*

*Yap1*, a yeast mutant which lacks YAP1, a methylglyoxal responsive element and oxidative responsive transcription factor was used to study MG toxicity in yeast and abiotic stress tolerance of glyoxalases in transformed yeast. The ORF of JcGLYI/II/GR was excised from pGEX-4T-1-JcGLYI/II/GR by digestion with restriction enzymes and ligated into the yeast expression vector p424. Frozen EZ-yeast transformation II$^{TM}$ kit (Zymo Research, USA) was used for transforming the vector constructs into yeast. The transformed cells were selected by their capacity to grow in complete synthetic medium (SC), lacking Trp (p424 selection marker). To determine the abiotic stress tolerance, yeast cells were transformed with p424 and p424-JcGLYI/II, the transformed cells were grown on SC-TRP medium supplemented independently with NaCl (200mM), PEG (5%), PEG+NaCl or MG (5mM) and the growth was observed by measuring the OD at 600nm for 36 h at 30$^{o}$C.

### *qRT- PCR analysis of JcGLYI/II and GR*

cDNA synthesis was done with total RNA isolated from leaf and root of control and treated plants. Primers were designed for JcGLYI/II, GR and 18S rRNA (Table 5).

qRT- PCR was performed according to Mudalkar et al.(2014) using SYBR mix (Kapa biosystems, USA) and Eppendorf Realplex MasterCycler (Eppendorf, Germany). The analysis was done using the formula: $F=2^{-(\Delta Ct\ treated - \Delta Ct\ control)}$(Livak and Schmittgen 2001).

### *Enzyme activities of purified and crude protein extracts*

Enzyme activities of GLY I and II were determined according to (Mustafiz et al. 2010). The reaction mixture for GLY1 had 0.1 M sodium phosphate buffer (pH 7.5), 1.7mM of GSH, 16mM of $MgSO_4$ and 1mM MG as substrate and in the presence of $Mg^{2+}/Ni^{2+}/Zn^{2+}/Co^{2+}$ metal ions. The mixture was incubated in dark for about 7 min. After incubation, 25µg of leaf, root or purified protein was added and the volume was made up to 1ml. The GLYII assay mixture contained 50mM tris HCl pH 7.2, 300µM SLG and 100µg of leaf, root or purified protein. The increase in absorbance was measured for 3 min at 240nm using a spectrophotometer (Eppendorf, Germany) at 25$^{o}$C. Specific activity was measured by taking extinction coefficient (ε) of SLG as 3.37 $mM^{-1}$ $cm^{-1}$ and expressed in units /mg of protein. Glutathione reductase (GR) activity was determined according to Contreras et al (2005). The reaction mixture contained 0.1M phosphate buffer, pH 7.0, 0.5mM oxidized Glutathione (GSSG), and 90 mM NADPH. After the addition of NADPH, its oxidation was monitored at 340nm for 1 min, and the activity was calculated using ε of NADPH as 56.2 $mM^{-1}cm^{-1}$.

### *Quantification of total glutathione*

GSSG and GSH levels were determined by Contreras et al (2005). 0.5g leaf tissue was extracted with 5% w/v sulfosalicylic acid and total glutathione (GSH+GSSG) was detected by incubating with reaction mixture containing 60µM 5,5-dithio-bis-(2-nitrobenzoic acid),and 0.66U of GR and NADPH. The colour developed was estimated at 412nm by using spectrophotometer.100µl of neutralized homogenate was incubated with 20µl of 1M 2-Vinyl pyridine for 1hour at room temperature. Then reaction mixture was added and calibration curve was prepared using 2 to 40nmol of GSH in the same reaction mixture.

### *Statistical analysis*

Samples from three biological replicates were collected at regular intervals and mean values were represented together with standard deviation (SD), for *in vitro* experiments. Analysis of variance (ANOVA) was used for further data analysis and the level of significance was set to 0.05. Statistical significance of the differences within a treatment at different time periods was indicated with capital letters and between the treatments was represented with small letters. Microsoft excel 2010 was used for data processing. Statistical analysis was performed using software, Sigma plot 11.0.

## Results and discussion

ROS generated during abiotic stress is the major cause for protein oxidation and lipid peroxidation generating toxic molecules including MDA and MG. MG is also known to be synthesized non-enzymatically from triose sugars during glycolysis in plants (Kalapos 1999). It is naturally produced in all living organisms including bacteria, yeast, animals and plants wherein its levels increase in response to various abiotic stresses. Therefore, MG is not just considered as metabolic by-product but also as an important component to activate plant defence mechanisms. Although many proteins are known to play an important role in abiotic stress tolerance in plants, very few were identified that are responsible for the detoxification of MG. In our previous study, we have reported a significant increase in MG levels when *J. curcas* plants were subjected to salinity, drought and combined salinity and drought stress compared to control. This rise in MG triggered the expression of JcAKR which was involved in its detoxification (Mudalkar et al. 2016a). The present study is focussed on the characterisation of glyoxalases from *J. curcas* wherein, the MG detoxification potentials of JcGLYI and II were investigated in bacteria and yeast. The endogenous role of these genes in abiotic stress tolerance was also studied along with JcGR.

### *Cloning, sequencing and analysis*

Transcriptome of J. curcas was screened for genes having significant homology with glyoxalases, GR and these genes were amplified from leaf cDNA of Jatropha using

gene specific primers containing restriction enzyme sites (Table 5). PCR products of 1140, 777 and 1224 bp were obtained for JcGLYI, II and GR, respectively. These were gel purified and cloned into pTZ57R vector and the presence of the insert was confirmed by plasmid PCR and sequencing, using insert specific primers. GLYI's are monomeric/dimeric and some of them have also evolved into a multigenic family in plants such as Arabidopsis and rice. Monomeric or dimeric proteins may have single active site or two active sites with a metal coordination site (Mustafiz et al. 2014). GLYII proteins are monomeric belonging to the superfamily of metallo-beta-lactamases (Kaur et al. 2013; Mustafiz et al. 2011; Singla-Pareek et al. 2008; Yadav et al. 2007). In silico analysis of glyoxalases from *J. curcas* revealed that JcGLY1gene encodes for a protein of 379 amino acids having two possible active sites with a molecular weight of 41.7 kDa and a theoretical pI of 6.38 presuming it to be a monomeric protein. The consensus sequence of LHVVY at N-terminal, which is also conserved in *A. thaliana, B. napus* and *M. truncatula* was found in JcGLYI, whereas DPDG sequence was observed at C-terminal region which is conserved among bacteria, yeast, humans and plants (Fig. 23) (Kaur et al. 2013). JcGLYII was also a monomeric protein with a molecular weight of 28.7 kDa and pI of 5.7 having a conserved THxHxDH motif which is a characteristic feature of glyoxalse II, observed in yeast, humans, *Arabidopsis* and *B. juncea* (Fig. 24) (Ridderstrom and Mannervik 1997a; Saxena et al. 2005; Schilling et al. 2003; Yadav et al. 2007). Conserved domain data analysis (CDD) of JcGLYI gave a specific hit to glyoxalase I showing conserved regions for lactoyl glutathione lyase belonging to a superfamily of structurally related metallo-proteins which include glyoxalase I and proteins involved in antibiotic resistance. JcGLYII had a specific hit with hydroxyacyl glutathione hydrolase with multidomains for metal-dependent hydrolase and metallo-beta-lactamase II superfamily. Translated cDNA sequence of JcGR gave a protein sequence of 407 amino acids that encodes for a cytosolic protein having a molecular weight of 44 kDa and a theoretical pI of 5.57. The conserved domain analysis gave a specific hit for pyridine nucleotide-disulphide oxidoreductase showing conserved domains for superfamily of

Rossmann-fold NAD(P)+ binding proteins and multi domains for glutathione-disulphide reductases of plants (Table 6). The multiple sequence alignment of JcGR with other organisms showed conserved domains of IGxGSGG at N-terminal and GTCVxxGCVPKK domain that forms a redox center/redox active disulphide bridge which aids in transferring the reducing equivalents to glutathione from FAD (Fig. 25) (Couto et al. 2016). This conservation of glyoxalases and GR from *E. coli* to humans and plants indicates their evolutionary importance in abiotic stress tolerance. Phylogenetically, JcGR clustered with *H. brasiliensis* which also belongs to the same family as that of Jatropha while, JcGLYI and II grouped with plant species of various families and they are first to be characterized from Euphorbiaceae (Fig. 26, 27 and 28). Moreover, JcGLYI showed maximum homology and grouped with $Ni^{2+}$ specific GLYIs from *E. coli*, *O. sativa*, *Z. mays*, *P. trichocarpa* and *T. aestivum* which possess two active sites in a single peptide, thus giving a clue that JcGLY1 is a monomeric Ni specific protein (Kaur et al. 2013). Recent findings showed that $Zn^{2+}$ dependent GLYI are known to have unique short amino acid sequence regions which are absent in $Ni^{2+}$ dependent enzymes. The multiple sequence alignment of JcGLYI indicated the absence of these short regions thus indicating its $Ni^{2+}$ dependency. Further, the presence of long N – terminal sequence which is a characteristic feature of $Zn^{2+}$ activated GLYI was present in JcGLYI. This could be presumably because, most of $Zn^{2+}$ activated proteins are also known to be activated by $Ni^{2+}$, $Co^{2+}$, $Mg^{2+}$ and $Mn^{2+}$. The presence of this long arm may possibly help the stabilization of quaternary structure of the $Ni^{2+}$ specific JcGLYI (Suttisansanee et al. 2015).

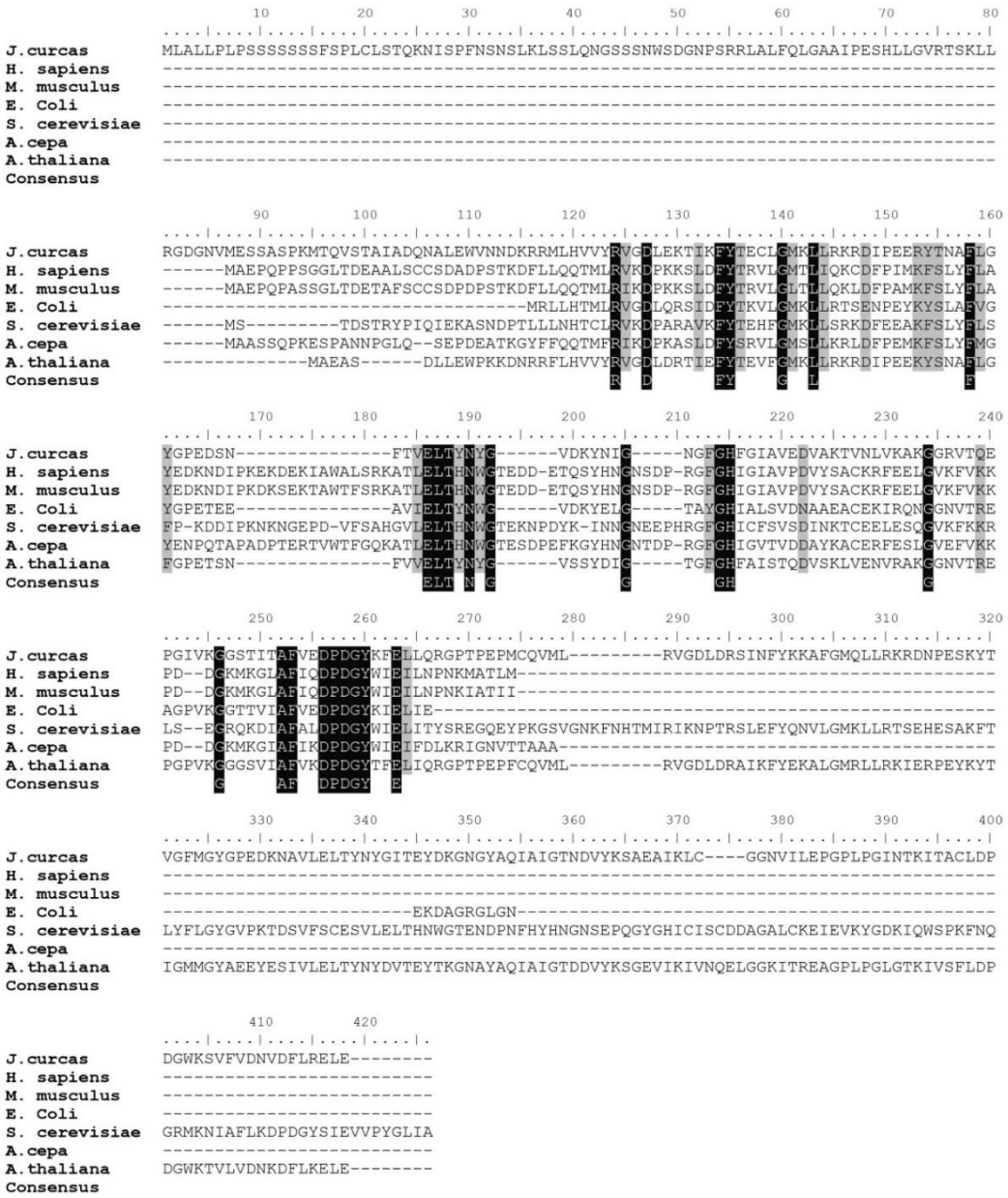


**Fig. 23.** Multiple sequence alignment of JcGLYI with deduced amino acid sequence from various organisms including bacteria, yeast and plants.

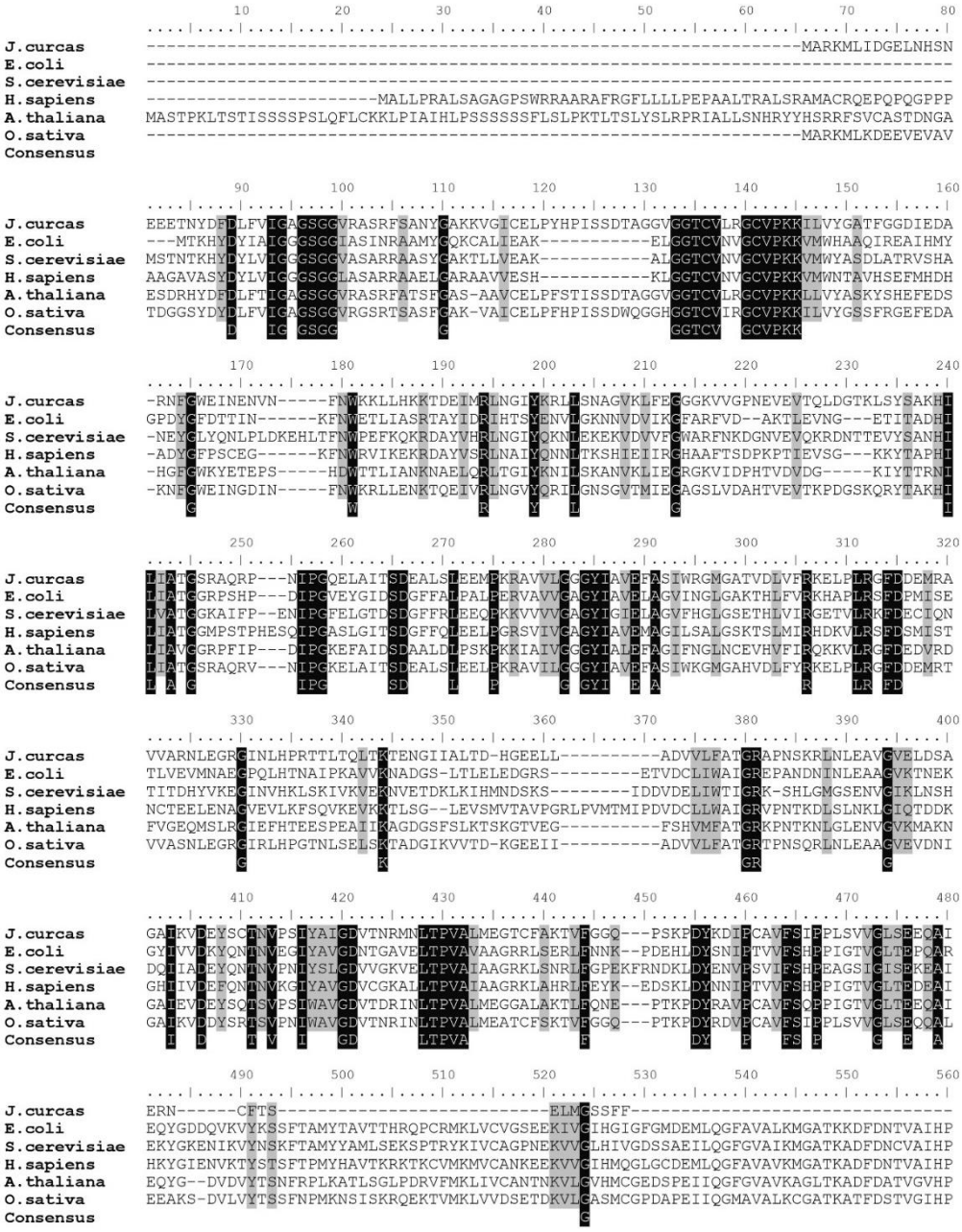


**Fig. 24.** Multiple sequence alignment of JcGLYII with other plants, *E.coli*, Saccharomyces and humans.

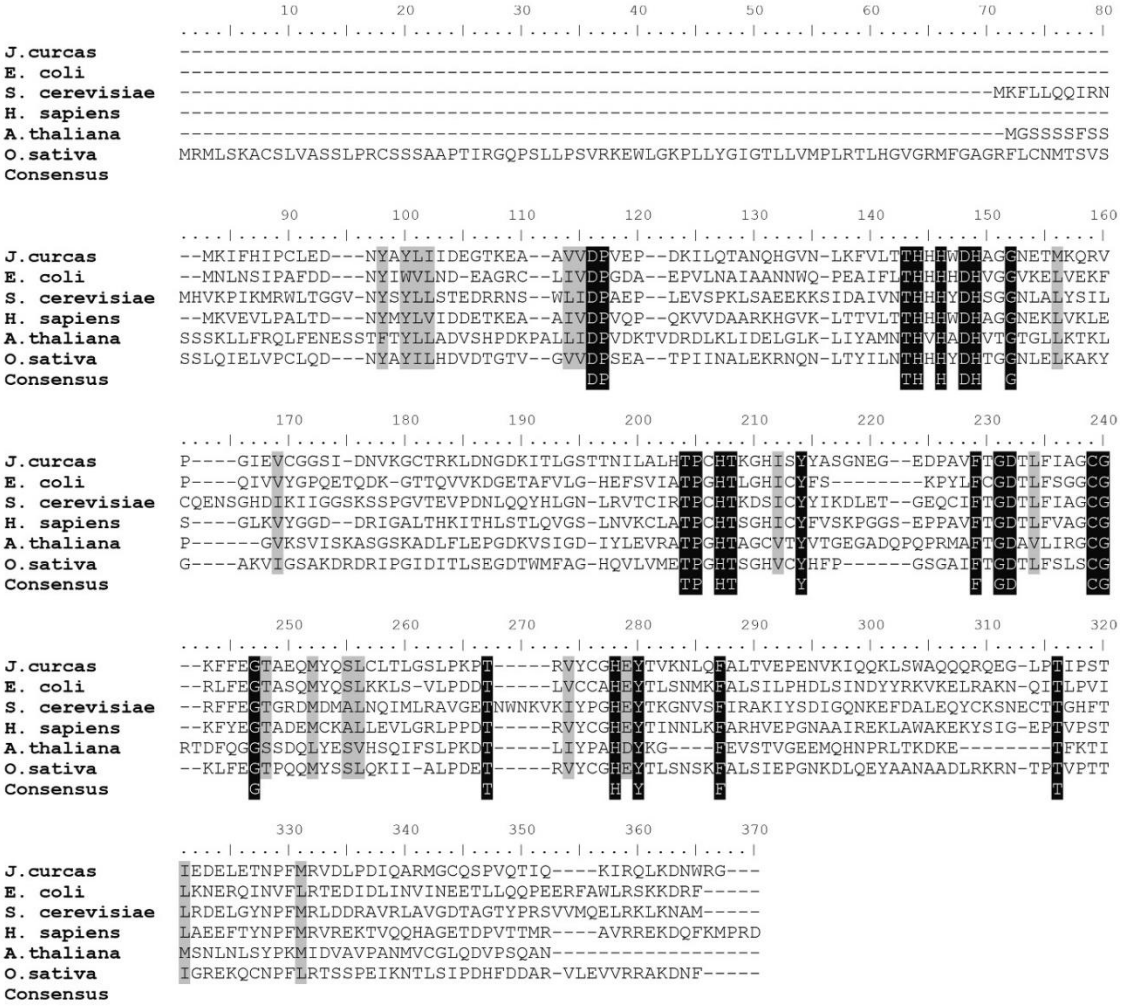


**Fig. 25.** JcGR-Multiple alignment of deduced amino acid sequence with other organism.

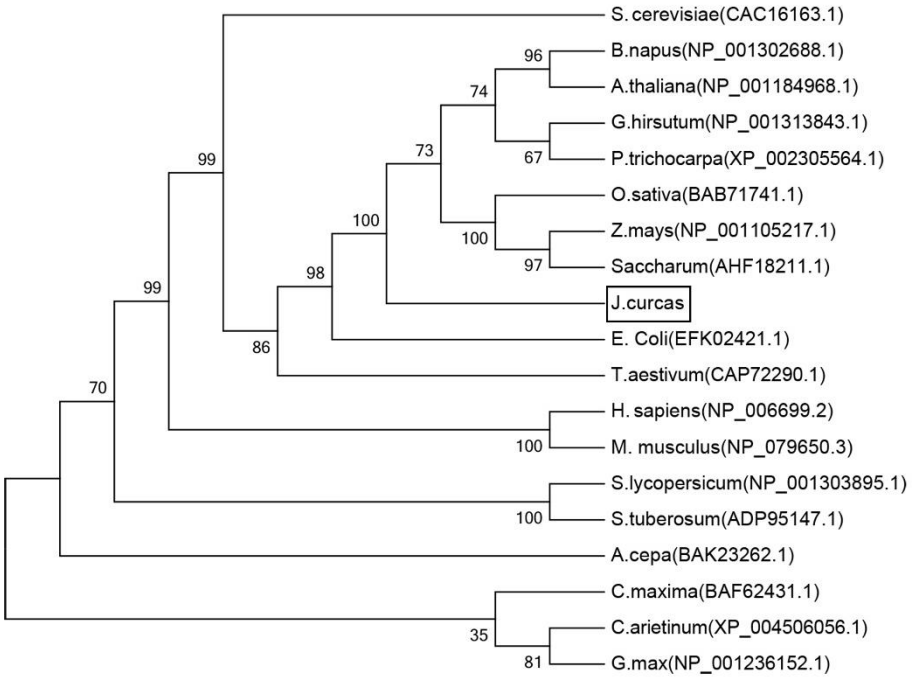


**Fig. 26.** Evolutionary relationships of taxa for JcGLYI. The evolutionary history was inferred using the Neighbor-Joining method. The bootstrap consensus tree inferred from 500 replicates is taken to represent the evolutionary history of the taxa analyzed. Branches corresponding to partitions reproduced in less than 50% bootstrap replicates are collapsed. The percentage of replicate trees in which the associated taxa clustered together in the bootstrap test (500 replicates) is shown next to the branches. The evolutionary distances were computed using the Poisson correction method and are in the units of the number of amino acid substitutions per site. The analysis involved 20 amino acid sequences. All positions containing gaps and missing data were eliminated. There were a total of 128 positions in the final dataset. Evolutionary analyses were conducted in MEGA7.

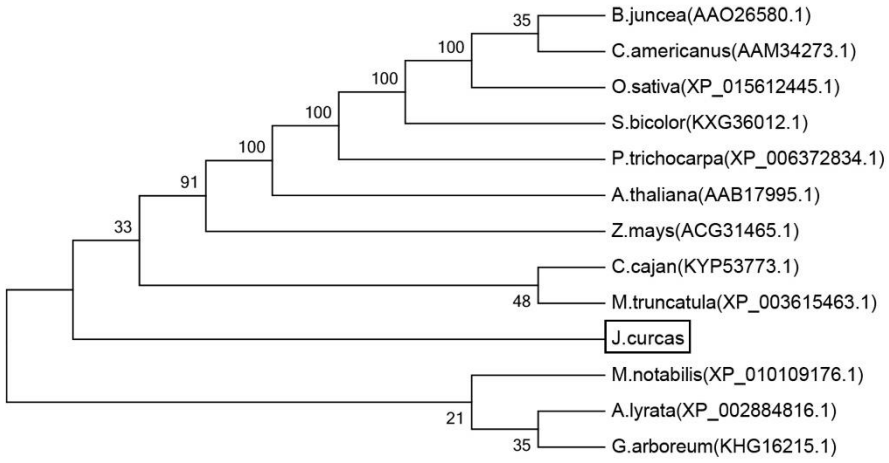


**Fig. 27.** Evolutionary relationships of taxa for JcGLYII. The analysis involved 13 amino acid sequences and there were a total of 219 positions in the final dataset. The evolutionary history was inferred using the Neighbor-Joining method. The bootstrap consensus tree inferred from 500 replicates is taken to represent the evolutionary history of the taxa analyzed. Branches corresponding to partitions reproduced in less than 50% bootstrap replicates are collapsed. The percentage of replicate trees in which the associated taxa clustered together in the bootstrap test (500 replicates) is shown next to the branches. The evolutionary distances were computed using the Poisson correction method and are in the units of the number of amino acid substitutions per site. The analysis involved 20 amino acid sequences. All positions containing gaps and missing data were eliminated. There were a total of 128 positions in the final dataset. Evolutionary analyses were conducted in MEGA7.

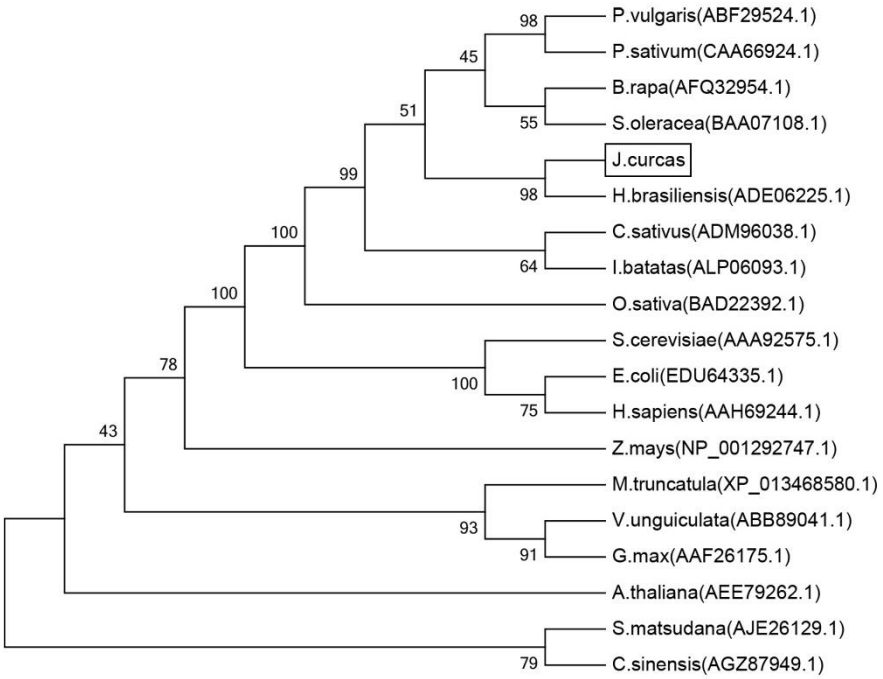


**Fig. 28.** Evolutionary relationships of taxa JcGR. The analysis involved 19 amino acid sequences and there were a total of 340 positions in the final dataset.

**Table 5:** List of Primers used in the study for target gene amplification

| S. No. | Primer | Sequence 5'-3' | Product size (bp) |
|---|---|---|---|
| 1 | JcGLY1 BF | gtaggatccATGCTAGCACTGCTGCCACTG | 1140 |
| | JcGLY1 ER | ccggaattccggTCACTCCAGTTCCCTGAG | |
| 2 | JcGLY2 EF | ccggaattccggATGAAAATATTTCATATCCCT | 777 |
| | JcGLY2 XR | gtactcgagTTAGCCTCTCCAATTGTC | |
| 3 | JcGR BF | gtaggatccATGGCAAGGAAAATGCTTATC | 1224 |
| | JcGR ER | ccggaattccggTCAAAAGAAAGAAGACCCCAT | |
| 4 | JcGLY1 qRTF | GCCTACACCTGAGCCAATGT | 182 |
| | JcGLY1 qRTR | TCAGTTCCAGCACAGCATTC | |
| 5 | JcGLY2 qRTF | GAGGGCACTAAAGAAGCAGC | 174 |
| | JcGLY2 qRTR | ACCACAGACCTCAATCCCAG | |
| 6 | JcGR qRTF | TTGGTGGAGGGTACATTGCT | 177 |
| | JcGR qRTR | TCAAAGTCGTCCTAGGGTGC | |

### *Protein expression, purification and enzyme assay*

JcGLYI, II and GR proteins were expressed in *E.coli* BL-21 (DE3) cells with GST as fusion protein in pGEX4T-1 vector and SDS-PAGE analysis showed that the cells transformed with only pGEX4T-1 expressed GST protein with a molecular mass of 26.5 kDa whereas GST fused JcGLYI, II and GR gave 68.7 kDa, 54.7 kDa and 70 kDa bands, respectively (Fig. 29A, B and C). The expression of protein was further confirmed by performing western blot analysis with anti-GST antibody (Fig. 29D, E and F). MALDI-TOF followed by MASCOT search analysis of GST cleaved JcGLYI and II gave hit to probable glyoxalases I and II of *J. curcas* with MS score of 57 and 40 and sequence coverage of 15 and 8 respectively. Whereas, JcGR matched with *P. sativum* with 9% coverage and 66 MS score (Table 7).

Glyoxalases are metalloenzymes and they require divalent metal ions for their activity. Previously, GLYI's were categorised either as $Zn^{2+}$ or $Ni^{2+}/Co^{2+}$ dependent enzymes, where the former was believed to be present in eukaryotes and latter in prokaryotes. However, recent reports have shown the presence of both the forms in prokaryotes and eukaryotes (Kaur et al. 2013). GLYI from *B. juncea* is a $Zn^{2+}$ metalloenzyme whereas Ni2+ specific GLYI was identified from rice (Deswal and Sopory 1998; Veena et al. 1999). Binding of metal ion as a cofactor plays a key role in the formation of active sites and changing structural conformation of the enzyme (Suttisansanee et al. 2011). Enzyme kinetic analysis was performed to establish $V_{max}$ and $K_m$ values in the presence of different metal ions. The $V_{max}$ of GST cleaved JcGLYI with hemithioacetal as substrate and $Zn^{2+}$, $Mg^{2+}$, $Ni^{2+}$, $Co^{2+}$ metal ions as individual cofactors was 0.869, 0.931, 1.088 and 0.284 mmol $min^{-1}$ $mg^{-1}$ protein respectively (Table 8). The $V_{max}$ values were almost similar for $Zn^{2+}$ and $Mg^{2+}$ since most of the enzymes that are dependent on $Zn^{2+}$ were also known to be activated by $Mg^{2+}$ (Sukdeo and Honek 2007). At saturating substrate concentrations, the $K_m$ values of JcGLYI showed varying affinities towards hemithioacetal depending on the metal ion used. Higher affinity and turnover number of JcGLYI were observed in the presence of $Ni^{2+}$ when compared to other metal ions

as indicated by the Km (17 µM) and $K_{cat}$ values (14.7 $sec^{-1}$) (Table 8). The high catalytic efficiency ($K_{cat}/K_m$) of JcGLYI with $Ni^{2+}$ as cofactor, its sequence analysis and phylogenetic relationship with other GLYIs' indicated the Ni specific nature of JcGLYI. The JcGLYI activity was significantly higher than that of purified OsGLY1 from rice which was reported to be 0.13 mmol $min^{-1}$ $mg^{-1}$ (Mustafiz et al. 2014). The specific activities and turnover numbers of GLYI varied significantly from species to species, wherein the $K_{cat}$ values ranged from 1.38 to 1120 $s^{-1}$ (Clugston et al. 1998; Ridderstrom et al. 1997b; Suttisansanee et al. 2011; Vander Jagt and Han 1973). The catalytic efficiency of JcGLYI was lower than that of *S. cerevisiae* (*Kcat*/*Km* - 0.35 x 107), Homo sapiens (2.7 x $10^7$) and *E. coli* (1.24 x $10^7$), while it was higher than that of *O. sativa* (0.71 x $10^6$) and *C. acetobutylicum* (2.6 x $10^3$). The specific activity of purified JcGLYII with SLG as substrate was 0.913 mmol $min^{-1}$ $mg^{-1}$ while, $K_m$ and $K_{cat}$ were found to be 189 µM and 7.65 $sec^{-1}$ respectively (Table 8). The affinity of JcGLYII towards SLG was lower when compared to *B. juncea* (BjGLYII) and *O. sativa* (OsGLYII) whereas it was higher than that of *S. cerevisiae* permeabilized cells (Martins et al. 1999; Saxena et al. 2005; Yadav et al. 2007). Purified JcGR gave a specific activity of 0.1205 mmol $min^{-1}$ $mg^{-1}$ protein and $K_m$ was 66.09 µM and $K_{cat}$ 3.37 $sec^{-1}$ (Table 8).

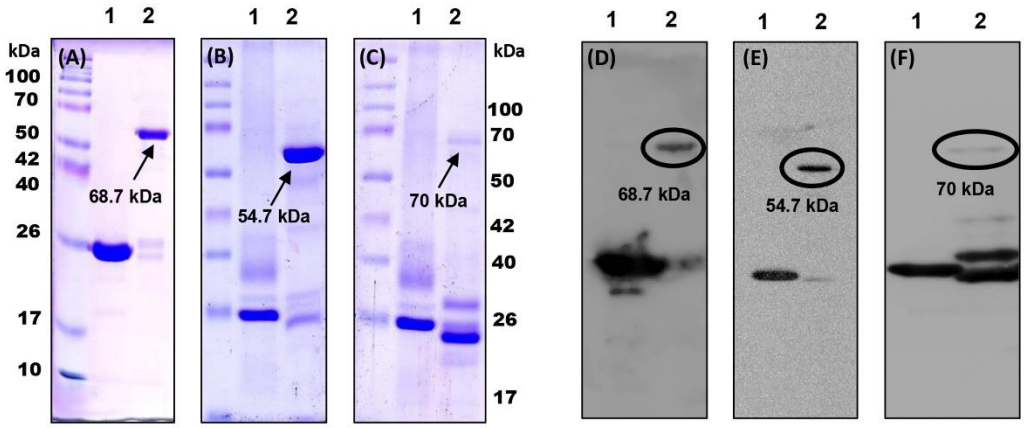


**Fig. 29.** Overexpression, purification and western blot analysis of JcGLYI, II and GR. 12% SDS-PAGE of GST and GST fused **(A)** JcGLYI, **(B)** JcGLYII and **(C)** JcGR stained with coomassie brilliant blue R 250 and Western blot for corresponding GST fused proteins **(D)** JcGLYI, **(E)** JcGLYII and **(F)** JcGR with anti-GST antibody. In all planes, lane 1 represents GST protein and lane 2 the corresponding GST fused targeted protein.

**Table 6:** Conserved regions of JcGLYI, II and GR

| Protein identified | Specific hit | Non-specific hits | Superfamily | Multi domains |
|---|---|---|---|---|
| JcGLYI (*Jatropha curcas* Glyoxalase 1) | Cd07233, Glyoxalase I | 1. TIGR00068: Lactoylglutathione lyase<br>2. PRK10291: Glyoxalase I<br>3. pfam00903: Glyoxalase/Bleomycin resistance protein/Dioxygenase superfamily<br>4. COG0346: Catechol 2,3-dioxygenase or other lactoylglutathione lyase family enzyme | 1. cl14632: This domain superfamily is found in a variety of structurally related metalloproteins, including the type I extradiol dioxygenases, glyoxalase | 1. PLN02300: lactoylglutathione lyase<br>2. TIGR02295: 3,4-dihydroxyphenylacetate 2,3-dioxygenase ;This enzyme catalyzes the second step in the degradation of 4-hydroxyphenylacetate to succinate and pyruvate |
| JcGLYII (*Jatropha curcas* Glyoxalase 2) | PLN02469, hydroxyacylglutathione hydrolase | 1.TIGR03413, hydroxyacylglutathione hydrolase<br>2. smart00849, Metallo-beta-lactamase superfamily<br>3. pfam00753, Metallo-beta-lactamase superfamily<br>4. COG1237, Metal-dependent hydrolase, beta-lactamase superfamily II | 1.cl00446, Metallo-beta-lactamase superfamily ; | 1.COG0491, Glyoxylase or a related metal-dependent hydrolase, beta-lactamase superfamily II<br>2. PLN02398, hydroxyacylglutathione hydrolase |
| JcGR (Jatropha curcas Glutathione reductase) | Pfam00070, Pyridine nucleotide-disulphide oxidoreductase | 1.pfam02852, Pyridine nucleotide-disulphide oxidoreductase, dimerization domain | 1. pfam02852, Pyridine nucleotide-disulphide oxidoreductase, dimerization domain<br>2. cl21454, Rossmann-fold NAD(P)(+)-binding proteins | 1.TIGR01424, glutathione-disulfide reductase, plant<br>2.PLN02507, glutathione reductase<br>3.COG1249, Pyruvate/2-oxoglutarate dehydrogenase complex<br>4. pfam07992, Pyridine nucleotide-disulphide oxidoreductase COG1249, Pyruvate/2-oxoglutarate dehydrogenase complex. |

**Table 7:** Identification of JcGLYI, II and GR with MALDI and MASCOTsearch analysis

| Protein identified | Peptide sequences matched | Theoretical Mr/pI | Accession no. | Sequence coverage (%) | Reference organism | MS/MS score |
|---|---|---|---|---|---|---|
| JcGLY1 | 1. R.GDGNVMESSASPK.M<br>2. R.YTNAFLGYGPEDSNFTVELTYNYGVDK.Y<br>3.K.LCGGNVILEPGPLPGINTK.I | 42kDa/6.4 | gi/802633310 | 15 | *Jatropha curcas* | 57 |
| JcGLY2 | 1. R.QEGLPTIPSTIEDELETNPFMR.V | 29kDa/5.79 | gi/802778276 | 8 | *Jatropha curcas* | 40 |
| JcGR | 1. K.HILIATGSR.A<br>2. K.ELPLRGFDDEMR.A<br>3. K.VGICELPFHPISSETIGGVGGTCVIR.G | 54kDa/6.59 | GSHRC PEA | 9 | *Pisum sativum* | 66 |

**Table 8:** Enzyme kinetics of GST-JcGLYI, II and GR with specific substrates respectively

| Enzyme | Substrate | Metal ion | Substrate concentration (mM) | Specific activity (µmol $min^{-1}$ $mg^{-1}P$) |
|---|---|---|---|---|
| JcGLY1 | Methylglyoxal | $Zn^{2+}$ | 1 | 6.7±0.15 |
| | | $Mg^{2+}$ | 1 | 6.5±0.1 |
| | | $Ni^{2+}$ | 1 | 3.2±0.12 |
| | | $Co^{2+}$ | 1 | 3.0±0.05 |
| JcGLY2 | SLG | - | 1 | 3.8±0.01 |
| JcGR | GSSG | - | 1 | 1.0±0.1 |

*MG detoxification and abiotic stress tolerance in bacteria and yeast*

Complementation in mutants with loss of function has been generally used for functional analysis of plant genes. Since obtaining a plant mutant for most of the genes is not feasible, heterologous systems such as bacteria and yeast are widely used. In order to assess the protective role of glyoxalases and GR, the relative genes were cloned in pGEX4T$^{-1}$ and p424 vectors for studies in bacteria and yeast respectively. In bacteria, MG decreased cell viability in control cells whereas the cells harbouring GLY I and II showed resistance and survived to a larger extent when they were supplemented with either NaCl (200mM), PEG (5%) or both NaCl and PEG as well as MG (5mM), thus protecting the bacteria from these oxidative stress inducing agents (Fig. 30A, B, C and D). Our results clearly corroborated with the decreased tolerance observed in E.coli mutants for GLXII and GLXII-2 (ΔgloB and ΔgloC respectively) to MG (Reiger et al. 2015). Also, bacteria when harboured with JcGR showed resistance and survived against NaCl, PEG and both the treatments. Interestingly, JcGR showed mild resistance against MG treatment suggesting that increased GSH turnover by GR aid in MG detoxification by inherent glyoxalases of bacteria, thus facilitating its active growth (Fig. 30E).

JcGly1, II and JcGR also showed similar type of protection when transformed into yeast, where the transformed yeast cells exhibited better growth against aforesaid stress causing agents (Fig. 31A, B and C). MG was found to activate several signal transduction pathways in yeast including transcription factors such as Yap1 and Msn2, and triggers a Hog1 mitogen-activated protein (MAP) kinase cascade in *S. cerevisiae*. However, when it crosses over threshold levels, it results disturbances in this signal transduction and thus becoming toxic to the yeast (Maeta et al. 2004; 2005). Overexpression of glyoxalases I and II in deletion mutants Δglo1 and 2 of *S. cerevisiae* prevented the sensitivity caused by MG (Ispolnov et al. 2008). Our results clearly showed that both glyoxalases and MG can be considered as markers for plant abiotic stress responses. Glyoxalases from other plant species including rice, sugarbeet, Arabidopsis were also proved to be potential detoxifiers of MG as they conferred enhanced tolerance to various abiotic stressors such as NaCl and $H_2O_2$ (Mustafiz et al. 2014; Wu et al. 2013; Yadav et al. 2007). In the present study, there was an increased viability in cells exposed to MG and abiotic stress, due to the presence of JcGLYI, II

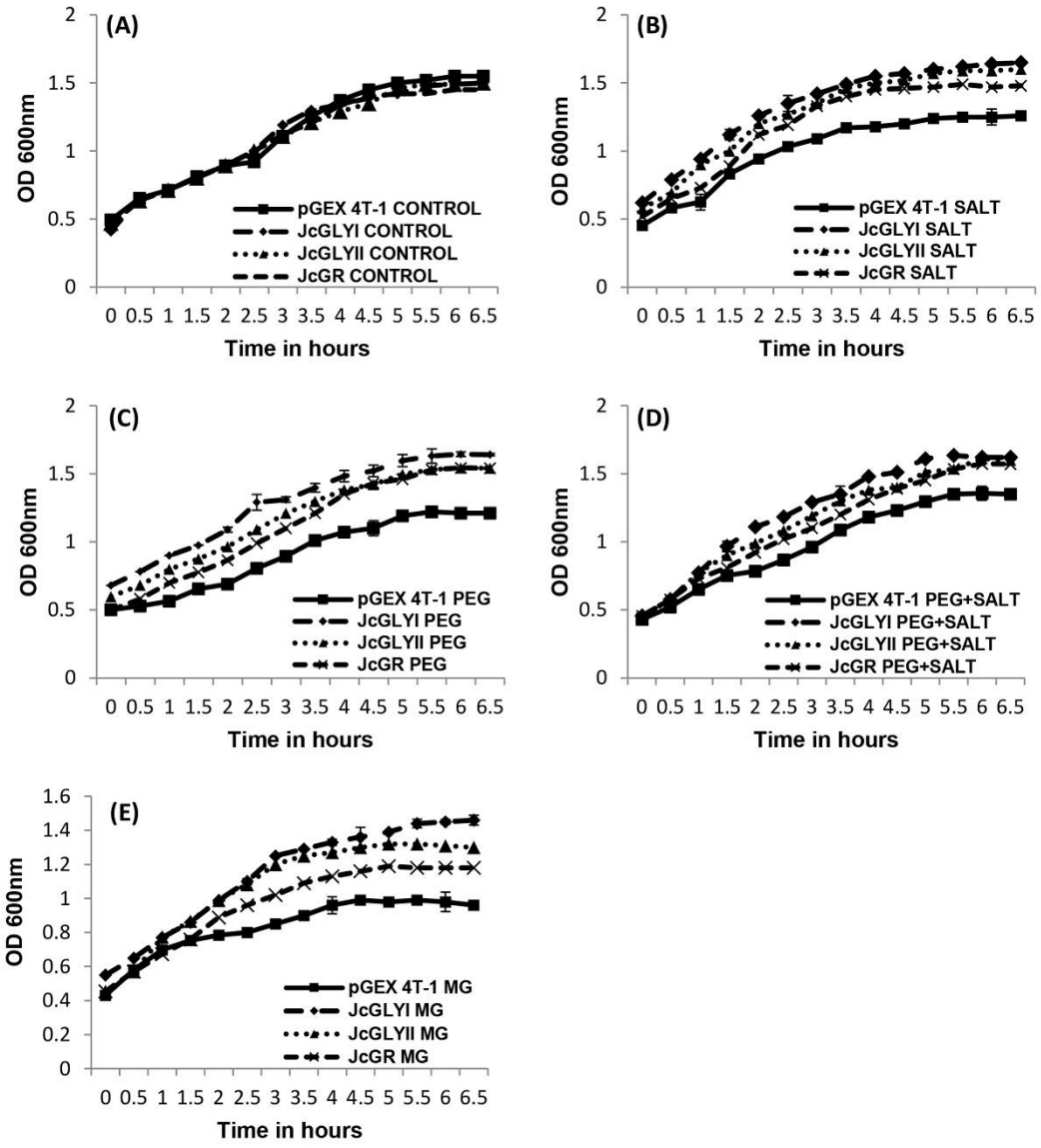


**Fig. 30.** Bacterial cells expressing GST and GST-JcGLYI, II and GR were grown in LB broth supplemented with ampicillin till $O.D_{600}$-0.5, the cultures were induced with 1mM IPTG **(A)** untreated control **(B)** 200mM NaCl, **(C)** 5% PEG or **(D)** 5% PEG+200mM NaCl for salt, osmotic and osmotic+salt stress, respectively and $O.D_{600}$ was measured respectively for each treatment. Data are the mean ± SD (n=3).

and JcGR which could act as stress protective enzymes in bacteria and yeast by overcoming the harmful effects of abiotic stress.

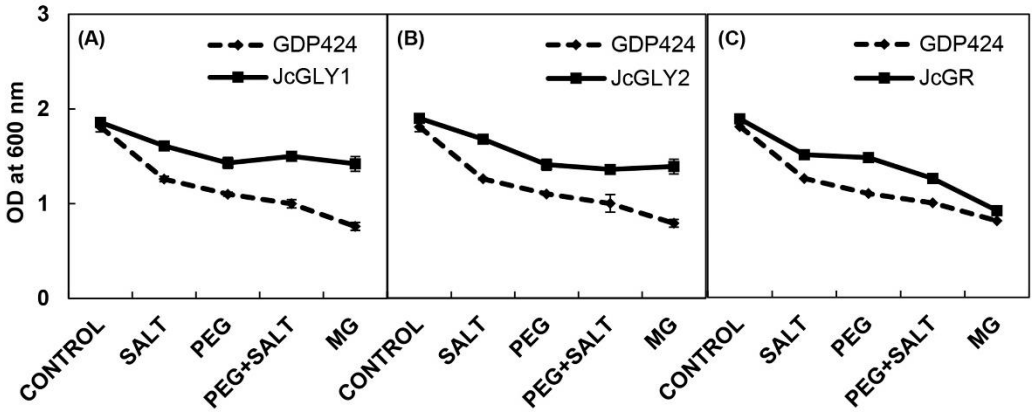


**Fig. 31.** Yeast growth for abiotic stress tolerance. Vector p424 and the construct p424-JcGLYI, II and GR were introduced into Yap-1 cells and the transformed cells were selected by their capacity to grow in complete synthetic medium (SC), lacking Trp (p424 selection marker). To determine the abiotic stress tolerance, yeast cells were grown in liquid SC-TRP medium supplemented independently with NaCl (200mM), PEG (5%), PEG+NaCl or MG (5mM) and the growth was observed by measuring the OD at 600nm for 36 h at 30°C for **(A)** JcGLYI, **(B)** JcGLYII and **(C)** JcGR. Data are the mean ± SD (n=3).

### *Role of glyoxalases and glutathione reductase in abiotic stress tolerance in J. curcas*

Abiotic stress tolerance is a multigenic trait which is controlled at multiple loci and glyoxalases are considered to be the primary components involved in plant defence mechanism where they are expressed in a time-dependent and differential manner during various abiotic stresses such as salinity, heat, desiccation, cold, metal and abscisic acid/ salicylic acid treatment (Kaur et al. 2014; Yadav et al. 2007). The upregulation of glyoxalases and other antioxidant systems such as GR was observed when plants were exogenously treated with selenium, nitric oxide, proline and glycine betaine by alleviating drought and salinity stress in rape seed, wheat and cultured tobacco cells, respectively (Hasanuzzaman and Fujita 2011; Hoque et al. 2008; Mostofa and Fujita 2013). In order to assess the interaction of glyoxalases and glutathione reductase in *J. curcas* during abiotic stress tolerance, the transcript abundance of these genes was analysed by qRT-PCR. One month old Jatropha plants subjected to salinity,

drought or combined stresses showed differential expression patterns of JcGLYI, JcGLYII and JcGR genes in roots and leaves. There was an upregulation of JcGLYI gene in drought (D) and combined drought and salinity (DS) stress at 7 (D-8.5, DS-7.5 folds) and 15DAS (D- 2.1, DS- 3.6 folds) which decreased at 21DAS in leaves; whereas in roots it got upregulated at 7DAS (D-1.5, DS-2 folds) and has not shown much difference at 15 and 21DAS (Fig. 32A, B). GLYII is a successor of GLYI and showed coordinated expression with that of GLYI. While JcGLYI has not shown any significant upregulation in Jatropha under salt stress, the transcript levels of JcGLYII were upregulated at 7 and 15DAS in leaf, whereas in root the transcript levels reduced during severe stress (21DAS) except in DS root (2 folds) (Fig. 32C, D). JcGR transcripts were also upregulated under drought and combined stress throughout the experimental periods. JcGR increased to 2.5, 6.5 and 4 folds at 7DAS for salt, drought and combined stress respectively when compared to control unstressed plants. However, the expression decreased at 15DAS which eventually increased at 21DAS (Fig. 32E, F).

Further, enzyme activities of these three key enzymes during various time points under different stress conditions were assessed to understand the stress tolerance potential of Jatropha. The activities of JcGLY1 and JcGLYII enzymes in leaf extracts showed enhancement under drought and combined stress during 7 DAS which decreased eventually as the stress progressed (Fig. 33A, C). Roots showed much dynamic behaviour of enzyme activities wherein, the activities were more at 7 DAS which decreased at15 DAS and further increased by 21 DAS when compared to control plants (Fig. 33B, D). However, there was no significant increment in activities of these enzymes under salt stress except at 7 DAS which is in accordance with their transcript levels. We infer from our results that the glyoxalase system involving GLYI and GLYII is highly active under drought stress rather than salt, signifying either the salt tolerance nature of Jatropha or involvement of other MG detoxifying enzymes like glutathione independent glyoxalases and AKRs. In our experiments, Jatropha exhibited morphological and physiological stability under salt stress till 15 DAS suggesting its salt tolerance nature. Mineral uptake occurs through xylem along with water and severe

drought decreases the water conduction as a result, the mineral uptake is also disturbed. Salinity interferes with uptake of essential nutrients from soil and excess sodium in soil replaces many essential metal ions such as $Ca^{2+}$, $Mg^{2+}$, $Zn^{2+}$, and $Ni^{2+}$ ions. $Zn^{2+}$ is an essential micronutrient to plants where, its deficiency leads to decrease in growth hormones, which results in reduced internodal length. Whereas, $Mg^{2+}$ is an integral part of chlorophyll which is essential for photosynthesis and plant growth and $Ni^{2+}$ is an important component of urease (Cakmak 2000; Polacco et al. 2013; Verbruggen and Hermans 2013). Apart from regulating the growth hormone biosynthesis, the availability of these metal ions also determine the activity of GLYI. In turn, it was reported that the exogenous application of hormones such as ABA/salicylic acid increased GLYI activity suggesting the interrelation of metal availability/growth hormone synthesis and GLY1 activity (Mostofa and Fujita 2013). Further, the phytoremediating ability of *J. curcas* justifies the presence of metal dependent JcGLYI enzyme wherein excess metals are translocated to various tissues by metallothioneins and phytochelatins and these sequestered metals could serve as cofactors for other metal dependent enzymes such as GLY1. In Jatropha, the gradual decrease in metal dependent JcGLYI activity and mRNA levels during severe stress (21DAS) compared to moderate stress (7 DAS) could be due to the imbalance in mineral uptake and ion homeostasis as a result of drought and salt stress. However, the activities of JcGLY1 and JcGLYII in leaves and roots of stressed samples were more when compared to control samples throughout the experimental periods indicating the active participation of these two enzymes in MG detoxification under abiotic stress. A similar increase in GLYI and GLYII activities was also observed in onion bulbs when the callus was subjected to drought and salt stress (Hossain and Fujita 2009). Also, there was a significant difference between the activities of both the enzymes in leaves and roots at 21 DAS presumably indicating effective stress sensing mechanisms of roots as they are the first to sense the soil originated abiotic stress. It is also evident from our results that combined drought and salt stress showed additive effects when compared to individual stresses on Jatropha. Depending on the type and severity of the stress conditions, in

addition to glyoxalase system, plants usually operate glutathione independent pathways to detoxify MG. These pathways involve proteins such as AKRs/ aldose reductases, aldehyde dehydrogenases and DJ1/GLXIII which were reported to exhibit combinatorial effects (Ghosh et al. 2016; Kwon et al. 2013; Misra et al. 1995; Sengupta et al. 2015; Turoczy et al. 2011; Yamauchi et al. 2011). The down regulation of JcGLYI and II along with GR at 15DAS in this study could also be attributed to the involvement of AKRs wherein, the expression and activity of JcAKR was high at 15DAS when subjected to salt, drought and drought+salt stress (Mudalkar et al. 2016). Therefore, a co-ordinated regulation between glutathione dependent and independent glyoxalases and AKRs could be an important strategy for detoxifying MG for abiotic stress tolerance in plants.

MG is known to reduce the levels of GSH which is an important antioxidant and glyoxalases not only detoxify MG but also recycle GSH thus maintaining its regeneration and homeostasis. GR is another enzyme, actively involved in the regeneration of GSH wherein it helps in the reduction of GSSG to GSH. In plants, GR proportionately showed enhanced activity in response to various stresses including NaCl and drought, thus indicating its role in abiotic stress tolerance (Meloni et al. 2003). It was also shown that exogenous application of GSH will reduce MG levels in GLYI transformed tobacco plants providing an evidence for interdependence of glyoxalase and glutathione metabolic systems (Yadav et al. 2005a). In Jatropha, GR was significantly upregulated in all the three stress treatments, nevertheless, highest activity was observed in combined stress treatment (Fig. 33 E, F). Reduced glutathione is also required for conversion of DHA to ASA which in turn acts as important non-enzymatic antioxidant by dehydroascorbate reductase. Thus, a higher ratio of GSH: GSSG is important for cell survival to combat various abiotic and biotic stresses (Noctor et al. 1998). In the present study, *J. curcas* plants showed an increased total glutathione content during all stress treatments at 7 DAS with a higher GSH: GSSG ratio (Fig. 34). Though, the levels of total glutathione was reduced during severe stresses, Jatropha maintained higher GSH content, which can be correlated with higher GR activity, in

order to provide tolerable amounts of reductants for various antioxidative defence reactions.

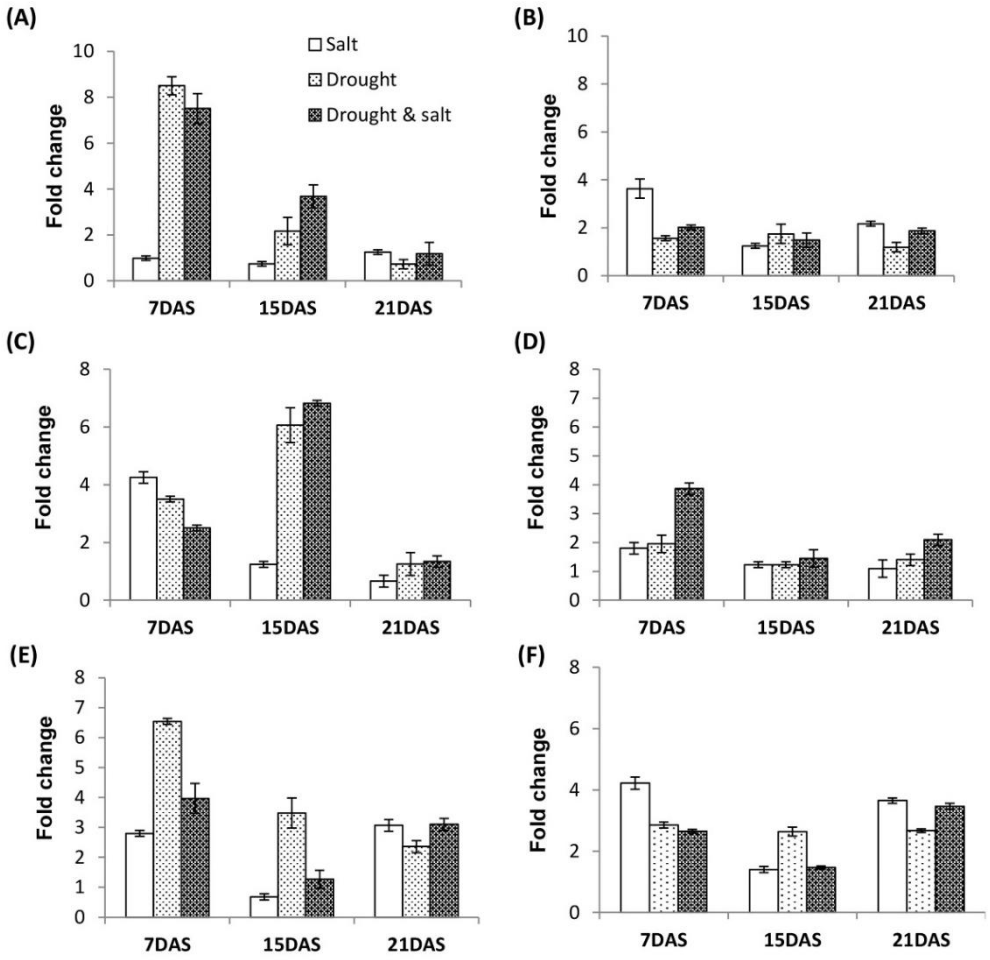


**Fig. 32.** qRT-PCR analysis of targeted genes. JcGLYI **(A)** leaf **(B)** root. JcGLYII **(C)** leaf **(D)** root and JcGR **(E)** leaf, **(F)** root at 7, 15 and 21DAS during salt, drought and drought + salt stress. Data presented is the mean ± SD (n=3).

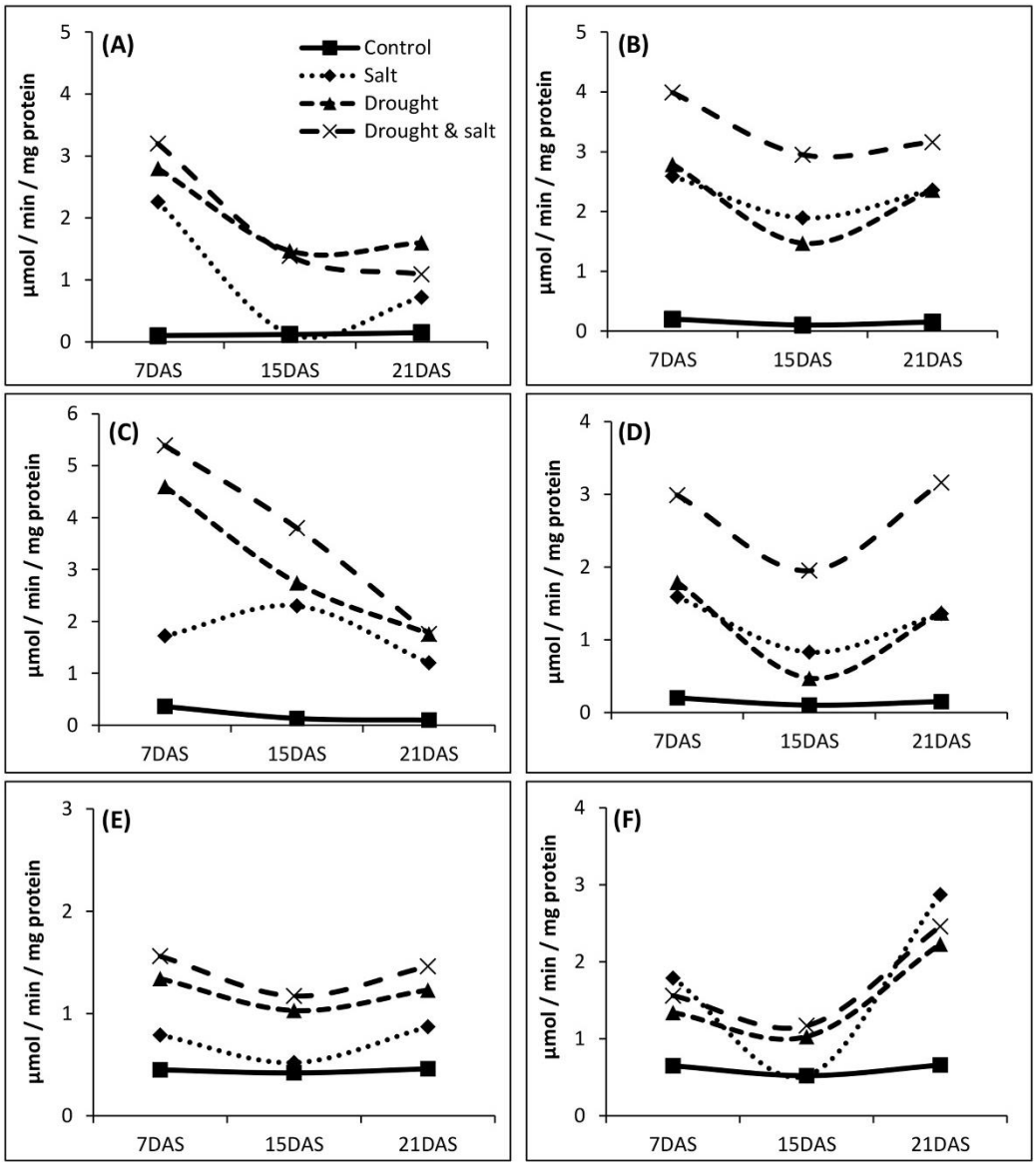


**Fig. 33.** Enzyme activities of targeted genes. JcGLYI **(A)** leaf **(B)** root. JcGLYII **(C)** leaf **(D)** root and JcGR **(E)** leaf, **(F)** root at 7, 15 and 21DAS during salt, drought and drought + salt stress and untreated control, with 2mM MG as substrate. Data presented are the mean ± SD (n=3).

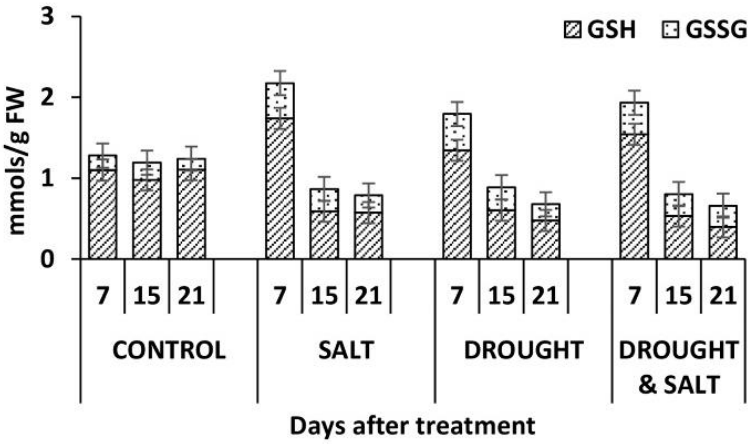


**Fig. 34. Total glutathione content.** Ratio of reduced (GSH) and oxidised glutathione (GSSG) in control and treated plants at 7, 15 and 21 DAS. Mean± SD (n=3) was taken for presentation of the data.

## Conclusions

JcGLYI, II and JcGR were successfully characterised from *J. curcas* which provided evidence that these enzymes could protect yeast and bacteria against MG induced-oxidative stress. Also, *J. curcas* effectively regulates the *GLYI*, *II* and *GR* genes in response to individual or combined abiotic stresses by up-regulating their mRNA expression and subsequently enhancing the MG detoxifying activity. The data demonstrated that JcGLYI, II and/or GR genes could be considered as effective markers or candidate genes for MG detoxification under abiotic stress tolerance.

# Chapter V

# Role of metallothionin (JcMT2) in detoxification of heavy metals from soil

# Chapter - V

Heavy metals are hazardous to the environment and may cause harmful effects to living organisms. Plant species differ in their ability to take up metals to transport and storage (Clemens 2006; Ensley 2000; Sheoran et al. 2011). Cd is a non-essential element and is highly toxic for plants, while Cu is an essential micronutrient at lower concentration, involved in electron transfer reactions by superoxide dismutase, cytochrome c oxidase and plastocyanin. Higher doses of these metals may cause metabolic disorders and growth inhibition for most of the plant species and often leading to death (Hall 2002). Plants have developed several mechanisms to absorb heavy metals from the contaminated soils which include sequestration, compartmentalization, chelation or exclusion (Clemens 2006; Hall 2002). Of all the detoxification mechanisms, chelation of heavy metals is most effective, which has been known to play an important role in metal binding through phytochelatins (PCs) and MTs (Cobbett and Goldsbrough 2002; Domènech et al. 2006; Domenech et al. 2007a; Guo et al. 2003). Phytochelatins are synthesized enzymatically from glutathione with the help of the enzyme phytochelatin synthase and consists of repeating units of ɣ-glutamyl cysteine i.e., $(\gamma\text{-Glu-Cys})_n\text{-Gly}$ where n=2-11. PCs are known to play an important role in the detoxification of Cd, Cu, Zn and are identified in wide variety of organisms including yeast, mammals and plants (Cobbett and Goldsbrough 2002). MTs are cysteine rich, low molecular weight metal binding proteins and have the ability to chelate metals by forming the mercaptide bonds between the cysteine residues and participate in the transport, sequestration and storage of metals. MTs are found in almost all the living forms such as bacteria, yeast, Fungi, animals and also plants

(Domenech et al. 2007b; Ferraz et al. 2012; Gonzalez-Mendoza et al. 2007; Palacios et al. 2011; Robinson et al. 1993; Zhou and Goldsbrough 1994). Mammalian MTs contain 20 cysteine residues arranged in Cys-Cys or Cys-x-Cys patterns lacking aromatic amino acids and are known to protect animals from Cd toxicity (Domenech et al. 2007b). Plant MTs are highly diverse in patterns of arrangement of Cys residues, their distribution and content. Based on the arrangement of the cysteine residues, Plant MTs are classified into four different types which also differ in their pattern of expression (Cobbett and Goldsbrough 2002; Freisinger 2008; 2009; 2011; Guo et al. 2003). All the four types of MTs have been characterized in *Arabidopsis thaliana* and *Oryza sativa* (Zhou et al. 2006; Zhou and Goldsbrough 1995). Type 1 MTs contain six Cys-Xaa-Cys motifs; equally distributed into two cysteine rich domains and their transcripts were mostly found in the subterranean tissues (Cobbett and Goldsbrough 2002; Ma et al. 2003; Yang et al. 2009). Type 2 MTs are abundant in the aerial organs (Cozza et al. 2013; Domènech et al. 2006; Mir et al. 2004; Zhang et al. 2012; Zhigang et al. 2006) and they also are known to possess two cysteine rich domains separated by a spacer region. The structure of QsMT2 has been studied by spectroscopic studies, suggesting a hairpin model where the two cysteine rich domains interact with the metal to form a cluster (Domènech et al. 2007) similarly MT2 from *Cicer arietinum* is known to form a single metal-thiolate cluster (Wan and Freisinger 2009). The type 3 MT gene transcripts have been mainly identified from ripening fruits and developing embryos and are known to contain four and six cysteine residues at N and C-terminals respectively (Freisinger 2007; Jordan et al. 2005). The transcripts of type 4 genes are profusely found in seeds and are comprised of three cysteine rich domains (Rodríguez-Llorente et al. 2010). Apart from metal chelation, MTs are known to play an important role during senescence, root development, seed germination, in alleviating oxidative stress caused due to abiotic stress as well as in ROS detoxification. (Akashi et al. 2004; Hassinen et al. 2011; Hassinen et al. 2009; Kumar et al. 2012; Lee et al. 2004; Yang et al. 2011; Yuan et al. 2008; Zhu et al. 2009).

*Jatropha curcas* (L.), commonly known as physic nut is a shrub belonging to Euphorbiaceae family. It has a high seed oil content of up to 50% and hence it is widely

grown as an economically important biofuel plant. The seed oil is used to produce biodiesel after trans esterification and also in making of soaps and bio pesticides. The seed cake is used as organic fertilizer, combustible fuel and for the production of biogas. *Jatropha* is also known for its tolerance to different abiotic stresses (Eswaran et al. 2010; Gao et al. 2008; Yadav et al. 2009). Of late *Jatropha* has been proposed as a potential crop for phytoremediation of heavy metals such as nickel, copper, arsenic, chromium, zinc, lead, cadmium and coal fly ash (Mangkoedihardjo 2008; Yan et al. 2008) and also for the soils contaminated with lubricating oils (Agamuthu et al. 2010). However the heavy metal tolerance at molecular level has never been reported in *Jatropha*.

In our present study, we have clearly demonstrated the role of JcMT2a to confer metal tolerance in bacteria and yeast and hence signifying its importance in metal homeostasis. qRT- PCR was performed to analyse the accumulation of *JcMT2a* transcripts in leaves and roots. The role of *J. curcas* in phytoremediating metals has been studied suggesting its use for phytoremediation of metal contaminated sites.

## Materials and methods

### *Plant material and treatments*

The seeds of *J. curcas* were surface sterilized with 0.4% sodium hypochlorite for 5 minutes and were washed thoroughly with sterile water. Sterilized seeds were germinated in petri plates containing sterile wet blotting paper. After germination, the seedlings were transferred to pots containing red soil and sand (1:1). Plants were grown in a greenhouse under controlled conditions at 28±2ºC and ~70% humidity for one month. For the experiment on metal treatment, one month old plants were transferred to ½ strength Hoagland's nutrient solution and allowed to acclimatize. 6-week-old plants were submerged in aqueous solutions of $CuSO_4$ and $CdCl_2$ at different concentrations (250, 500, 1000 µM) for 48 h. Control plants were submerged in ½ strength Hoagland's nutrient without metal. Following the treatment, roots and leaves

of the treated as well as the control plants were frozen in liquid nitrogen and stored at -80$^0$C.

### *RNA isolation and first strand cDNA synthesis*

Total RNA was isolated from 100 mg of frozen leaf and root tissues, of both metals treated and control plants using Plant Spectrum RNA isolation kit (Sigma-Aldrich, USA). RNA purity was checked by means of spectrophotometer (Nano drop 2000 spectrophotometer, Thermo Fisher Scientific) and its integrity was checked by agarose gel electrophoresis. Following isolation, cDNA synthesis was performed by using RevertAid$^{TM}$ first strand synthesis kit (Fermentas Life Sciences, Germany) according to the manufacturer's protocol. The cDNA was stored at −20 °C until use.

### *Primer synthesis and cDNA amplification*

MT gene sequences from *Ricinus communis* (MT-like, Accession number: L02306.1), *Atropa belladona* (MT2b, AJ297968.1), *Quercus suber* (MT-like, AJ277599.2), *Thlaspi caerulescens* (MT2, AY847455.1), *Populus* spp. (MT2b, AY594298.1), *Codonopsis lanceolata* (MT2-like, AY833717.1), *Brassica juncea* (MT2-like, Y10853.1) *Pringlea antiscorbutica* (MT2-like, AY333930.1) *Salix matsudana* (MT2b, EF157298.1) *Puccinellia tenuiflora* (MT-like, JQ279061.1) available in the databases were aligned using the Clustal W software (Thompson et al. 1994) and primers were designed from the conserved region of the aligned sequences (Fig 35). All the primers used in the study were listed in Table 9. cDNA and genomic DNA was amplified using JcMTF and JcMTR at $T_m$ 60$^0$C to obtain partial *JcMT2* sequence. The PCR product was cloned in pTZ57RT vector (Fermentas Life Sciences, Germany) and later sequenced.

### *RACE (Rapid Amplification of cDNA Ends) PCR*

Gene specific primers were designed to carry out 3'- and 5'- RACE to get full length cDNA sequence using "SMART$^{TM}$ RACE cDNA amplification kit" (Clonetech, USA) following manufacturer's instructions. The specific primers for 3'RACE and 5'RACE (Table 9) were designed from the partial sequence of *JcMT2*. The amplified PCR

products were gel extracted using "QIAquick Gel extraction kit" (Qiagen, Netherlands) and sequenced. The resulting sequence was designated as *JcMT2a*. The full length cDNA sequence obtained was submitted to NCBI to get the accession number.

### *Cloning, heterologous expression, purification and heavy metal tolerance assay of recombinant JcMT2a in Escherichia coli*

The coding region of JcMT2 protein (JcMT2a) was obtained by PCR amplification with the primers JcMT2BF and JcMT2ER (Table 9) which encompassed the *Bam*HI and *Eco*RI sites, respectively. The amplified fragment was digested with the restriction endonucleases, and sub cloned into a pGEX-4T-1 (Amersham Pharmacia Biotech) expression vector digested with the same enzymes. The recombinant plasmid, pGEX-4T1-JcMT2a, was confirmed by sequencing and was transformed into competent cells of *E. coli* BL21 (DE3) for protein expression. A parent vector without inserts was used as a negative control. JcMT2 fusion protein was expressed in *E. coli* and induced with 1 mM isopropyl β-D-thiogalactoside (IPTG) for 4 h at 30 °C. Cells were harvested by centrifugation for 15 min at 12,000 rpm and resuspended in 1xPBS and later the cells were lysed by sonication in the presence of 0.5% β -mercaptoethanol to prevent protein oxidation. After sonication, cellular debris was pelleted by centrifugation for 20 min at 16,000 rpm (Kubota 7780, Tokyo, Japan) and the fusion protein GST-JcMT2a was isolated from the supernatant by affinity chromatography using CL-Agarose column from Genei$^{TM}$ GST-Fusion protein purification kit (Bangalore Genei, Bangalore, India). Selected fractions were confirmed by 12% SDS-PAGE.

To further investigate the metal tolerance of transformed *E.coli*, the cells harbouring GST and GST-JcMT2a protein were induced in presence of 1mM IPTG and 300 µM $CuSO_4$, 300 µM $CdCl_2$ or 300 µM $ZnCl_2$. Bacterial growth was monitored at 1 h. intervals at $OD_{600}$ simultaneously spot assay was performed by making fivefold dilutions of the grown cultures and spotting was performed on LB with ampicillin plates, supplemented with 1mM IPTG and 300 µM $CuSO_4$, 300 µM $CdCl_2$ or 300 µM $ZnCl_2$ respectively. The plates were grown at $37^0$C for 12 hrs and were photographed.

### *Yeast functional complementation assays*

The yeast vector p424-JcMT2a was constructed as follows: the JcMT2a coding region was excised from pGEX-4T-1-JcMT2a by digestion with *Bam*HI/*Eco*RI and ligated into the yeast expression vector p424 under the transcriptional control of the yeast glyceraldehyde-3-phosphate dehydrogenase (GPD) promoter. The p424 vector also contains the CYC1 (cytochrome c oxidase) terminator, the 2 µ replication origin and the TRP1 tryptophan marker. Two copper-sensitive *Saccharomyces cerevisiae* strains: DTY3 and DTY4, referred to hereafter as *cup1s* and *cup1*$^{\Delta}$, respectively (Longo et al. 1996) and one cadmium sensitive mutant *yap-1* were used for the study. Vector p424 and the construct p424-JcMT2a were introduced into *cup1*$^{\Delta}$ and *yap-1* cells using Frozen EZ-yeast transformation II$^{TM}$ kit (Zymo Research, USA). The transformed cells were selected by their capacity to grow in complete synthetic medium (SC), lacking Trp (p424 selection marker) and Ura (*cup1*$^{\Delta}$ strain selection marker) (SC–Trp–Ura medium) for *cup1*$^{\Delta}$ mutants and SC-Trp medium for *yap1* mutant. For the functional complementation experiments, cultures of *cup1*$^{\Delta}$ yeast cells carrying either p424 or p424-JcMT2a and *cup1s* were grown in SC–Trp–Ura medium and *yap-1* were grown in SC-TRP medium at 30 $^{0}$C and 220 rpm, to $OD_{600}$=1.0. 10-fold dilutions were performed and 3µl of each dilution were spotted on SC plates and on SC supplemented with 75 µM $CuSO_4$ plates for Cu sensitive mutants and 75µM $CdCl_2$ for Cd sensitive mutants. Plates were incubated for 3 d at 30 $^{0}$C and photographed.

### *Real-time PCR (qRT-PCR) of JcMT2a gene under heavy metal stress*

Quantification of gene expression by real-time PCR analysis was performed using Eppendorf Realplex MasterCycler (Eppendorf, Germany) using the KAPA SYBR FAST (Mastermix (2X) Universal) (KAPA Bio systems, USA) real time PCR. To establish reference points for MT-expression, primers were designed for *Jatropha curcas* Actin and 18SrRNA mRNA partial sequences. Actin was used as the reference gene for internal standardization when measuring responses for the root tissue samples.

However, qPCR expression of 18SrRNA proved to be more stable than actin for leaf tissue samples. Expression levels of mRNA for *JcMT2a* were measured by qPCR using the primer pairs (qRTF and qRTR) listed in Table 9. Expression levels of the target genes were calculated by comparing the cycle threshold value (Ct) to the reference gene. The relative quantification (comparative method) was calculated using the $2^{-\Delta\Delta Ct}$ method (Livak and Schmittgen 2001). All samples were normalized to the ΔCt value of a reference gene sample to obtain a ΔΔCt value = (ΔCt treated−ΔCt control). The final relative expression was calculated using the following formula $F=2^{-(\Delta Ct\ treated-\Delta Ct\ control)}$. The experiment was performed twice in triplicates for each sample.

### *Scanning electron microscopy (SEM) and Energy dispersive x-ray spectroscopy (EDAX) analysis*

To study the distribution of metals within the plant tissues, stem and root of the treated and control plants were harvested and cut into 1-1.5cm sections. These sections were placed in 2.5% glutaraldehyde for 24-48 hrs. They were then rinsed with 0.1M phosphate buffer (pH-6.8), 3 times; 30min per rinse and then post fixed in 1% Osmium tetra oxide for 2hrs. The sections were then rinsed in deionized water and dehydrated in a graded ethanol series for at least 30 min per exchange. Free hand sections of stem and root tissues with thickness of 3-5mm were taken and mounted on aluminium stubs, dried under vacuum, gold coated and observed under ESEM/EDAX XL30 (Netherlands). The data on the elemental composition were expressed in percentage weight of element.

### *Statistical analysis*

The data were processed using Microsoft excel 2010. The parameters were represented as mean ± standard deviation with sample size n=3 for qPCR and ESEM/EDAX analysis. The data were further analysed by one way analysis of variance (ANOVA), the comparisons were tested with Holm-Sidak method, and the level of significance was set to 0.05. The statistical analysis was performed using Sigma Plot 11.0.

Table 9: List of specific primers used in the study

| S. No. | Primer name | 5'-3' Primer sequence | Role |
|---|---|---|---|
| 1. | JcMTF | TCTTGCTGTGGAGGAAACTG | Partial JcMT2 |
| | JcMTR | GCAGTTGTCGCCACACTT | fragment |
| 2. | 5'RACE | GCAGTTGTCGCCACACTT | 5' and 3' |
| | 3'RACE | TCTTGCTGTGGAGGAAACTG | JcMT2 RACE |
| 3. | JcMT2BF | CGCGGATCCATGTCTTCTTGCTGTGGTGG | Heterologous |
| | JcMT2ER | CCGGAATTCTCATTTACAGTTGCAAGGAT | Gene expression |
| 4. | JcActF | GAGCAGAGAGATTCCGATGC | qRT-PCR |
| | JcActR | GCAATGCCAGGGAACATAGT | Reference gene1 |
| 5. | Jc18F | CCTGCGGCTTAATTTGACT | qRT-PCR |
| | Jc18R | TTAGCAGGCTGAGGTCTC | Reference gene2 |
| 6. | qRTF | GCAAGTGTGGCAGCGGTTGT | qRT-PCR |
| | qRTF | CCGCCGATCTCATTTACAGT | JcMT2a gene |

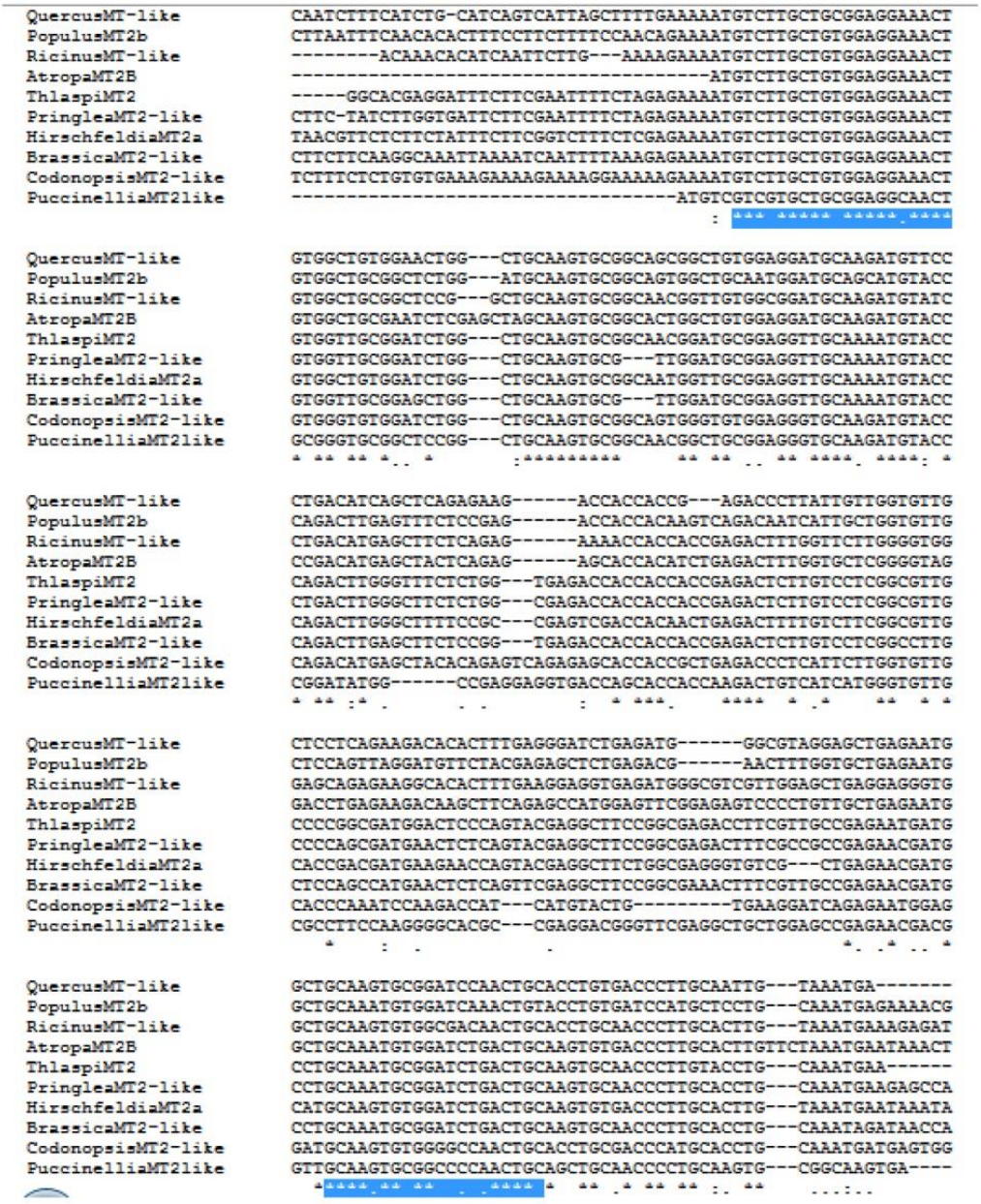


**Fig. 35.** Sequence alignment of MT2 from different plants which were used to design primers JcMTF and JcMTR from the conserved regions highlighted in blue using Clustal W.

## Results

### *Sequence characterization and deduced amino acid comparison*

A 618 bp long cDNA sequence was generated by 5' and 3' RACE, having an open reading frame of 246 bp with 66 bp of 5' UTR (untranslated region) and 309 bp of 3' UTR. This complete sequence was submitted to NCBI (GenBank accession number Bank It 1560107 *JcMT2a* JX501994). The sequence analyses of cDNA and genomic DNA regions from the leaf showed the presence of two introns (Fig. 39). The coding region of JcMT2 protein represented an 80 amino acid protein with a molecular weight of 7.965 kDa and a pI of 5.18 having 6 C-X-C motifs, 3 at N terminal (CCXXXCGCXXXCKCXXXCGGC) and 3 at C terminal (CKCXXXCTCXXCNCK), typical of MT type 2 proteins. JcMT2 characterised in our study also has 3 aromatic amino acids in its protein sequence (Fig. 37 and 38). When BLAST analysis was performed with the protein sequence of JcMT2a, it showed maximum identity with 74% of sequence matching with MT2 of *Ricinus communis*, 73% similarity with MT protein of *Gossypium hirsutum*, 71% with MT2a of *Salix matsudana* and 70% with the MTs of *Elaeagnus umbellate*, *Quercus suber* and *Fagus sylvatica* (Fig. 36).

### *Protein expression and purification of GST-JcMT2a protein*

The *E.coli* BL21 (DE3) cells were overexpressed with JcMT2a protein as a carboxy terminal fusion of GST. Similarly cells, expressing only GST, were considered as control. The overexpressed proteins were found in the soluble fractions and were purified with affinity chromatography; purity was checked by SDS-PAGE. In SDS-PAGE analysis, a protein corresponding to the size of GST (26.5KDa) was detected in crude lysate of induced BL-21 cells containing the vector pGEX4T-1 and a unique protein corresponding to the predicted size (34KDa) of the GST-JcMT2a fusion protein was detected in crude lysates of cells transformed with plasmid pGEX4T-1-JcMT2a (Fig 40A and B).

Sequences producing significant alignments:

| Accession | Description | Max score | Total score | Query coverage | E value | Max ident | Links |
|---|---|---|---|---|---|---|---|
| AAV74186.1 | metallothionein-like protein [Gossypium hirsutum] | 95.1 | 95.1 | 69% | 1e-23 | 73% | |
| ABM21761.1 | metallothionein-like protein MT2A [Salix matsudana] | 92.0 | 92.0 | 69% | 1e-22 | 71% | |
| XP_002532329.1 | conserved hypothetical protein [Ricinus communis] >sp\|P30564.1\|MT2_RICCO RecName: Full=Metallothionein-like protein type 2 >gb\|AAC37473.1\| metallothionein [Ricinus communis] >gb\|EEF30056.1\| conserved hypothetical protein [Ricinus communis] | 90.9 | 90.9 | 69% | 4e-22 | 74% | G |
| AAC62105.1 | metallothionein homolog [Elaeagnus umbellata] | 88.6 | 88.6 | 69% | 3e-21 | 70% | |
| CAC39481.2 | metallothionein-like protein [Quercus suber] | 88.6 | 88.6 | 69% | 3e-21 | 70% | |
| XP_002308156.1 | predicted protein [Populus trichocarpa] >gb\|EEE91679.1\| predicted protein [Populus trichocarpa] | 88.2 | 88.2 | 69% | 3e-21 | 71% | U G M |
| ABK95520.1 | unknown [Populus trichocarpa] >gb\|ABK96343.1\| unknown [Populus trichocarpa x Populus deltoides] | 88.2 | 88.2 | 69% | 5e-21 | 71% | M |
| ABF50984.1 | metallothionein [Bruguiera gymnorhiza] | 87.4 | 87.4 | 69% | 9e-21 | 70% | |
| CAA10232.1 | metallothionein-like protein class II [Fagus sylvatica] | 86.7 | 86.7 | 69% | 2e-20 | 67% | |
| AEJ37038.1 | type 2 metallothionein [Malus x domestica] | 85.5 | 85.5 | 67% | 5e-20 | 65% | |
| ACN97424.1 | metallothionein-like protein [Pyrus pyrifolia] | 85.5 | 85.5 | 67% | 5e-20 | 65% | |
| ACJ12936.1 | metallothionein-like protein [Pyrus pyrifolia] | 85.5 | 85.5 | 67% | 5e-20 | 65% | |
| ABQ44281.1 | metallothionein type 2 [Sesbania drummondii] | 85.5 | 85.5 | 69% | 5e-20 | 67% | |
| O24058.1 | RecName: Full=Metallothionein-like protein type 2 >gb\|AAC23697.1\| metallothionein-like protein [Malus x domestica] | 85.5 | 85.5 | 67% | 5e-20 | 65% | |
| ABD97258.1 | metallothionin 2 [Camellia sinensis] | 84.7 | 84.7 | 67% | 1e-19 | 64% | |
| ADM86706.1 | metallothionein-like protein [Cicer microphyllum] | 84.7 | 84.7 | 69% | 1e-19 | 67% | |
| AAT02524.1 | metallothionein 2a [Populus trichocarpa x Populus deltoides] | 84.7 | 84.7 | 69% | 1e-19 | 68% | |
| Q39459.2 | RecName: Full=Metallothionein-like protein 2; Short=MT-2 >emb\|CAA65009.1\| class I type 2 metallothionein [Cicer arietinum] | 84.7 | | | | | |

**Fig. 36.** Sequence alignment of genomic and cDNA regions of *JcMT2a.*

```
                1        10        20        30        40        50        60        70        80 83
                |--------+---------+---------+---------+---------+---------+---------+---------+--|
          JMT2  MSSCCGGNCGCGSGCKCGSGCGGCKMYPDMSFS-EKNTAETQVLGVAPEKARFVDGGEVGV-GAEN-GCKCGDNCTCNPCNCK
RicinusMT2like   MSCCGGNCGCGSGCKCGNGCGGCKMYPDMSFS-EKTTTETLVLGVGAEKAHF-EGGEMGVVGAEEGGCKCGDNCTCNPCTCK
NelumboMT2A      MSCCGGNCGCGSGCKCGSGCGGCKMYPDFSFSGERATTETIVVGVAPQKAYF-EGSEMSF-GAENEGCKCGSNCTCNPCNCK
ElaeisMT2a       MSCCGGNCGCGSGCKCGTGCGGCKMYPDMAEE-RSTTTQTVIMGVAPQKGQV-EGFEMAT-GSENGGCKCGSNCTCDPCNCK
SesbaniaMT2      MSCCGGNCGCGSSCKCGTGCGGCKMYPDLSYA-EKTTTETLVMGVAPVKVQF-EGAEMGV-AAENGGCKCGSNCPCDPCNCK
SalviaMT2a       MSCCSGNCGCGSSCKCGNGCTGCGMYPDLSYSERSGAAETLVLGVAPQKTYF-EGSEMGM-GEDENGCKCGANCTCDPCNCK
Consensus        .mSCCgGNCGCGSgCKCG.GCgGCkMYPD.sfs.e..tt#Tl!lGVapqKa.f.#G.Emg..ga##.GCKCG.NCtC#PCnCK
```

**Fig. 37.** Multiple alignment of JcMT2a protein sequence with MT2 like proteins of *Ricicnus, Nelumbo, Elaeis, Sesbania* and *Salvia.*

### *Heavy metal tolerance of transformed bacteria*

To determine heavy metal tolerance of transformed bacteria, the culture media was supplemented with 300µM $CuSO_4$, $CdCl_2$ and $ZnSO_4$ respectively. The *E.coli* cells expressing GST-JcMT2a were more tolerant to metal stress than cells expressing only the GST protein, which was evident from the data on growth curves (Fig. 41). Compared to Zn, the tolerance was more for Cu and Cd metals and similar results were obtained for spot assay when the cells were grown in the presence and absence of metals (Fig. 42).

### *Yeast functional complementation assays*

To test and confirm the functional role of JcMT2a, the gene was expressed in Cd and Cu sensitive yeast mutants respectively for both control (without metal) and metal supplemented media. The *Saccharomyces cerevisiae yap1* locus encodes a transcription factor related to mammalian AP-1 complex that positively controls various genes involved in metal and oxidative stress tolerance in yeast (Kuge and Jones 1994). CUP1 in Yeast was induced by copper and encodes Cu-thionein. The $cup1^s$ mutant has single copy of MT gene whereas $cup1^\Delta$ has no functional copies of CUP1 (Hamer et al. 1985). The cells transformed with p424-JcMT2a could survive on media supplemented with the metals, while the cells harbouring just the vector were able to grow on control media without metal but could not survive under metal stress (Fig. 43A, 43B). Furthermore, the *yap1*-p424-JcMT2a was able to tolerate a concentration of 40 µM Cd and DTY4-p424-JcMT2a tolerated a concentration of 125 µM of Cu.

### *Transcript analysis of JcMT2a gene by qRT-PCR*

The expression level of *JcMT2a* mRNA was assessed by quantitative real time PCR to different Cd and Cu concentrations and exposure times, with 18SrRNA and actin as internal controls for leaf and root tissue respectively. The specificity of the designed primers was indicated by the single peak in the melting curve. The expression of *JcMT2a* was prominently up-regulated for both Cu and Cd stress in the leaf tissue while

a down regulation was recorded in the root tissue. The highest induction of MT2 was approximately 400-fold increase when young plants of *J. curcas* were treated with 1000µM Cu for 48hrs (Fig. 44).

**ORF FINDER RESULTS**

**MSSCCGGNCGCGSGCKCGSGCGGCKMYPDMSFSEKNTAETQVLGVAPEKARFVDGGEVGVG AENGCKCGDNCTCNPCNCK***

1. **Total amino acids – 80 AA**
2. **Total ORF length – 240 bp**
3. **Total Cysteines – 14**
4. **C-X-C Motifs - 6**
5. **3 C-X-C motifs at N terminal and 3 at C terminal end**
6. **Molecular weight – 7965 Da**
7. **Isoelectric Point – 5.18**

```
67  atgtcttcttgctgtggtggaaattgcggctgcggctccggctgc
     M   S   S   C   C   G   G   N   C   G   C   G   S   G   C
112 aagtgtggcagcggttgtggcggatgcaagatgtatcctgacatg
     K   C   G   S   G   C   G   G   C   K   M   Y   P   D   M
157 agtttctccgagaaaaacaccgccgagactcaggttctcggagtt
     S   F   S   E   K   N   T   A   E   T   Q   V   L   G   V
202 gcaccggagaaggcacgctttgtcgatggaggtgaggtcggcgtt
     A   P   E   K   A   R   F   V   D   G   G   E   V   G   V
247 ggagctgagaacggatgcaagtgcggtgacaactgcacctgcaat
     G   A   E   N   G   C   K   C   G   D   N   C   T   C   N
292 ccttgcaactgtaaatga 309
     P   C   N   C   K   *
```

**Fig. 38.** Protein parameters and ORF finder results of JcMT2a protein

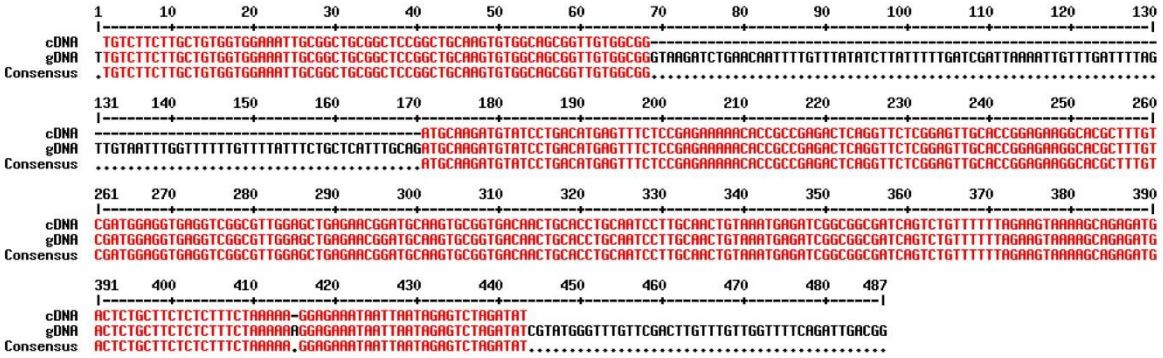


**Fig. 39.** BLAST analysis showing the sequence alignment and percentage similarity of JcMT2a with MT's of other plant species

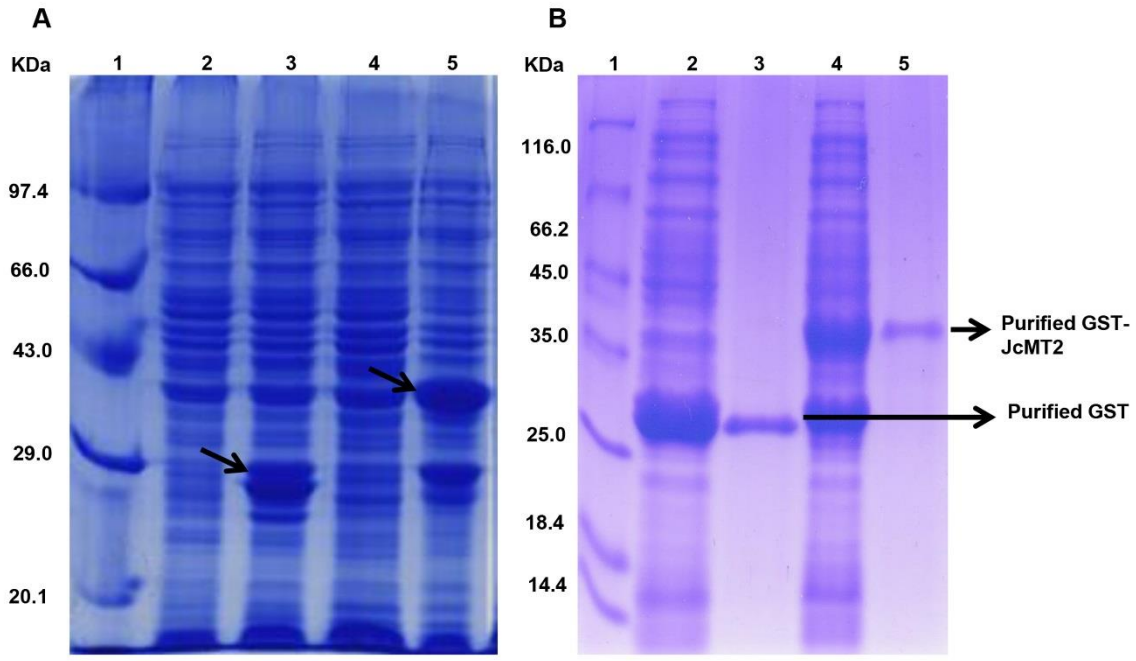


**Fig. 40. (A) Over-expression of JcMT2a recombinant protein in *E.coli* BL21 (DE3) cells:** 12% SDS-PAGE of GST-JcMT2a fusion protein and GST protein was induced by 1mM IPTG, isolated at 6 h of the induction from *E.coli* cells. Lane1: Medium range marker, Lane 2: *E.coli* BL21 cell lysate, Lane 3: *E.coli* BL21 with GST cell lysate induced with IPTG, Lane 4: GST- JcMT2a without IPTG induction, Lane 4: GST- JcMT2a with IPTG induction. **(B) 12% SDS-PAGE of purified GST and GST-JcMT2a protein**: Lane 1: Medium range Molecular weight marker, Lane 2: IPTG induced GST cell lysate, Lane 3: Purified GST protein, Lane 4: IPTG induced GST-JcMT2a cell lysate, Lane 5: Purified GST-JcMT2a protein

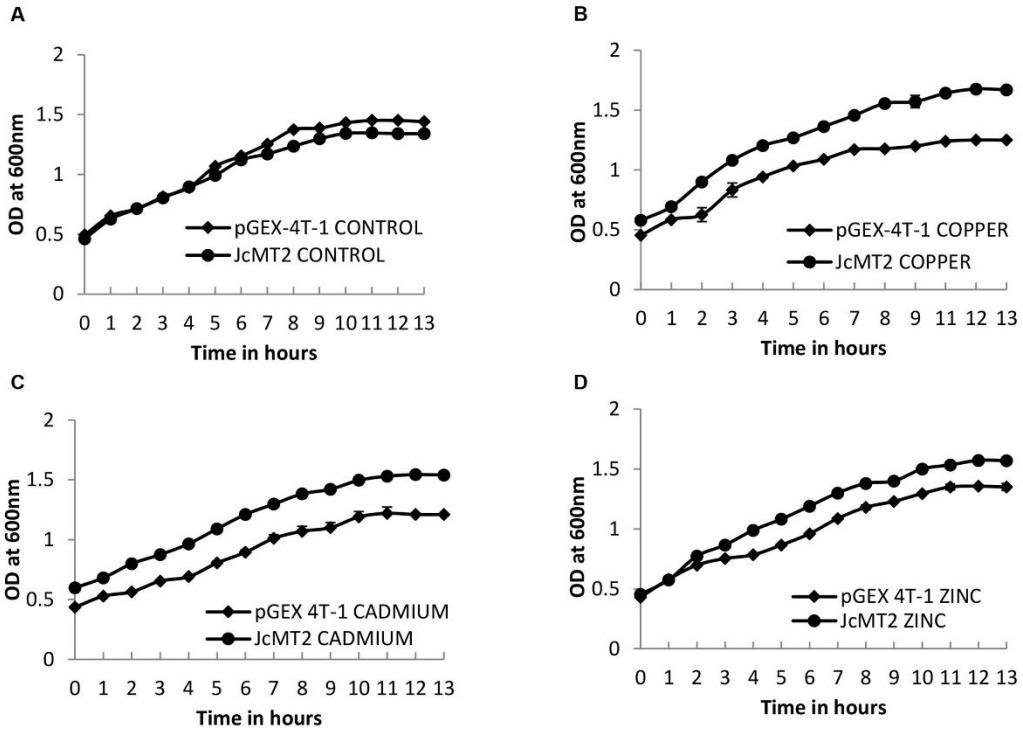


**Fig. 41. Heavy metal tolerance of *E.coli* BL21 cells expressing GST or GST-JcMT2a:** Bacterial growth curve of *E.coli* cells transformed with empty pGEX-4T-1 vector and pGEX-4T-1-JcMT2a, induced with 1mM IPTG and either in the absence of metal ions (A), or in the presence of 300 μM $CuSO_4$ (B), 300 μM $CdCl_2$ (C), 300 μM $ZnSO_4$(D) at $OD_{600}$=0.5.

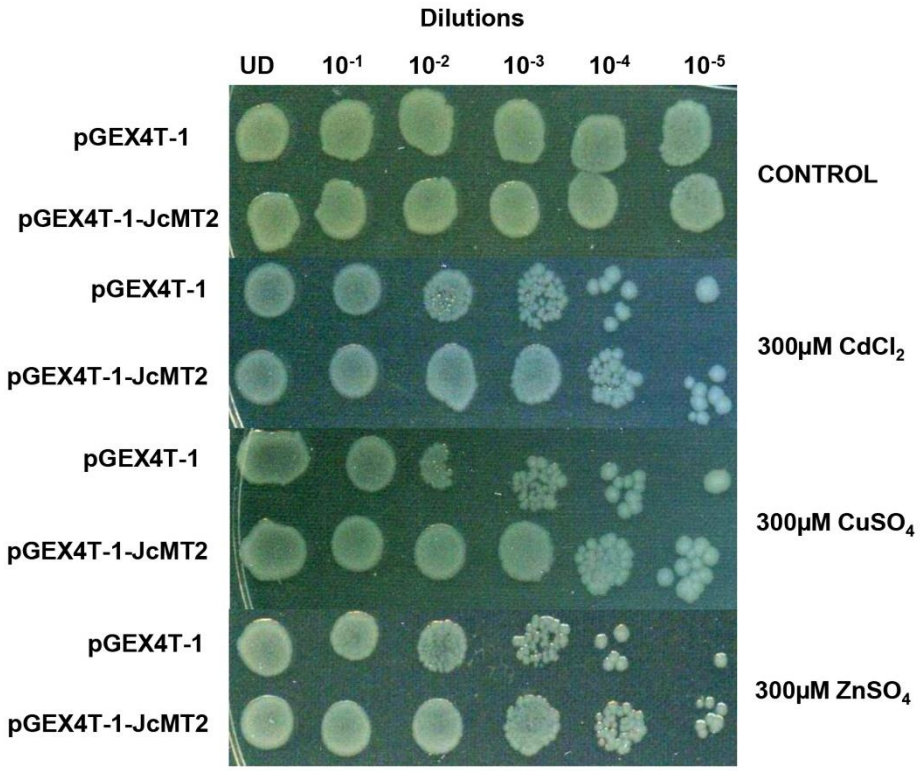


**Fig. 42. Spot assay of *E.coli* BL21 cells expressing GST or GST-JcMT2a:** *E.coli* cells transformed with empty pGEX-4T-1 vector and pGEX-4T-1-JcMT2a and spotted on LB with ampicillin plates supplemented with 1mM IPTG and either in the absence of metal ions- control or in the presence of 300 µM $CuSO_4$, 300 µM $CdCl_2$, 300 µM $ZnSO_4$.

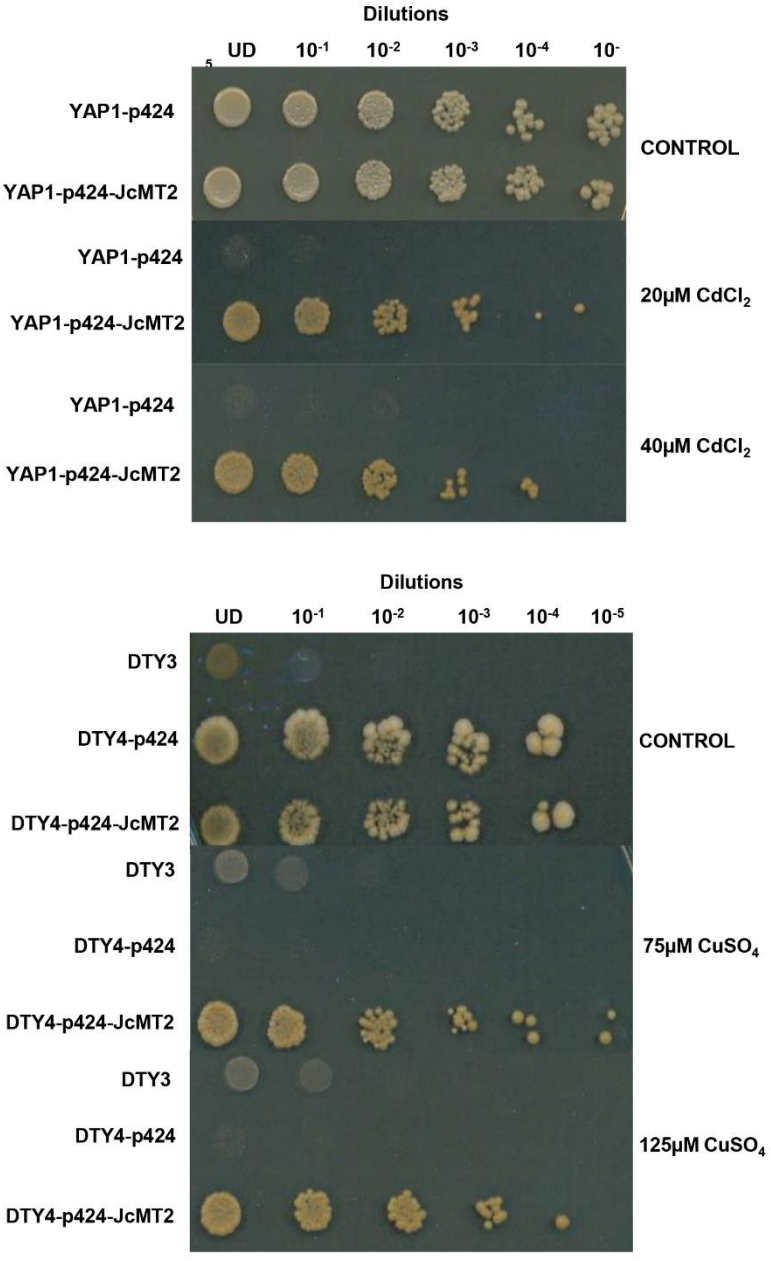


**Fig. 43:**

**(A) Functional complementation of yeast mutants on selective media:** *yap-1* (Cadmium sensitive) mutant, transformed with empty vector p424 or with p424-JcMT2a. The cells were grown to $OD_{600}$=1.0, 10-fold dilutions were performed and 3µl of each dilution were spotted on SC-TRP plates supplemented without or with 20 µM and 40 µM $CdCl_2$.

(**B) Functional complementation of yeast mutants on selective media:** DTY4 (Copper sensitive) mutant was transformed with empty vector P424 or with p424-JcMT2a and DTY3 (parental cells with single CUP1 gene) were taken for the study. The cells were grown to $OD_{600}$=1.0, 10-fold dilutions were performed. 3µl of each dilution were spotted on SC-URA-TRP plates supplemented without or with 75 µM and 125 µM $CuSO_4$.

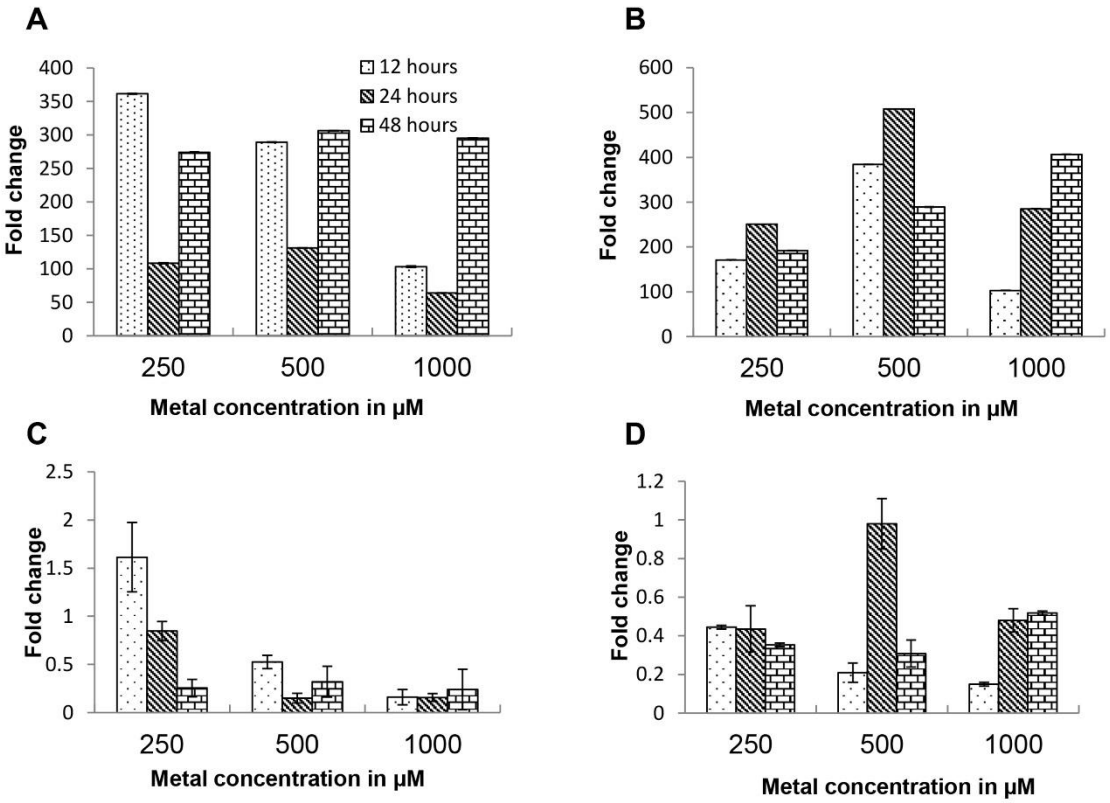


**Fig. 44. Transcript analysis of JcMT2a gene under heavy metal stress:** qRT-PCR analysis of *JcMT2a* gene under heavy metal stress from leaf tissue cadmium(A), copper (B) stress and root tissue cadmium (C), copper (D) stress at different time points (12, 24, 48 hours) and concentrations (250, 500, 1000 µM) of the metals respectively. Total RNA was isolated from control and treated plants, converted to cDNAs, subjected to qRT-PCR. The relative expression of gene ***JcMT2a*** was expressed by $2^{-\Delta\Delta C_T}$. The vertical bars represent the mean ± SD.

### *SEM EDAX analysis*

The SEM-EDAX analysis of individual particles deposited inside the metal treated stem and root was scanned. According to the chemical composition examined by the SEM-EDAX, most abundant particles were C, Al, Fe, Mg, N, Ca, and K with minor constituents such as Si, S, Cl, Cu and Cd. The data for cadmium, copper, chloride and sulphur are presented in the Table 10. The plants supplemented with Cu accumulated it more in the root tissue (Table 10) whereas Cd was found accumulating in both root and stem tissues (Table 11).

## Discussion

Plant MTs are known to perform many physiological roles including essential metal storage, heavy metal detoxification, metal homeostasis (Gonzalez-Mendoza et al. 2007; Usha et al. 2009), alleviating several abiotic stresses (Singh et al. 2011; Usha et al. 2009; Zhou et al. 2005), developmental regulation (Yuan et al. 2008) and ROS scavenging (Akashi et al. 2004; Yang et al. 2011; Zhu et al. 2009). However the crucial role of MTs in plants has not been properly elucidated because of the difficulty in purifying the native proteins (Freisinger 2011; Zhou and Goldsbrough 1995).

In our study, we have cloned a gene encoding *JcMT2a* from *J. curcas*. The comparison of genomic and cDNA sequences revealed the presence of two intronic regions in *JcMT2a* which were correlated with the type 2 MTs of *Oryza sativa* which also is known to have two introns (Hsieh and Huang 1998; Zhou et al. 2006). *JcMT2a* encodes a low molecular weight cysteine rich protein with 80 amino acids and with a molecular weight of 7.96 kDa with 6 C-X-C motifs, which were equally distributed on both N and C terminal ends of the protein. The arrangement of the cysteine residues determines the ability of MTs to bind and chelate the metals. Unlike mammalian MTs which lack aromatic amino acids, most of the plant MTs possesses one or two of them (Domènech et al. 2006). The JcMT2a protein has a tyrosine and two phenylalanine residues but the distribution of the C-X-C motifs was similar to plant type 2 MTs as is seen for *Arabidopsis* MT2a where the first pair of cysteines in JcMT2a was present as

Cys-Cys at 4$^{th}$ and 5$^{th}$ positions followed by two C-x-C motifs and a Cys-Gly-Gly-Cys at the N-terminal region.

**Table 10:** Accumulation of elements (% weight) in the root and leaf tissues of copper-treated (500 and 1000µM) and untreated (control) plants

| Sample | % weight of element | | | Level of significance | | |
|---|---|---|---|---|---|---|
| Cadmium stress | 0(µM) | 500(µM) | 1000(µM) | 0*500 | 0*1000 | 500*1000 |
| Cu Root | 0.37±0.01 | 0.37±0.05 | 0.36±0.12 | ns | ns | ns |
| Cd Root | 0.2±0.08 | 1.10±0.19 | 1.44±0.11 | *** | *** | ** |
| Cl Root | 0.45±0.07 | 0.39±0.02 | 0.29±0.02 | ns | *** | ns |
| S Root | 1.65±0.27 | 1.83±0.06 | 1.8±0.06 | ns | ns | ns |
| Cu Stem | 0.45±0.01 | 0.35±0.02 | 0.45±0.07 | ns | ns | ns |
| Cd Stem | 0.64±0.03 | 2.16±0.24 | 2.8±0.52 | *** | *** | ns |
| Cl Stem | 0.15±0.05 | 0.24±0.08 | 0.23±0.01 | ns | ns | ns |
| S Stem | 0.64±0.02 | 0.73±0.02 | 0.66±0.13 | ns | ns | ns |

**Table 11:** Accumulation of elements (% weight) in the root and leaf tissues of cadmium-treated (500 and 1000µM) and untreated (control) plants

| Sample | % weight of element | | | Level of significance | | |
|---|---|---|---|---|---|---|
| Copper stress | 0(µM) | 500(µM) | 1000(µM) | 0*500 | 0*1000 | 500*1000 |
| Cu Root | 0.37±0.01 | 3.11±0.54 | 3.65±0.15 | *** | *** | ns |
| Cd Root | 0.2±0.08 | 0.47±0.06 | 0.26±0.02 | *** | ns | *** |
| Cl Root | 0.43±0.07 | 0.24±0.06 | 0.57±0.03 | *** | ** | *** |
| S Root | 1.65±0.2 | 1.64±0.1 | 2.3±0.19 | ns | ** | ** |
| Cu Stem | 0.45±0.01 | 0.38±0.07 | 0.67±0.01 | ns | *** | *** |
| Cd Stem | 0.64±0.03 | 0.81±0.13 | 0.91±0.02 | ns | *** | ns |
| Cl Stem | 0.15±0.05 | 0.35±0.07 | 0.19±0.03 | *** | ns | *** |
| S Stem | 0.64±0.02 | 0.31±0.08 | 0.69±0.07 | *** | ns | *** |

The C-terminal had 3 Cys-X-Cys motifs and the two cysteine rich domains were separated by a non-cysteine spacer region containing 40 amino acids. This non-cysteine rich spacer region is proposed to play an important role in stabilization and subcellular localization of MTs. Presence of C-X-C motifs, their arrangement and conservation among different plant species are some of the important characteristics suggesting that *JcMT2*a encodes a type-2 MT protein which may be involved in heavy metal homeostasis by chelating the metals in its C-X-C motifs.

It is difficult to isolate native MT protein from plants owing to its low molecular weight and susceptibility to proteolysis. The first plant MT protein that was purified and metal binding studies performed was wheat early cysteine-labelled protein ($E_c$-1), which plays an important role in zinc binding and its storage during embryogenesis (Loebus et al. 2011; Peroza et al. 2009a; Peroza et al. 2009b). Due to the difficulties in isolating native protein, a recombinant protein was developed in this study by cloning *JcMT2a* gene in heterologous expression vector pGEX 4T-1 and the clone was expressed in *E. coli* BL21 (DE3) cells. After the isolation of purified protein with GST affinity column, a clear band corresponding to the GST fused JcMT2a protein with a molecular weight of 34 kDa was observed in the SDS-PAGE analysis (Fig 40B). To assess the survival ability of the bacteria expressing GST and GST fused JcMT2a protein under metal stress; the cells were grown in presence of Cu, Cd and Zn at a concentration of 300µM. The results showed increased tolerance and metal resistance of the GST fused bacteria to the metal ions compared to the cells expressing GST alone (Fig 41) similar results were obtained when bacterial spotting studies were performed (Fig 42) (Sekhar et al. 2011). Thus JcMT2a protein played an important role in metal homeostasis and cell survivability of the prokaryotic model, *E. coli*. This could probably be due to the metal chelating ability of GST fused JcMT2a protein, expressed in the transformed bacteria. Similarly, GST fused *PjMTs*, *SbMT2* and *QsMT2* from *Prosopis julifora*, *Salicornia brachiata* and *Quercus suber* respectively showed metal tolerance by their ability to bind Cd, Zn and Cu (Chaturvedi et al. 2012).

To examine and confirm the functional role of JcMT2a, yeast complementation studies were performed in *Saccharomyces cerevisiae* mutants, since yeast serves as a eukaryotic model to study the genes involved in various metabolic pathways of the higher eukaryotic organisms. The mutants used for the study were, two copper-sensitive yeast strains: DTY3 and DTY4 (*cup1s* and *cup1*$^{\Delta}$, respectively). The cells with vector alone were able to grow only on control media but could not survive under metal stress. Four MTs from *Arabidopsis* were expressed in Cu sensitive and Zn sensitive yeast mutants, all the four MTs provided tolerance and showed accumulation to both Cu and Zn (Guo et al. 2008). Type 2 MT from *Typha latifolia* restored metal tolerance when expressed in Cu sensitive yeast mutant (Zhang et al. 2004). An increased tolerance against Cd, Zn, Cu and NaCl was observed in transgenic yeast expressing *ThMT3* from *Tamarix hispida* (Yang et al. 2011). *QsMT2* from *Quercus suber* could restore Cu tolerance to MT-deficient, Cu sensitive yeast mutant. But when yeast complementation studies were performed for *McMT1* from *Festuca rubra*, it could not confer heavy metal tolerance in yeast. Therefore, it is evident from our present study that the expression of JcMT2a in yeast mutants led to metal tolerance, and this may be due to the ability of JcMT2a to sequester and bind metals thus protecting the metal sensitive yeast strains from metal stress.

Most of the genes are regulated differently at different levels of translation and post translation for a particular heavy metal treatment. Several reports have shown the involvement of MT genes associated with various abiotic stresses, ROS detoxification, during senescence, heat shock, wounding, during developmental stages and heavy metal stress (van Hoof et al. 2001), but their expression is complex and diversified in plants. In this study, young plants of *J. curcas* were exposed to increasing concentrations of Cu and Cd metals to varying time periods to study *JcMT2a* transcript level under metal stress. *JcMT2a* gene expression in response to Cu and Cd addition was independent of metal dosage and also its expression did not increase linearly with exposure time, which is similar to what has been found in other MTs such as *HtMT2*, *PtdMTs* and *AvMT2* from *Helianthus, Populus, Avicennia* respectively (Chang et al.

2004; Kohler et al. 2004). The nonlinearity may also be due to the presence of other important metal binding proteins such as phytochelatins which are known to chelate Cd in plants and also due to the overlapping functions of PCs and MTs (Guo et al. 2008). Earlier studies with MT2 gene have revealed its expression in the aerial parts of the plant including stems, flowers and in leaves (Guo et al. 2003). In our study, *JcMT2a* gene expression was significantly high in the aerial leaf tissue compared to root tissue for both Cu and Cd stress. When exposed to Cu, the expression of *MT1a* and *MT2b* from *Arabidopsis* was more in root whereas the transcripts of *MT2a* and *MT3* were more in the leaves. *TyMT* from *Typha latifolia* also showed differential expression pattern between root and shoot (Zhang et al. 2004). Hence the expression of *JcMT2a* is tissue-specific suggesting MT synthesis is a direct consequence of metal stress in *J. curcas.* Thus JcMT2a may be involved in Cu and Cd homeostasis and may be a possible candidate for use in genetic engineering approaches for phytoremediation. The ability of *Jatropha* to maintain homeostasis and to tolerate heavy metals may be due to sequestration, compartmentalization, chelation or exclusion of excess of metals by the plant. Also, in *Arabidopsis, AtMT2* expression was increased due to Cu and Cd stress. (Lee et al. 2004) observed an increased expression of *AtMT2a* in *Arabidopsis* seedlings exposed to Cd while an enhanced resistance to Cd was seen in *Vicia faba* guard cells expressing *AtMT2a*. QsMT2 from cork tissue showed an enhanced gene expression under oxidative stress. *SbMT2* gene from *Salicornia* was upregulated by Zn, Cu, salt and drought stress, whereas it was unaffected by Cd stress. MTs other than MT2 such as *ThMT3* from *Tamarix hispida* and *AmMT3* from *Avicennia marina* were known to show an induced gene expression due to Cd and Cu in leaves respectively (Usha et al. 2009).

Phytoremediation is a process where plants are used for cleaning up of the contaminated environments which includes herbicides, insecticides, industrial wastes comprising of metals and toxic chemicals. Of these, metal stress poses a serious problem to the plants by generation of reactive oxygen species (ROS) and free radicals leading to oxidative stress. Most of the plant species exhibit the presence of exclusion and sequestering

mechanisms that moderate metal uptake by roots and stimulate their accumulation in aerial tissues (Olivares et al. 2013). *Jatropha* and *Ricinus* are not accumulators for Cd, however they could be used for phytoremediation of metal polluted soil by phyto-stabilization which prevents leaching into the soil and ground water, thus decreasing the bioavailability to various living forms. To study the uptake and distribution of metals in the young plants of metal treated *J. curcas.* SEM/EDAX analysis was performed. Cu was seen to be accumulating only in the root but no significant traces of it were found in the stem tissue (Table 10), substantiating a slow translocation rate of Cu between the tissues exhibiting an exclusion mechanism of phytoremediation. Increase in the levels of Cd as compared to the control tissue was noticed both in root and stem (Table 11), indicating the ability of *J. curcas* in translocation and retention of heavy metals from root to the aerial parts of the plant, thus showing its efficacy in metal sequestration capacity (Bhargava et al. 2012; Kuzovkina et al. 2004; Mac Farlane and Burchett 2000; Rabier et al. 2008). The ability of Jatropha to extract heavy metals from coal fly ash was reported and the extraction ability was enhanced by adding plant nutrients and chelating agents such as EDTA since the young plants of *Jatropha* were grown in Hoagland's nutrient medium, their ability to extract heavy metals must have been enhanced which is evident from our results obtained for both Cu and Cd treated plants. Similarly, addition of organic waste such as brewery spent grain (BSG) enhanced the plant growth which in turn helped in remediating hydrocarbon contaminated soils. Forest tree MTs are also known to be involved in metal tolerance and accumulation and hence may play an important role in environmental clean-up (Jamil et al. 2009). Genes other than *MT2a* such as *MT2b* and *MT1*a are crucial in maintaining Cu homeostasis and are inducible by Cu stress; also *MT2a* is Cu inducible in young leaves and root tips. Increased *MT2b* expression was seen in *Populus* when the plants were grown in Cd and Zn contaminated soils. PCs are known to participate in transport of Cd from roots and shoots as a mechanism to alleviate Cd accumulation in *Arabidopsis*. Transgenic *Arabidopsis* plants expressing *CcMT1* from *cajanus cajan* showed a higher accumulation of Cu and Cd in the roots as compared to the shoots (Gong et al. 2003). *QsMT2* from *Quercus suber* has shown the ability to bind Cd, thus

bridging the gap between phytochelatins and metallothioneins. In our present study, the differential accumulations of Cu and Cd in root and leaf tissues of *Jatropha* plants treated with metals may be attributed to the differential expression of proteins such as JcMT2a, other MTs and PCs, since all of them tend to have an overlapping function, thus protecting the plant from deleterious effects of metal stress. Our study clearly demonstrates the strategy of *J. curcas* to survive in presence of high concentration of metals possibly by detoxifying mechanisms such as exclusion, sequestration, chelation, and compartmentalization. Our data also suggest that *JcMT2a* from *J. curcas* may be involved in Cu and Cd homeostasis and may be a possible candidate for use in genetic engineering approaches for phytoremediation. In conclusion, *Jatropha* could be a potential plant for phytoremediation to clean heavy metals from the environment as this biofuel tree species is known for faster growth rates resulting superior above ground biomass yields.

## Conclusion

Our experiments on Cu and Cd stress clearly implied a role for JcMT2a protein in protecting and conferring resistance in transformed bacterial cells and the metal sensitive yeast mutants to higher concentrations of external metal ions. *JcMT2a* gene could be a candidate for genetic engineering of plants to confer metal tolerance. Our data on SEM/EDAX analysis also clearly demonstrated the phytoremediation potential of *Jatropha curcas*. Hence *Jatropha* plantations could serve dual purpose including phytoremediation and biodiesel production.

# Summary and Conclusions

# Chapter VI

**Growth and photosynthetic responses of *Jatropha curcas L.* to water and salinity stresses:** Utilization of non-arable land for growing biofuel feedstock will unriddle the scuffle for land usage between food crops and biofuel trees. *Jatropha curcas* is a biofuel tree species which is known for its high oil content, abiotic stress tolerance and phytoremediation. In the current study, we established its potency for abiotic stress tolerance including interactive drought and salt stress with emphasis on its growth and photosynthetic parameters. *J. curcas* plants were treated for 7, 15, 21 days with individual and interactive drought and salt stress by continuous water withholding and 200mM NaCl treatment. With progression of stress there was a decrease in leaf relative water content, stem height and width, number of nodes and total fresh weight of the plant. Gas exchange parameters including photosynthetic rates ($P_n$), stomatal conductance ($g_s$), transpiration rates (E) and apparent quantum efficiency were significantly decreased under stress treatments. This decrease was more pronounced under combined treatment of drought and salt stress when compared to the individual stress treatment. Water use efficiency (WUEi) was retained till 7 DAS (days after stress) but decreased under prolonged stress treatments. Our results on photosystem II efficiency showed a decreased yield and photochemical quenching and an increased non-photochemical quenching. Also, Progressive drought and salinity stress induced a gradual accumulation of $H_2O_2$ and lipid peroxidation in *J.curcas.* The levels of proline which acts as an osmolyte increased with stress severity. In conclusion, *J. curcas* demonstrated morphological, physiological and biochemical adaptive mechanisms under progressive drought and salinity stress.

**Detoxification potential and expression of aldo-keto reductase (*JcAKR*) from *J. curcas.***

Abiotic stress leads to the generation of reactive oxygen species (ROS) which further results in the production of reactive carbonyls (RCs) including methylglyoxal (MG). MG, an α, β-dicarbonyl aldehyde, is highly toxic to plants and the mechanism behind its detoxification is not well understood. Aldo-keto reductases (AKRs) play a role in detoxification of reactive aldehydes and ketones. In the present study, we cloned and characterised a putative AKR from *Jatropha curcas* (JcAKR). Phylogenetically, it forms a small clade with AKRs of *Glycine max* and *Rauwolfia serpentina*. JcAKR was heterologously expressed in *E.coli* BL-21(DE3) cells and the identity of the purified protein was confirmed through MALDI-TOF analysis. The recombinant protein had high enzyme activity and catalytic efficiency in assays containing MG as the substrate. Protein modelling and docking studies revealed MG was efficiently bound to JcAKR. Under progressive drought and salinity stress, the enzyme and transcript levels of JcAKR were higher in leaves compared to roots. Further, the bacterial and yeast cells expressing JcAKR showed more tolerance towards PEG (5%), NaCl (200mM) and MG (5mM) treatments compared to controls. Our data strongly project JcAKR as a possible and potential target even in other crops for the improvement of abiotic stress tolerance.

**Characterization of glyoxalase genes (*JcGlyI* and *JcGlyII*) from *J.curcas* and elucidation of their role in glyoxalase - glutathione cycle.**

We characterized three crucial enzymes, glyoxalase I, II (JcGLYI, JcGLYII) and glutathione reductase (JcGR) that are known to play key role in metabolite degradation and oxidative stress tolerance. Methylglyoxal (MG) produced during abiotic stress causes severe damage to plants and glyoxalases along with glutathione (GSH) detoxify MG to non-toxic compounds. Our transcriptome analysis of Jatropha revealed the presence of putative JcGLYI, JcGLYII and JcGR. The Conserved Domain Database (CDD) analysis of JcGLYI showed two active sites for metal and glutathione binding while JcGLYII had β-lactamase domain. The three corresponding genes were heterologously expressed in *E.coli* BL-21 (DE3) individually and the purified proteins were analysed through MALDI-TOF analysis. JcGLYI, II and JcGR showed specific activity of 1.08, 0.913 and 0.12 mmol $min^{-1}$ $mg^{-1}$ protein with hemithioacetal, S-D-

lactoyl glutathione (SLG) and oxidised glutathione (GSSG) as substrates respectively. JcGLYI Sequence alignment, phylogenetic analysis together with its enzyme kinetics indicated its Ni specificity. Bacterial and yeast growth curves confirmed their protective role against PEG (5%), NaCl (200mM) and MG (5mM). The mRNA expression levels and enzyme activities of these three important enzymes in leaves and roots under drought, salt and combined stress conditions along with total glutathione content were assessed. Our results clearly demonstrated the expression and activities of GLYI and GLYII in corroboration with GR under the drought and salt stress which actively metabolised harmful MG into less toxic compounds, suggesting their protective role in abiotic stress tolerance in *J. curcas*.

**Molecular cloning and characterization of type 2 metallothionein gene (*JcMT2*) from *J. curcas* to understand its role in metal stress tolerance.**

In the present study, we have cloned a gene encoding JcMT2a protein from *Jatropha curcas* L., a promising biofuel tree species. Full length sequence of *JcMT2a* gene was isolated using RACE PCR. Heterologous expression of JcMT2a in *Escherichia coli* and its purification has shown distinct bands corresponding to the GST and GST-fused JcMT2a protein. Significant tolerance was observed in *E. coli* cells expressing recombinant GST-JcMT2a for zinc, copper and cadmium metals compared to cells expressing GST alone. JcMT2a also restored Cu and Cd tolerance in the metal sensitive yeast mutants. Quantitative real time PCR showed a significant increase in *JcMT2a* transcripts with Cu and Cd in the leaf compared to root tissue. Our Scanning electron microscopy and energy dispersive x-ray spectroscopy (SEM-EDAX) analysis clearly demonstrate that *J. curcas* could be a potential candidate for phytoremediation to clean heavy metals from the environment, in addition to its non-edible oil seed yields for biodiesel production.

## Major conclusions

**1.** Our data on phenology of *Jatropha* showed that drought, salinity and combined drought and salinity stress significantly restricted plant growth with simultaneous reduction in leaf water content. Reduced stomatal conductance ($g_s$) limited the $CO_2$

supply and as a result there was a reduction in photosynthetic rate ($P_n$) with a decrease in quantum yield of photosystem II, electron transport rate (ETR) and photochemical quenching (PQ) with simultaneous increase in non-photochemical quenching (NPQ) in the stressed *J. curcas* plants compared to control. In conclusion, *J. curcas* demonstrated morphological, physiological and biochemical adaptive mechanisms under progressive drought and salinity stress.

**2.** Our experiments on salinity and drought stress on *Jatropha* clearly implied a role for *JcAKR* in protecting the plant from abiotic stress as well as conferring resistance in transformed bacterial and yeast cells. JcAKR protein sequence was confirmed by MALDI-TOF analysis. The transcript levels and enzyme activity of AKR increased in response to drought and salt stress. Our data demonstrate that, *JcAKR* from *J. curcas* is involved in MG detoxification and could be a possible candidate for use in genetic engineering approaches to confer abiotic stress tolerance even in crop plants.

**3.** JcGLYI and II from *J.curcas* provided protection against MG induced- oxidative stress in yeast and bacteria. Also, *J.curcas* effectively regulates the *JcGLYI, II* and *GR* genes in response to drought and salinity stress by up-regulating their mRNA expression and subsequently enhancing the MG detoxifying activity and thus could be considered as markers or candidate genes for MG detoxification and abiotic stress tolerance.

**4.** Our experiments on Cu and Cd stress clearly implied a role for JcMT2a protein in protecting and conferring resistance in transformed bacterial cells and the metal sensitive yeast mutants to higher concentrations of external metal ions. Our data further suggests that *JcMT2a* gene could be a potential candidate for genetic engineering of plants to confer metal tolerance. Our results on SEM/EDAX analysis also clearly demonstrated the phytoremediation potential of *Jatropha curcas*. We conclude that *Jatropha* plantations could serve dual purpose including phytoremediation and biodiesel production.

# Literature cited

Agamutu P, Abioye OP, Aziz AA (2010) Phytoremediation of soil contaminated with used lubricating oil using *Jatropha curcas*. *Journal of Hazardous Materials* 179: 891-894

Agrawal C, Sen S, Chatterjee A, Rai S, Yadav S, Singh S, Rai L (2015) Signal Perception and Mechanism of Salt Toxicity/Tolerance in Photosynthetic Organisms: Cyanobacteria to Plants. Stress Responses in Plants. Springer, pp 79-113

Aguilera J, Prieto J (2001) The *Saccharomyces cerevisiae* aldose reductase is implied in the metabolism of methylglyoxal in response to stress conditions. *Current Genetics* 39, 273-283

Akashi K, Nishimura N, Ishida Y, Yokota A (2004) Potent hydroxyl radical scavenging activity of drought-induced type-2 metallothionein in wild watermelon. *Biochemical and Biophysical Research Communications* 323: 72–78

Angelopoulos K, Dichio B, Xiloyannis C (1996) Inhibition of photosynthesis in olive trees (*Olea europaea* L.) during water stress and rewatering. *Journal of Experimental Botany* 47: 1093-1100

Apel K, Hirt H (2004) Reactive oxygen species: metabolism, oxidative stress, and signal transduction. *Annual Review of Plant Biology* 55: 373-399

Asada K (1999) The water-water cycle in chloroplasts: scavenging of active oxygens and dissipation of excess photons. *Annual Review of Plant Biology* 50: 601-639

Ashraf M, Foolad M (2007) Roles of glycine betaine and proline in improving plant abiotic stress resistance. *Environmental and Experimental Botany* 59: 206-216

Belleghem FV, Cuypers A, Semane B, Smeets K, Vangronsveld J (2007) Subcellular localization of cadmium in roots and leaves of *Arabidopsis thaliana*. *New Phytologist* 173: 495–508

Bhargava A, Carmona FF, Bhargava M, Srivastava S (2012) Approaches for enhanced phytoextraction of heavy metals. *Journal of Environmental Management* 105: 103-120

Boo YC, Jung J (1999) Water Deficit—Induced Oxidative Stress and Antioxidative Defenses in Rice Plants. *Journal of Plant Physiology* 155: 255-261

Bowler C, Fluhr R (2000) The role of calcium and activated oxygens as signals for controlling cross-tolerance. *Trends in Plant Science* 5: 241-246

Cakmak I (2000) Possible roles of zinc in protecting plant cells from damage by reactive oxygen species. *New Phytologist* 146: 185-205

Chang Q, Petrash JM (2008) Disruption of aldo-keto reductase genes leads to elevated markers of oxidative stress and inositol auxotrophy in *Saccharomyces cerevisiae*. *BBA Molecular Cell Research* 1783, 237-245

Chang T, Liu X, Xu H, Meng K, Chen S, Zhu Z (2004) A metallothionein-like gene htMT2 strongly expressed in internodes and nodes of *Helianthus tuberosus* and effects of metal ion treatment on its expression. *Planta* 218: 449-455

Chaturvedi AK, Mishra A, Tiwari V, Jha B (2012) Cloning and transcript analysis of type 2 metallothionein gene (SbMT-2) from extreme halophyte *Salicornia brachiata* and its heterologous expression in *E. coli*. *Gene* 499: 280-287

Chen M, Lv S, Meng Y (2010) Epigenetic performers in plants. *Development, Growth & Differentiation* 52: 555-566.

Chen Y, Cai J, Yang F, Zhou B, Zhou L (2015) Ascorbate peroxidase from *Jatropha curcas* enhances salt tolerance in transgenic Arabidopsis. *Genetics and Molecular Research* 14: 4879-4889.

Chinnusamy V, Zhu J-K (2009) Epigenetic regulation of stress responses in plants. *Current Opinion in Plant Biology* 12: 133-139.

Choudhary P, Gupta S, Swarnkar P (2003) Plant Responses Under Water Stress. *Glimpses in Plant Sciences and Biotechnology*: 293.

Clemens S (2006) Toxic metal accumulation, responses to exposure and mechanisms of tolerance in plants. *Biochimie* 88: 1707-1719.

Clugston SL, Barnard JF, Kinach R, Miedema D, Ruman R, Daub E, Honek JF (1998) Overproduction and characterization of a dimeric non-zinc glyoxalase I from *Escherichia coli*: evidence for optimal activation by nickel ions. *Biochemistry*, 37: 8754-8763

Cobbett C, Goldsbrough P (2002) Phytochelatins and metallothioneins: roles in heavy metal detoxification and homeostasis. *Annual Review of Plant Biology* 53: 159–182.

Cobbett CS, Goldsbrough PB (2000) In: Raskin I, Ensley BD, editors. Phytoremediation of toxic metals: Using Plants to clean up the environment, Wiley, New York. pp. 247-269.

Contreras L, Moenne A, Correa JA (2005) Antioxidant responses in *Scytosiphon lomentaria* (phaeophyceae) inhabiting copper-enriched coastal environments1. *Journal of Phycology* 41: 1184-1195.

Cornic G (2000) Drought stress inhibits photosynthesis by decreasing stomatal aperture–not by affecting ATP synthesis. Trends in plant science 5: 187-188

Couto N, Wood J, Barber J (2016) The role of glutathione reductase and related enzymes on cellular redox homoeostasis network. *Free Radical Biology and Medicine* 95: 27-42.

Cozza R, Bruno L, Bitonti MB (2013) Expression pattern of a type-2 metallothionein gene in a wild population of the psammophyte *Silene nicaeensis*. *Protoplasma* 250: 381-389.

Cushman JC, Bohnert HJ (2000) Genomic approaches to plant stress tolerance. *Current Opinion in Plant Biology* 3: 117-124.

Deswal R, Sopory SK (1998) Biochemical and immunochemical characterization of *Brassica juncea* glyoxalase I. *Phytochemistry* 49: 2245-2253.

Dhar MK, Vishal P, Sharma R, Kaul S (2014) Epigenetic dynamics: role of epimarks and underlying machinery in plants exposed to abiotic stress. *International journal of genomics* 2014: 187146.

Domènech J, Mir G, Huguet G, Capdevila M, Molinas M et al. (2006) Plant metallothionein domains: functional insight into physiological metal binding and protein folding. *Biochimie* 88: 583–593.

Domenech J, Tinti A and Torreggiani A (2007) In: Biopolymer Res Trends, Nemeth TS, editors. Research progress on metallothioneins: Insights into structure, metal

binding properties and molecular function by spectroscopic investigations. Nova Science Publishers, Inc. pp. 11-48.

Domenech J, Tinti A, Capdevila M, Atrian S, Torreggiani A (2007) Structural study of the zinc and cadmium complexes of a type 2 plant (*Quercus suber*) metallothionein: insights by vibrational spectroscopy. *Biopolymers* 86(3): 240-248.

Domenech, J, Orihuela R, Mir G, Molinas M, Atrian S et al. (2007) The Cd (II)-binding abilities of recombinant *Quercus suber* metallothionein, QsMT: bridging the gap between phytochelatins and metallothioneins. *Journal of Biological Inorganic Chemistry* 12: 867–882.

Du J, Yang J-L, Li C-H (2012) Advances in metallotionein studies in forest trees. *Plant Omics* 5: 46.

El-Shabrawi H, Kumar B, Kaul T Reddy MK, Singla-Pareek SL, Sopory SK (2010) Redox homeostasis, antioxidant defense, and methylglyoxal detoxification as markers for salt tolerance in Pokkali rice. *Protoplasma* 245: 85-96.

Escalona JM, Flexas J, Medrano H (2000) Stomatal and non-stomatal limitations of photosynthesis under water stress in field-grown grapevines. *Functional Plant Biology* 27: 87-87.

Eswaran N, Parameswaran S, Sathram B, Anantharaman B, Raja KKG et al. (2010) Yeast functional screen to identify genetic determinants capable of conferring abiotic stress tolerance in *Jatropha curcas*. *BMC Biotechnology* 10: 23.

Fehér-Juhász E et al., (2014) Phenotyping shows improved physiological traits and seed yield of transgenic wheat plants expressing the alfalfa aldose reductase under permanent drought stress. *Acta Physiologiae Plantarum* 36, 663-673.

Ferraz P, Fidalgo F, Almeida A, Teixeira J (2012) Phytostabilization of nickel by the zinc and cadmium hyperaccumulator Solanum nigrum L. Are metallothioneins involved? *Plant Physiology and Biochemistry* 57: 254-260.

Freisinger E (2006) Spectroscopic characterization of a fruit-specific metallothionein: *M. acuminata* MT3. *Inorganica Chimica Acta* 360 (1): 369-380.

Freisinger E (2008) Plant MTs—long neglected members of the metallothionein superfamily. *Dalton Transactions* 6663-6675.

Freisinger E (2009) Metallothioneins in plants. Met Ions Life Sci 5: 107-153

Freisinger E (2011) Structural features specific to plant metallothioneins. *Journal of Biological Inorganic Chemistry* 16: 1035–1045.

Gao S, Yan R, Cao M, Yang W, Wang S, Chen F (2008) Effects of copper on growth, antioxidant enzymes and phenylalanine ammonia-lyase activities in *Jatropha curcas* L. seedling. *Plant Soil Environment* 54(3): 117–122.

Gavidia I, Pérez-Bermúdez P, Seitz HU (2002) Cloning and expression of two novel aldo-keto reductases from *Digitalis purpurea* leaves. *European Journal of Biochemistry* 269, 2842-2850.

Ghosh A, Kushwaha HR, Hasan MR et al (2016) Presence of unique glyoxalase III proteins in plants indicates the existence of shorter route for methylglyoxal detoxification. *Scientific Reports* 6:18358.

Gong J-M, Lee DA, Schroeder JI (2003) Long-distance root-to-shoot transport of phytochelatins and cadmium in Arabidopsis. *Proceedings of the National Academy of Sciences* 100(17): 10118-10123.

Gonzalez-Mendoza D, Moreno AQ, Zapata-Perez O (2007) Coordinated responses of phytochelatin synthase and metallothionein genes in black mangrove, *Avicennia germinans*, exposed to cadmium and copper. *Aquatic Toxicology* 83: 306–314.

Grant AW, Steel G, Waugh H, Ellis EM (2003) A novel aldo-keto reductase from *Escherichia coli* can increase resistance to methylglyoxal toxicity. *FEMS Microbiology Letters* 218, 93-99.

Gulshan, K., Rovinsky, S.A., Moye-Rowley, W.S., 2004. YBP1 and its homologue YBP2/YBH1 influence oxidative stress tolerance by non-identical mechanisms in *Saccharomyces cerevisiae*. *Eukaryotic Cell* 3, 318–330.

Guo GJ, Meetam M, Goldsbrough PB (2008) Examining the specific contributions of individual Arabidopsis metallothioneins to copper distribution and metal tolerance. *Plant Physiology* 146: 1697-1706.

Guo WJ, Bundithya W, Goldsbrough PB (2003) Characterization of the Arabidopsis metallothionein gene family: tissue-specific expression and induction during senescence and in response to copper. *New Phytologist* 159: 369–381.

Hall JL (2002) Cellular mechanisms for heavy metal detoxification and tolerance. *Journal of Experimental Botany* 53: 1–11.

Hamer DH, Thiele DJ, Lemontt JE (1985) Function and auto regulation of yeast copperthionein. *Science* 228: 685–690.

Hao X, Li P, Feng Y, Han X, Gao J, Lin E, Han Y (2013) Effects of fully open-air [$CO_2$] elevation on leaf photosynthesis and ultrastructure of *Isatis indigotica* Fort. *PloS One* 8: e74600.

Hasanuzzaman M, Fujita M (2011) Selenium pretreatment upregulates the antioxidant defense and methylglyoxal detoxification system and confers enhanced tolerance to drought stress in rapeseed seedlings. *Biological Trace Element Research* 143: 1758-1776.

Hassinen V, Tuomainen M, Peräniemi S, Schat H, Kärenlampi S, Tervahauta A (2009) Metallothioneins 2 and 3 contribute to the metal-adapted phenotype but are not directly linked to Zn accumulation in the metal hyperaccumulator, *Thlaspi caerulescens*. *Journal of Experimental Botany* 60: 187-196.

Hassinen V, Vallinkoski V-M, Issakainen S, Tervahauta A, Kärenlampi S, Servomaa K (2009) Correlation of foliar MT2b expression with Cd and Zn concentrations in hybrid aspen (*Populus tremula* × *P. tremuloides*) grown in contaminated soil. *Environmental Pollution* 157: 922-930.

Hassinen V, Vallinkoski VM, Issakainen S, Tervahauta A, Karenlampi S, Servomaa K (2009) Correlation of foliar MT2b expression with Cd and Zn concentrations in hybrid aspen (*Populus tremula* x *tremloides*) grown in contaminated soil. *Environmental Pollution* 157: 922-930.

Hassinen VH, Tervahauta AI, Schat H, Karenlampi SO (2011) Plant metallothioneins-metal chelators with ROS scavenging activity? *Plant Biology* 13: 225-232.

Hassinen VH, Tuomainen T, Peraniemi S, Karenlampi SO and Tervahauta AI (2009) Metallothionein 2 and 3 contribute to the metal adapted phenotype but are not

directly linked to Zn accumulation in the metal hyperaccumulator, *Thlapsi caerulescens*. *Journal of Experimental Botany* 60(1): 187-196.

Herbette S, Lenne C, Leblanc N, Julien JL, Drevet JR, Roeckel-Drevet P (2002) Two GPX-like proteins from *Lycopersicon esculentum* and *Helianthus annus* are antioxidant enzymes with phospholipid hydroperoxide glutathione peroxidase and thioredoxin peroxidase activities. *European Journal of Biochemistry*, 269: 2414-2420.

Hodges DM, DeLong JM, Forney CF, Prange RK (1999) Improving the thiobarbituric acid-reactive-substances assay for estimating lipid peroxidation in plant tissues containing anthocyanin and other interfering compounds. *Planta* 207: 604-611.

Hoque MA, Banu MNA, Nakamura Y, Shimoishi Y, Murata Y (2008) Proline and glycinebetaine enhance antioxidant defense and methylglyoxal detoxification systems and reduce NaCl-induced damage in cultured tobacco cells. *Journal of Plant Physiology* 165: 813-824.

Hoque TS, Okuma E, Uraji M, Furuichi T, Sasaki T, Hoque MA, Nakamura Y, Murata Y (2012) Inhibitory effects of methylglyoxal on light-induced stomatal opening and inward $K^+$ channel activity in Arabidopsis. *Bioscience, Biotechnology and Biochemistry* 76, 617–619.

Hossain MA, Fujita M (2009) Purification of glyoxalase I from onion bulbs and molecular cloning of its cDNA. *Bioscience, Biotechnology and Biochemistry* 73: 2007-2013.

Hsieh HM and Huang PC (1998) Promoter structure and activity of type I rice metallothionein-like gene. *Mitochondrial DNA* 9(1): 9-18.

Hyndman D, Bauman DR, Heredia VV, Penning TM (2003) The aldo-keto reductase superfamily homepage. *Chemico-Biological Interactions* 143, 621-631.

Ispolnov K, Gomes R, Silva MS, Freire A (2008) Extracellular methylglyoxal toxicity in *Saccharomyces cerevisiae*: role of glucose and phosphate ions. *Journal of Applied Microbiology* 104: 1092-1102.

Jaleel CA, Manivannan P, Wahid A, Farooq M, Al-Juburi HJ, Somasundaram R, Panneerselvam R (2009) Drought stress in plants: a review on morphological

characteristics and pigments composition. *International Journal Agriculture and Biology* 11: 100-105.

Jamil S, Abhilash PC, Singh N, Sharma PN (2009) *Jatropha curcas*: A potential crop for phytoremediation of coal fly ash. *Journal of Hazardous Material* 172: 269-275.

Jarboe LR (2011) YqhD: a broad-substrate range aldehyde reductase with various applications in production of biorenewable fuels and chemicals. *Applied Microbiology and Biotechnology* 89, 249-257.

Jez J, Bennett M, Schlegel B, Lewis M, Penning T (1997) Comparative anatomy of the aldo–keto reductase superfamily. *Biochemical Journal* 326, 625-636.

Jha B, Mishra A, Jha A, Joshi M (2013) Developing transgenic Jatropha using the SbNHX1 gene from an extreme halophyte for cultivation in saline wasteland. *PLoS One* 8: e71136.

Jia D, Jing-Li Y, Cheng-Hao L (2012) Advances in metallothionein studies in forest trees. *Plant Omics Journal* 5(1): 46-51.

Johansen KS, Svendsen I, Rasmussen SK (2000) Purification and cloning of the two domain glyoxalase I from wheat bran. *Plant Science* 155: 11-20.

Jordan RH, Turley RB, Defauw SL, Steele M (2005) Characterization of cDNA encoding metallothionein 3 from cotton (*Gossypium hirsutum* L.). *DNA Sequence* 16(2): 96-102.

Jung BG, Lee KO, Lee SS, Chi YH, Jang HH, Kang SS, Lee K, Lim D, Yoon SC, Yun D-J (2002) A Chinese cabbage cDNA with high sequence identity to phospholipid hydroperoxide glutathione peroxidases encodes a novel isoform of thioredoxin-dependent peroxidase. *Journal of Biological Chemistry* 277: 12572-12578.

Kalapos MP (1999) Methylglyoxal in living organisms: chemistry, biochemistry, toxicology and biological implications. *Toxicology Letters* 110, 145–175.

Kanayama Y, Mizutani R, Yaguchi S, Hojo A, Ikeda H, Nishiyama M, Kanahama K, (2014) Characterization of an uncharacterized aldo-keto reductase gene from peach and its role in abiotic stress tolerance. *Phytochemistry* 104, 30-36.

Kaur C, Singla-Pareek SL, Sopory SK (2014) Glyoxalase and methylglyoxal as biomarkers for plant stress tolerance. *Critical Reviews in Plant Sciences* 33: 429-456.

Kaur C, Vishnoi A, Ariyadasa TU, Bhattacharya A, Singla-Pareek SL, Sopory SK (2013) Episodes of horizontal gene-transfer and gene-fusion led to co-existence of different metal-ion specific glyoxalase I. *Scientific Reports* 3: 3076.

Kaur C, Vishnoi A, Ariyadasa TU, Bhattacharya A, Singla-Pareek SL, Sopory SK (2013) Episodes of horizontal gene-transfer and gene-fusion led to co-existence of different metal-ion specific glyoxalase I. *Scientific Reports* 3: 3076.

Khan K, Agarwal P, Shanware A, Sane VA (2015) Heterologous expression of two Jatropha aquaporins imparts drought and salt tolerance and improves seed viability in transgenic *Arabidopsis thaliana*. *PLoS One* 10: e0128866.

Kiani SP, Grieu P, Maury P, Hewezi T, Gentzbittel L, Sarrafi A (2007) Genetic variability for physiological traits under drought conditions and differential expression of water stress-associated genes in sunflower (*Helianthus annuus* L.). *Theoretical and Applied Genetics* 114: 193-207.

Kim J-M, To TK, Ishida J, Morosawa T, Kawashima M, Matsui A, Toyoda T, Kimura H, Shinozaki K, Seki M (2008) Alterations of lysine modifications on the histone H3 N-tail under drought stress conditions in *Arabidopsis thaliana*. *Plant and Cell Physiology* 49: 1580-1588.

Ko J, Kim I, Yoo S, Min B, Kim K, Park C (2005) Conversion of methylglyoxal to acetol by *Escherichia coli* aldo-keto reductases. *Journal of Bacteriology* 187, 5782-5789.

Kohler A, Blaudez D, Chalot M and Martin F (2004) Cloning and expression of multiple metallothioneins from hybrid poplar. *New Phytologist* 164: 83-93.

Kuge S, Jones N (1994) YAP1 dependent activation of TRX2 is essential for the response of *Saccharomyces cerevisiae* to oxidative stress by hydroperoxides. *EMBO Journal* 13: 655–664.

Kumar G, Kushwaha HR, Sabharwal VP et al. (2012) Clustered metallothionein genes are co-regulated in rice and ectopic expression of OsMT1e-P confers multiple

abiotic stress tolerance in tobacco via ROS scavenging. *BMC Plant Biology* 12:107.

Kumar S and Gadagkar SR (2001) Disparity Index: A simple statistic to measure and test the homogeneity of substitution patterns between molecular sequences. *Genetics* 158, 1321-1327.

Kumar S, Stecher G, Tamura K (2016) MEGA7; Molecular evolutionary genetics analysis version 7.0 for bigger datasets. *Molecular Biology and Evolution* 33: 1870-1874.

Kuzovkina YA, Knee M, Quigley MF (2004) Cadmium and Copper Uptake and Translocation in Five Willow (Salix L.) species. *International Journal of Phytoremediation* 6(3): 269–287.

Kwon K, Choi D, Hyun JK, Jung HS, Baek K, Park C (2013) Novel glyoxalases from *Arabidopsis thaliana*. *FEBS Journal* 280: 3328-3339.

Lee J, Shim D, Song WY, Hwang I and Lee Y (2004) Arabidopsis metallothioneins 2a and 3 enhance resistance to cadmium when expressed in *Vicia faba* guard cells. *Plant Molecular Biology* 54: 805-815.

Liang J, Zhou M, Zhou X, Jin Y, Xu M, Lin J (2013) JcLEA, a novel LEA-like protein from *Jatropha curcas*, confers a high level of tolerance to dehydration and salinity in *Arabidopsis thaliana*. *PloS One* 8, 12: e83056.

Liu B, Wang W, Gao J, Chen F, Wang S, Xu Y, Tang L, Jia Y (2010) Molecular cloning and characterization of a jasmonate biosynthetic pathway gene for allene oxide cyclase from *Jatropha curcas*. *Acta Physiologiae Plantarum* 32: 531-539.

Liu Y, Wu H, Kou L, Liu X, Zhang J, Guo Y, Ma E (2014) Two metallothionein genes in *Oxya chinensis*: molecular characteristics, expression patterns and roles in heavy metal stress. 9: e112759.

Liu Z, Zhang W, Gong X, Zhang Q, Zhou L (2015) A Cu/Zn superoxide dismutase from *Jatropha curcas* enhances salt tolerance of *Arabidopsis thaliana*. *Genetics and Molecular Research* 14: 2086-2098.

Livak KJ, Schmittgen TD (2001) Analysis of relative gene expression data using real time quantitative PCR and the 2−ΔΔCT method. *Methods* 25: 402–408.

Loebus J, Peroza EA, Bluthgen et al. (2011) Protein and metal cluster structure of the wheat metallothionein domain ɣ-$E_c$-1: the second part of the puzzle. *Journal of Biological Inorganic Chemistry* DOI 10.1007/s00775-011-0770-2.

Longo VD, Gralla EB, Valentine JS (1996) Superoxide dismutase activity is essential for stationary phase survival in *Sacchraromyces cerevisiae*. *Journal of Biological Chemistry* 271: 12275–12280.

Lüthy R, Bowie JU, Eisenberg D (1992) Assessment of protein models with three-dimensional profiles. *Nature* 356, 83–85.

Ma M, Lau PS, Jia YT, Tsang WK, Lam SKS et al. (2003) The isolation and characterization of type1 metallothionein (MT) cDNA from a heavy-metal-tolerant plant *Festuca rubra* cv. Merlin. *Plant Science* 164: 51-60.

Mac Farlane GR, Burchett MD (2000) Cellular distribution of copper, lead, and zinc in the grey mangrove, *Avicennia maria* (Forsk.) Vierh. *Aquatic Botany* 68: 45-59.

Macháčková I (1995) McKersie, BD, Leshem, YY: Stress and stress coping in cultivated plants. *Biologia Plantarum* 37: 380-380.

Maeta K, Izawa S, Inoue Y (2005) Methylglyoxal, a metabolite derived from glycolysis, functions as a signal initiator of the high osmolarity glycerol-mitogen-activated protein kinase cascade and calcineurin/Crz1-mediated pathway in *Saccharomyces cerevisiae*. *Journal of Biological Chemistry* 280: 253-260.

Maeta K, Izawa S, Okazaki S, Kuge S, Inoue Y (2004) Activity of the Yap1 transcription factor in *Saccharomyces cerevisiae* is modulated by methylglyoxal, a metabolite derived from glycolysis. *Molecular and Cell Biology* 24: 8753-8764.

Mahajan S, Tuteja N (2005) Cold, salinity and drought stresses: an overview. *Archives of Biochemistry and Biophysics* 444: 139-158.

Mangkoedihardjo S and Surahmaida (2008) *Jatropha curcas* L. for phytoremediation of lead and cadmium polluted soil. *World Applied Sciences Journal* 4(4): 519-522.

Mano JI (2012) Reactive carbonyl species: their production from lipid peroxides, action in environmental stress, and the detoxification mechanism. *Plant Physiology and Biochemistry* 59: 90-97.

Martins AM, Cordeiro CA, Ponces Freire AM (2001) In situ analysis of methylglyoxal metabolism in *Saccharomyces cerevisiae*. *FEBS Letters* 499: 41–44.

Meloni DA, Oliva MA, Martinez CA, Cambraia J (2003) Photosynthesis and activity of superoxide dismutase, peroxidase and glutathione reductase in cotton under salt stress. *Environmental and Experimental Botany* 49: 69-76.

Miller G, Suzuki N, CIFTCI-YILMAZ S, Mittler R (2010) Reactive oxygen species homeostasis and signalling during drought and salinity stresses. *Plant, Cell & Environment* 33: 453-467.

Mir G, Domènech J, Huguet G, Guo WJ, Goldsbrough P et,al., (2004) A plant type 2 MT from cork tissue responds to oxidative stress. *Journal of Experimental Botany* 55: 2483–2493.

Misra K, Banerjee AB, Ray S, Ray M (1995) Glyoxalase III from *Escherichia coli*: a single novel enzyme for the conversion of methylglyoxal into D-lactate without reduced glutathione. *Biochemical Journal* 305: 999-1003.

Mittler R, Blumwald E (2010) Genetic engineering for modern agriculture: challenges and perspectives. *Annual Review of Plant Biology* 61: 443-462.

Mittler R, Vanderauwera S, Gollery M, Van-Breusegem F (2004) Reactive oxygen gene network of plants. *Trends in Plant Science* 9: 490–498.

Morris GM et al., (2009) Autodock4 and AutoDockTools4: automated docking with selective receptor flexiblity. *Journal of Computational Chemistry* 16: 2785-91.

Mostofa MG, Fujita M (2013) Salicylic acid alleviates copper toxicity in rice (*Oryza sativa* L.) seedlings by up-regulating antioxidative and glyoxalase systems. *Ecotoxicology* 22: 959-973.

Mudalkar S, Golla R, Ghatty S, Reddy AR (2014b) De novo transcriptome analysis of an imminent biofuel crop, *Camelina sativa* L. using Illumina GAIIX sequencing platform and identification of SSR markers. Plant Molecular Biology 84: 159–171.

Mudalkar S, Golla R, Sengupta D, Ghatty S, Reddy AR (2014a) Molecular cloning and characterisation of metallothionein type 2a gene from *Jatropha curcas* L., a promising biofuel plant. *Molecular Biology Reports* 41, 113–124.

Mudalkar S, Sreeharsha RV, Reddy AR (2016) A novel aldo-keto reductase from *Jatropha curcas* L.(JcAKR) plays a crucial role in the detoxification of methylglyoxal, a potent electrophile. *Journal of Plant Physiology* 195: 39-49.

Mustafiz A, Ghosh A, Tripathi AK, Kaur C, Ganguly AK, Bhavesh NS, Tripathi JK, Pareek A, Sopory SK, Singla-Pareek SL (2014) A unique $Ni^{2+}$-dependent and methylglyoxal-inducible rice glyoxalase I possesses a single active site and functions in abiotic stress response. *Plant Journal* 78: 951-963.

Mustafiz A, Sahoo KK, Singla-Pareek SL, Sopory SK (2010) Metabolic engineering of glyoxalase pathway for enhancing stress tolerance in plants. *Methods in Molecular Biology* 639, 95–118.

Mustafiz A, Singh AK, Pareek A, Sopory SK, Singla-Pareek SL (2011) Genome-wide analysis of rice and Arabidopsis identifies two glyoxalase genes that are highly expressed in abiotic stresses. *Functional & Integrative Genomics* 11: 293-305.

Narawongsanont R, Kabinpong S, Auiyawong B, Tantitadapitak C (2012) Cloning and characterization of AKR4C14, a rice aldo–keto reductase, from Thai Jasmine rice. *Protein Journal* 31, 35-42.

Noctor G, Arisi A-CM, Jouanin L, Kunert KJ, Rennenberg H, Foyer CH (1998) Glutathione: biosynthesis, metabolism and relationship to stress tolerance explored in transformed plants. *Journal of Experimental Botany* 49: 623-647.

Oberschall A et al., (2000) A novel aldose/aldehyde reductase protects transgenic plants against lipid peroxidation under chemical and drought stresses. *Plant Journal*. 24, 437-446.

Olivares AR, Carillo-Gonzalez R, Gonzalez-Chavez MCA, Hernandez RMS (2013) Potential of castor bean (*Ricinus communis* L.) for phytoremediation of mine tailings and oil production. *Journal of Environmental Management* 114: 316-323.

Omar S, Elsheery N, Kalaji H, Ebrahim M, Pietkiewicz S, Lee C-H, Allakhverdiev S, Xu Z-F (2013) Identification and differential expression of two dehydrin cDNAs during maturation of *Jatropha curcas* seeds. *Biochemistry (Moscow)* 78: 485-495.

Omar SA, Fu Q-T, Chen M-S, Wang G-J, Song S-Q, Elsheery NI, Xu ZF (2011) Identification and expression analysis of two small heat shock protein cDNAs from developing seeds of biodiesel feedstock plant *Jatropha curcas*. *Plant Science* 181: 632-637.

Palacios O., Atrian S, Capdevila M (2011) Zn- and Cu-thioneins: a functional classification for metallothioneins? *Journal of Biological Inorganic Chemistry* 16: 991–1009.

Pe´rez JM, Arenas FA, Pradenas GA, Sandoval JM, Va´squez CC (2008) *Escherichia coli* YqhD exhibits aldehyde reductase activity and protects from the harmful effect of lipid peroxidation derived aldehydes. *Journal of Biological Chemistry* 283, 7346–7353.

Peng H, Zhang J (2009) Plant genomic DNA methylation in response to stresses: Potential applications and challenges in plant breeding. *Progress in Natural Science* 19: 1037-1045.

Peng X, Liu H, Wang D, Shen S (2016) Genome-wide identification of the *Jatropha curcas* MYB family and functional analysis of the abiotic stress responsive gene JcMYB2. *BMC Genomics* 17: 251.

Peroza EA, Kaabi AA, Meyer-Klaucke W, Wellenreuther G, Freisinger E (2009) The two distinctive metal ion binding domains of the wheat metallothionein $E_c$-1. *Journal of Inorganic Biochemistry* 103: 342-353.

Peroza EA, Schmucki, Guntert P, Freisinger E and Zerbe O (2009) The $\beta_E$-domain of wheat $E_c$-1 metallothionein: A metal-binding domain with a distinctive structure. *Journal of Molecular Biology* 387: 207-218.

Petrov v, Hille, J, Mueller-Roeber B, Gechev TS (2015) ROS-mediated abiotic stress-induced programmed cell death in plants. *Frontiers in Plant Science*. 6: 69.

PHILLIPS SA, THORNALLEY PJ (1993) The formation of methylglyoxal from triose phosphates. *European Journal of Biochemistry* 212: 101-105.

Polle A, Chen S (2015) On the salty side of life: molecular, physiological and anatomical adaptation and acclimation of trees to extreme habitats. *Plant, Cell & Environment* 38: 1794-1816.

Qin X, Gao F, Zhang J, Gao J, Lin S, Wang Y, Jiang L, Liao Y, Wang L, Jia Y (2011) Molecular cloning, characterization and expression of cDNA encoding translationally controlled tumor protein (TCTP) from *Jatropha curcas* L. *Molecular Biology Reports* 38: 3107-3112.

Qin X, Zheng X, Huang X, Lii Y, Shao C, Xu Y, Chen F (2014) A novel transcription factor JcNAC1 response to stress in new model woody plant *Jatropha curcas*. *Planta* 239: 511-520.

Rabbani N, Thornalley PJ (2012) Methylglyoxal, glyoxalase 1 and the dicarbonyl proteome. *Amino Acids* 42: 1133-1142.

Rabier J, Laffont-Schwob I, Notonier R, Fogliani B, Bouraïma-Madjèbi S (2008) Anatomical element localization by EDXS in *Grevillea exul* var. exul under nickel stress. *Environmental Pollution* 156: 1156-1163.

Ramachandran GN, Ramakrishnan C, Sasisekharan V (1963) Stereochemistry of polypeptide chain configurations. *Molecular Biology* 7: 95–99.

Rascher U, Liebig M, Lüttge U (2000) Evaluation of instant light-response curves of chlorophyll fluorescence parameters obtained with a portable chlorophyll fluorometer on site in the field. *Plant, Cell & Environment* 23: 1397-1405.

Reddy AR, Chaitanya KV, Vivekanandan M (2004) Drought induced responses of photosynthesis and antioxidant metabolism in higher plants. *Journal of Plant Physiology* 161: 1189-1202.

Reddy VS, Sopory SK (1999) Glyoxalase I from *Brassica juncea*: molecular cloning, regulation and its over-expression confer tolerance in transgenic tobacco under stress. *Plant Journal* 17: 385-395.

Reiger M, Lassak J, Jung K (2015) Deciphering the role of the type II glyoxalase isoenzyme YcbL (GlxII-2) in *Escherichia coli*. *FEMS Microbiology Letters* 362: 1-7.

Ridderström M, Mannervik B (1997) Molecular cloning and characterization of the thiolesterase glyoxalase II from *Arabidopsis thaliana*. *Biochemical Journal* 322: 449-454.

Robinson NJ, Tommey AM, Kuske C, Jackson PJ (1993) Plant metallothioneins. *The Journal of Biochemistry* 295: 1–10.

Rodríguez-Llorente ID, Pérez-Palacios P, Doukkali B, Caviedes MA, Pajuelo E (2010) Expression of the seed-specific metallothionein mt4a in plant vegetative tissues increases Cu and Zn tolerance. *Plant Science* 178: 327–332.

Rosenthal C, Mueller U, Panjikar S, Sun L, Ruppert M, Zhao Y, Stöckigt J (2006) Expression, purification, crystallization and preliminary X-ray analysis of perakine reductase, a new member of the aldo-keto reductase enzyme superfamily from higher plants. *Acta Crystallographica Section F: Structural Biology Communications* 62: 1286-1289.

Rupesh KS, Sivalingam A, Shweta S, Vikas YP, Zakwan A et al. (2011) Metallothionein-like gene from *Cicer microphyllumis* regulated by multiple abiotic stresses. *Protoplasma* 248: 839–847.

Saito R, Shimakawa G, Nishi A, Iwamoto T, Sakamoto K, Yamamoto H, Amako K, Makino A, Miyake C (2013) Functional analysis of the AKR4C subfamily of *Arabidopsis thaliana*: model structures, substrate specificity, acrolein toxicity, and responses to light and [CO2]. *Bioscience, Biotechnology and Biochemistry* 77, 2038-2045

Saito R, Yamamoto H, Makino A, Sugimoto T, Miyake C (2011) Methylglyoxal functions as Hill oxidant and stimulates the photoreduction of $O_2$ at photosystem I: a symptom of plant diabetes. *Plant, Cell & Environment* 34: 1454-1464.

Sali A and Blundell TL (1993) Comparative protein modelling by satisfaction of spatial restraints. *Journal of Molecular Biology* 234, 779–815.

Sato-Masumoto N, Ito M (2014) Two types of alcohol dehydrogenase from Perilla can form citral and perillaldehyde. *Phytochemistry* 104: 12-20.

Saxena M, Bisht R, Roy SD, Sopory S, Bhalla-Sarin N (2005) Cloning and characterization of a mitochondrial glyoxalase II from *Brassica juncea* that is upregulated by NaCl, Zn, and ABA. *Biochemical and Biophysical Research Communications* 336: 813-819.

Schilling O, Wenzel N, Naylor M, Vogel A, Crowder M, Makaroff C, Meyer-Klaucke W (2003) Flexible metal binding of the metallo-β-lactamase domain: glyoxalase II incorporates iron, manganese, and zinc *in vivo*. *Biochemistry* 42: 11777-11786.

Sekhar K, Priyanka B, Reddy VD, Rao KV (2011) Metallothionein 1 (CcMT1) of pigeonpea (*Cajanus cajan* L.) confers enhanced tolerance to copper and cadmium in *Escherichia coli* and *Arabidopsis thaliana*. *Environmental and Experimental Botany* 72: 131–139.

Sekhar KM, Sreeharsha RV, Reddy AR (2015) Differential responses in photosynthesis, growth and biomass yields in two mulberry genotypes grown under elevated $CO_2$ atmosphere. *Journal of Photochemistry and Photobiology B: Biology* 151: 172-179.

Sengupta D, Mudalkar S, Reddy AR (2012) Detoxification potential and expression analysis of eutypine reducing aldehyde reductase (VrALR) during progressive drought and recovery in *Vigna radiata* (L.) Wilczek roots. *Planta* 236, 1339-49.

Sengupta D, Naik D, Reddy AR (2015) Plant aldo-keto reductases (AKRs) as multi-tasking soldiers involved in diverse plant metabolic processes and stress defense: A structure-function update. *Journal of Plant Physiology* 179: 40-55.

Sheoran V, Sheoran AS, Poonia P (2011) Role of hyperaccumulators in phytoextraction of metals from contaminated mining sites. *Critical Reviews in Environmental Science and Technology* 41(2): 168-214.

Simpson PJ, Tantitadapitak C, Reed AM, Mather OC, Bunce CM, White SA, Ride JP (2009) Characterization of two novel aldo–keto reductases from Arabidopsis: expression patterns, broad substrate specificity, and an open active-site structure suggest a role in toxicant metabolism following stress. *Journal of Molecular Biology* 392, 465-480.

Singh RK, Anandhan S, Singh S, Patade VY, Ahmed Z, Pande V (2011) Metallothionein-like gene from *Cicer microphyllum* is regulated by multiple abiotic stresses. *Protoplasma* 248: 839-847.

Singla-Pareek SL, Yadav SK, Pareek A, Reddy M, Sopory S (2008) Enhancing salt tolerance in a crop plant by overexpression of glyoxalase II. *Transgenic Research* 17: 171-180.

Smits MM, Johnson MA (1981) Methylglyoxal: enzyme distributions relative to its presence in Douglas-fir needles and absence in Douglas-fir needle callus. *Archives of Biochemistry and Biophysics* 208: 431-439.

Sokol A, Kwiatkowska A, Jerzmanowski A, Prymakowska-Bosak M (2007) Up-regulation of stress-inducible genes in tobacco and Arabidopsis cells in response to abiotic stresses and ABA treatment correlates with dynamic changes in histone H3 and H4 modifications. *Planta* 227: 245-254.

Sreeharsha RV, Sekhar KM, Reddy AR (2015) Delayed flowering is associated with lack of photosynthetic acclimation in Pigeon pea (*Cajanus cajan* L.) grown under elevated $CO_2$. *Plant Science* 231: 82-93.

Stockinger EJ, Mao Y, Regier MK, Triezenberg SJ, Thomashow MF (2001) Transcriptional adaptor and histone acetyltransferase proteins in Arabidopsis and their interactions with CBF1, a transcriptional activator involved in cold-regulated gene expression. *Nucleic Acids Research* 29: 1524-1533.

Sukdeo N, Honek JF (2007) *Pseudomonas aeruginosa* contains multiple glyoxalase I-encoding genes from both metal activation classes. *Biochemica Biophysica Acta* 1774:756–63.

Sunkar R, Chinnusamy V, Zhu J, Zhu J-K (2007) Small RNAs as big players in plant abiotic stress responses and nutrient deprivation. *Trends in Plant Science* 12: 301-309.

Suttisansanee U, Honek JF (2011) Bacterial glyoxalase enzymes. *Semin Cell and Developmental Biology* 22: 285-292.

Suzuki N, Koussevitzky S, Mittler R, Miller G (2012) ROS and redox signalling in the response of plants to abiotic stress. *Plant, Cell & Environment* 35: 259-270.

Tamura K, Stecher G, Peterson D, Filipski A, Kumar S (2013) MEGA6: Molecular evolutionary genetics analysis version 6.0. *Molecular Biology and Evolution* 30: 2725-2729.

Tang M, Liu X, Deng H, Shen S (2011) Over-expression of JcDREB, a putative AP2/EREBP domain-containing transcription factor gene in woody biodiesel plant *Jatropha curcas*, enhances salt and freezing tolerance in transgenic *Arabidopsis thaliana*. *Plant Science* 181: 623-631.

Tariq M, Paszkowski J (2004) DNA and histone methylation in plants. *Trends in Genetics* 20: 244-251.

Thompson JD, Higgins DG, Gibson TJ (1994) CLUSTALW: improving the sensitivity of progressive multiple sequence alignment through sequence weighting, position-specific gap penalties and weight matrix choice. *Nucleic Acids Research* 22: 4673–4680.

Tsimilli-Michael M, Strasser RJ (2008) In vivo Assessment of Stress Impact on Plant's Vitality: Applications in Detecting and Evaluating the Beneficial Role of Mycorrhization on Host Plants. In: Varma A ed. Mycorrhiza: State of the Art, Genetics and Molecular Biology, Eco-Function, Biotechnology, Eco-Physiology, Structure and Systematics. Berlin, Heidelberg, Springer Berlin Heidelberg.

Tsuchimoto S, Cartagena J, Khemkladngoen N, Singkaravanit S, Kohinata T, Wada N, Sakai H, Morishita Y, Suzuki H, Shibata D (2012) Development of transgenic plants in Jatropha with drought tolerance. *Plant Biotechnology* 29: 137-143.

Turóczy Z, Kis P, Török K, Cserháti M, Lendvai Á, Dudits D, Horváth GV (2011) Overproduction of a rice aldo–keto reductase increases oxidative and heat stress tolerance by malondialdehyde and methylglyoxal detoxification. *Plant Molecular Biology* 75, 399-412.

Usha B, Prashanth SR, Parida A (2007) Differential expression of two metallothionein encoding genes during heavy metal stress in the mangrove species, *Avicennia marina* (Forsk.) Vierh. *Current Science* 93: 1215-1219.

Usha B, Venkataraman G, Parida A (2009) Heavy metal and abiotic stress inducible metallothionein isoforms from *Prosopis juliflora* (SW) D.C. show differences in binding to heavy metals in vitro. *Molecular Genetics and Genomics* 281: 99–108.

Van Hoof NALM, Hassinen VH, Hakvoort HWJ, Ballintijn KF, Schat H et al. (2001) Enhanced copper tolerance in *Silene vulgaris* (Moench) Garcke populations from copper mines is associated with increased transcript levels of a 2b-type metallothionein gene. *Plant Physiology* 4: 1519-1526.

Vander Jagt D, Robinson B, Taylor K, Hunsaker L (1992) Reduction of trioses by NADPH-dependent aldo-keto reductases. Aldose reductase, methylglyoxal, and diabetic complications. *Journal of Biological Chemistry* 267, 4364-4369.

Verbruggen N, Hermans C (2013) Physiological and molecular responses to magnesium nutritional imbalance in plants. *Plant Soil* 368: 87-99.

Wan X, Freisinger E (2009) The plant metallothionein 2 from *Cicer arietinum* forms a single metal-thiolate cluster. *Metallomics* 1: 489-500.

Wang F, Chen H, Li X, Wang N, Wang T, Yang J, Guan L, Yao N, Du L, Wang Y (2015) Mining and identification of polyunsaturated fatty acid synthesis genes active during Camelina seed development using 454 pyrosequencing. *BMC Plant Biology* 15: 147.

Wang R, Hanna MA, Zhou W-W, Bhadury PS, Chen Q, Song B-A, Yang S (2011) Production and selected fuel properties of biodiesel from promising non-edible oils: *Euphorbia lathyris* L., *Sapium sebiferum* L. and *Jatropha curcas* L. *Bioresource Technology* 102: 1194-1199.

Wang X, Han H, Yan J, Chen F, Wei W (2015) A new AP2/ERF transcription factor from the oil plant *Jatropha curcas* confers salt and drought tolerance to transgenic tobacco. *Applied Biochemistry and Biotechnology* 176: 582-597.

Wani S, Gosal S (2011) Introduction of OsglyII gene into *Oryza sativa* for increasing salinity tolerance. *Biologia Plantarum* 55: 536-540.

Wu C, Ma C, Pan Y, Gong S, Zhao C, Chen S, Li H (2013) Sugar beet M14 glyoxalase I gene can enhance plant tolerance to abiotic stresses. *Journal of Plant Research* 126: 415-425.

Wu Z, Xu X, Xiong W, Wu P, Chen Y, Li M, Wu G, Jiang H (2015) Genome-wide analysis of the NAC gene family in physic nut (*Jatropha curcas* L.). *PLoS One* 10: e0131890.

Xu D, Liu X, Guo C, Zhao J (2006) Methylglyoxal detoxification by an aldo-keto reductase in the cyanobacterium Synechococcus sp. PCC 7002. *Microbiology* 152: 2013-2021.

Yadav SK, Juwarkar AA, Phani KG, Thawale PR, Singh SK et al. (2009) Bioaccumulation and phyto-translocation of arsenic, chromium and zinc by *Jatropha curcas* L.: Impact of dairy sludge and bio fertilizer. *Bioresource Technology* 100(20): 4616-4622.

Yadav SK, Singla-Pareek SL, Kumar M, Pareek A, Saxena M, Sarin NB, Sopory S (2007) Characterization and functional validation of glyoxalase II from rice. *Protein Expression and Purification* 51: 126-132.

Yadav SK, Singla-Pareek SL, Ray M, Reddy M, Sopory S (2005a) Methylglyoxal levels in plants under salinity stress are dependent on glyoxalase I and glutathione. *Biochemical and Biophysical Research Communications* 337: 61-67.

Yadav SK, Singla-Pareek SL, Reddy M, Sopory S (2005b) Transgenic tobacco plants overexpressing glyoxalase enzymes resist an increase in methylglyoxal and maintain higher reduced glutathione levels under salinity stress. *FEBS Letters* 579: 6265-6271.

Yamauchi Y, Hasegawa A, Taninaka A, Mizutani M, Sugimoto Y (2011) NADPH-dependent reductases involved in the detoxification of reactive carbonyls in plants. *Journal of Biological Chemistry* 286: 6999-7009.

Yan R, Gao S, Yang W, Cao M, Wang S et al. (2008) Nickel toxicity induced antioxidant enzyme and phenylalanine ammonia-lyase activities in *Jatropha curcas* L. cotyledons. *Plant, Soil & Environment* 54: 294-300.

Yang J, Wang Y, Liu G, Yang C, Li C (2011) Tamarix hispida metallothionein-like ThMT3, a reactive oxygen species scavenger, increases tolerance against $Cd^{2+}$, $Zn^{2+}$, $Cu^{2+}$ and NaCl in transgenic yeast. *Molecular Biology Reports* 38(3): 1567-74.

Yang S, Chen, Wang S, Gong M (2015). Osmoregulation as a key factor in drought hardening-induced drought tolerance in *Jatropha curcas*. *Biologia Plantarum* 1-8.

Yang Y, Luo Z, Zhang M, Liu C, Gong M, Zou Z (2016) Molecular Cloning, Expression Analysis, and Functional Characterization of the $H^+$-Pyrophosphatase from *Jatropha curcas*. *Applied Biochemistry and Biotechnology* 178: 1273-1285.

Yang Z, Wu YR, Li Y, Ling HQ, Chu C (2009) OsMT1a, a type 1 metallothionein, plays the pivotal role in zinc homeostasis and drought tolerance in rice. *Plant Molecular Biology* 70: 219–229.

Yousuf PY, Hakeem KUR, Chandna R, Ahmad P (2012) Role of glutathione reductase in plant abiotic stress. In: Abiotic Stress Responses in Plants: Metabolism, Productivity and Sustainability. Springer. DOI: 10.1007/978-1-4614-0634-1_8.

Yuan J, Chen D, Ren Y, Zhang X, Zhao J (2008) Characteristic and expression analysis of a metallothionein gene, OsMT2b, downregulated by cytokinin suggests functions in root development and seed embryo germination of rice. Journal of Plant Physiology 146: 1637-1650.

Zhang D-Y, Chen G-Y, Gong Z-Y, Chen J, Yong Z-H, Zhu J-G, Xu D-Q (2008) Ribulose-1, 5-bisphosphate regeneration limitation in rice leaf photosynthetic acclimation to elevated $CO_2$. *Plant science* 175: 348-355.

Zhang D-Y, Chen G-Y, Gong Z-Y, Chen J, Yong Z-H, Zhu J-G, Xu D-Q (2008) Ribulose-1, 5-bisphosphate regeneration limitation in rice leaf photosynthetic acclimation to elevated $CO_2$. *Plant science* 175: 348-355.

Zhang FQ, Wang YS, Sun CC, Lou ZP, Dong JD (2012) A novel metallothionein gene from a mangrove plant *Kandelia candel*. *Ecotoxicology* 21(6): 1633-1641.

Zhang YW, Tan NFY, Wong YS (2004) Cloning and characterization of type 2 metallothionein-like gene from a wetland plant *Typha latifolia*. *Plant Science* 167: 869–877.

Zhigang A, Cuijie L, Yuangang Z, Yejie D, Wachter A et al. (2006) Expression of BjMT2, a metallothionein 2 from *Brassica juncea*, increases copper and cadmium tolerance in *Escherichia coli* and *Arabidopsis thaliana*, but inhibits root elongation in *Arabidopsis thaliana* seedlings. *Journal of Experimental Botany* 57: 3575–3582.

Zhou G, Xu Y, Li J, Yang L, Liu JY (2006) Molecular analyses of the metallothionein gene family in rice (*Oryza sativa* L.). *Journal of Biochemistry and Molecular Biology* 39(5): 595-606.

Zhou GK, Xu YF, Liu JY (2005) Characterization of a rice class II metallothionein gene: tissue expression patterns and induction in response to abiotic factors. *Journal of Plant Physiology* 162: 686–696

Zhou J, Goldsbrough PB (1994) Functional homologs of fungal metallothionein genes from Arabidopsis. *Plant Cell* 6: 875-884.

Zhou J, Goldsbrough PB (1995) Structure, organization and expression of the metallothionein gene family in Arabidopsis. Molecular Genetics and Genomics 248: 318–328.

Zhu J-K (2002) Salt and drought stress signal transduction in plants. *Annual Review of Plant Biology* 53: 247.

Zhu W, Zhao DX, Miao Q, Xue TT, Li XZ, Zheng C (2009) *Arabidopsis thaliana* metallothionein, AtMT2a, mediates ROS balance during oxidative stress. *Journal of Plant Biology* 52: 585–592.

# Publications

1. Shalini Mudalkar, Rachapudi Venkata Sreeharsha, Attipalli Ramachandra Reddy. Involvement of glyoxalases and glutathione reductase in conferring abiotic stress tolerance to *Jatropha curcas* L. *Environmental and Experimental Botany* (2017) 134:141-150
2. Shalini Mudalkar, Rachapudi Venkata Sreeharsha, Attipalli Ramachandra Reddy. A novel aldo-keto reductase from *Jatropha curcas* L. (JcAKR) plays a crucial role in the detoxification of methylglyoxal, a potent electrophile. *Journal of Plant Physiology* (2016) 195: 39-49.
3. Shalini Mudalkar, Ramesh Golla, Sreenivas Ghatty , Attipalli Ramachandra Reddy.De novo transcriptome analysis of an imminent biofuel crop, *Camelinasativa* L. using Illumina GAIIX sequencing platform and identification of SSR markers. *Plant Molecular Biology* (2014) 84:159–171.
4. Shalini Mudalkar, Ramesh Golla, Debashree Sengupta, Sreenivas Ghatty, Attipalli Ramachandra Reddy.Molecular cloning and characterisation of metallothionein type 2agene from *Jatropha curcas* L., a promising biofuel plant. *Molecular Biology Reports* (2014) 41:113–124.
5. Rachapudi V Sreeharsha, Shalini Mudalkar, Kambam T Singha, Attipalli R Reddy. Unravelling molecular mechanisms from floral initiation to lipid biosynthesis in a promising biofuel tree species, Pongamia pinnata (L.) using transcriptome analysis. *Scientific Reports* (2016) 6:34315
6. Kalva Madhana Sekhar, Venkata Sreeharsha Rachapudi, Shalini Mudalkar, Attipalli Ramachandra Reddy.Persistent stimulation of photosynthesis in short rotation coppice mulberry under elevated $CO_2$ atmosphere. *Journal of Photochemistry and Photobiology B: Biology* (2014) 137: 21–30.
7. Debashree Sengupta, Shalini Mudalkar, Attipalli R. Reddy.Detoxification potential and expression analysis of eutypine reducing aldehyde reductase (VrALR) during progressive drought and recovery in *Vignaradiata* (L.) Wilczek roots. *Planta* (2012) 236:1339-1349.
8. Debashree Sengupta, Golla Ramesh, Shalini Mudalkar, Koppolu Raja Rajesh Kumar, Pulugurtha Bharadwaja Kirti, Attipalli R. Reddy.Molecular Cloning and Characterization of γ-Glutamyl Cysteine Synthetase (VrγECS) from Roots

of *Vignaradiata* (L.) Wilczek under Progressive Drought Stress and Recovery. *Plant Molecular Biology Reporter* (2012) 30:894–903.

**Symposia / Workshops and Seminars attended**

- **Poster presentation- Interdrought V,** February 21-25, 2017, held at Hyderabad, India.
- **Poster presentation- International Plant Physiology Congress,** December 11-14 2015, held at New Delhi, India
- **Poster presentation- Plant gene discovery and Omics technologies,** February 17-18 2014held at Vienna, Austria
- **Oral presentation** in **Plant Science Colloquium** held on 14th March 2014 at department of Plant Sciences, University of Hyderabad, Hyderabad.
- **Participation** in **Bioquest 2015** organized by School of Life Sciences, University of Hyderabad, Hyderabad.
- **Genomics Training Workshop** for Quantitative PCR and Microarray under UoH – DBT – CREBB programme at University of Hyderabad, Hyderabad.
- **One year M.Sc. dissertation** research on "Cloning and characterization of metallothionein type 2 gene from *Vignaradiata*", 2009-2010 at Department of Plant Science, University of Hyderabad.
- **Participation** in "**All India Cell Biology Conference and International Workshop on Cell Cycle regulation**" Dec 10th-13th 2009, organized by School of Life Sciences, University of Hyderabad.